THE OIL FILM IN A CLOSING GAP.

By

HELGE CHRISTENSEN, B.Sc.

June 1960

Department of Mechanical Engineering,

The University of Leeds.

BEST COPY AVAILABLE.

VARIABLE PRINT QUALITY

PAGE NUMBERS ARE CLOSE TO THE EDGE OF THE PAGE.

SOME ARE CUT OFF

ABSTRACT

This Thesis presents a solution to a problem of elasto-hydrodynamics of normal approach ie, the motion of two elastic circular cylinders approaching each other along the line joining their centres and separated by a viscous film. Elastic deformation of the cylinders is accounted for, and the viscosity of the separating film is taken to be a function of pressure and temperature. A numerical method of solution making the use of an electronic computer is devised, and the problem is solved assuming a constant load being applied to the cylinders.

An investigation into the nature of the temperature rise in the oil film due to the motion showed that under certain circumstances this would be rather small, of the order of a few degrees centigrade. This makes the assumption of isothermal conditions in the lubricant film a reasonable approximation under these circumstances and the resulting simpler problem, where viscosity is regarded as a function of pressure alone, is given a more general numerical treatment.

It is found that a very large pressure may be developed in the fluid film at a finite separation of the two cylinders. As the film thickness is further reduced, the value of the maximum pressure goes down and as the film thickness approaches zero, the pressure distribution seems to converge to the Hertzian, dry contact form.

For a given load applied to the cylinders, the value of the maximum pressure reached seems to depend mainly upon the value of parameter αE, i.e. the product of the pressure coefficient of viscosity and the reduced Youngs modulus of the elastic system. It was found that the higher the value of αE, the higher the pressure would go for a given load under otherwise equal conditions. Furthermore, for a load high enough to produce sufficiently large pressures, a small increase in load will produce a large increase in maximum pressure. This gain is also dependent upon the parameter αE and is higher for increased values of αE.

Finally, a series of experiments were performed in order to check some of the theoretical predictions made. These experiments consisted of letting a loaded steel ball normally approach the polished surface of various materials, the surface being covered by a lubricant film, and measuring up the plastic deformations produced in the surface. These tests showed clearly the influence of the lubricant in that in every case the depth of the impression with lubricant was significantly larger than the ones produced under Hertzian, dry contact impacts, under otherwise equal conditions. The experimental results also indicate a correlation between the value of the parameter αE and pressure developed in the lubricant film as predicted by theory.

CONTENTS

NOTATION.

The following is a list of the main notation used. Special symbols are defined in the text.

E : Youngs modulus.

H : Initial central filmthickness

h : Filmthickness

h_o : Filmthickness at point of maximum pressure.

$P_{i\,j}$: Stress

P : Pressure.

P_o : Maximum pressure.

R : Radius of cylinders; $\therefore 1/R = 1/R_1 + 1/R_2$

T : Temperature.

t : Time.

u,v,w : Component velocities; also elastic displacements in the x,y,z directions.

V : Velocity of approach.

W : Load per unit length of cylinder.

x,y,z ; Cartesian Coordinates.

α : Pressure coefficient of viscosity.

$\gamma_{i\,j}$: Rate of shear strain; also direct strain.

δ : Elastic displacement.

ϵ_i : Rate of direct strain; also direct strain.

λ : Elastic constant = $(-2/\pi)\{[1-\nu_1^2]/E_1 + [1-\nu_2^2]/E_2\{$

μ : Dynamic viscosity; also micron = 1/10 000 cm

μ_0 : Dynamic viscosity under atmospheric conditions.

ν : Poissons ratio.

ρ : Density.

CHAPTER 1

INTRODUCTION

1.1 Elasto-Hydrodynamic Lubrication

The principles of hydrodynamics have long been applied to problems in lubrication. As long ago as 1886 O. Reynolds read his now classical paper on hydrodynamic lubrication to the Royal Society, and since that time much work has gone into elaboration of this theory. Most of this theory, however, is applied to journal bearings and thrust bearings, i.e., confined to cases where the pressures encountered are not very high and the assumptions are sufficiently close approximations. During the last 20 years, the theory has also been applied to such machine elements as gears, heavily loaded rollers etc., where the pressures encountered are very much higher. The consequence of this is that now the concept of constant viscosity of the lubricant must be abandoned and instead a variable viscosity must be used. Equally important, however, is the fact that now the boundary materials can no longer be assumed rigid structures, but that due consideration must be given to the deformation of these surfaces under the pressures and the influence this will have on the hydrodynamic film shape.

Problems of this sort then fall within the domain of Elasto-hydrodynamic Lubrication. Briefly, the solution of a problem in Elasto-Hydrodynamics consist of finding the proper solution of the following system of equations (fig. 1.1.1.)

1.1.

$$\frac{\partial}{\partial x}\left\{\frac{h^3}{\mu}\frac{\partial P}{\partial x}\right\}+\frac{\partial}{\partial z}\left\{\frac{h^3}{\mu}\frac{\partial P}{\partial z}\right\}=6U\frac{\partial h}{\partial x}+6W\frac{\partial h}{\partial z}-12V$$

1.1.1

$$h = C + f(x) + \lambda \int_{\Omega} P \ln(r)\,dr$$

where

h = oil film thickness.

P = pressure in the oil film.

μ = lubricant viscosity.

U = velocity in X direction.

W = velocity in Z direction.

V = velocity in normal direction.

$f(x)$ = undeformed geometry of film shape.

r = distance between a point where deformation is calculated and the pressure element producing it.

λ = constant, depending upon the elastic properties of boundaries.

C = an arbitrary additive constant.

Ω = Total area over which the pressure acts.

The first of these equations is the Reynolds equation governing the hydrodynamics. The second is the elastic equation controlling the deformation of the boundaries.

In 1916 Martin (1) assuming constant viscosity and rigid teeth, showed theoretically the possibility of hydrodynamic lubrication in gears.

COORDINATE SYSTEM

FIG 1·1·1

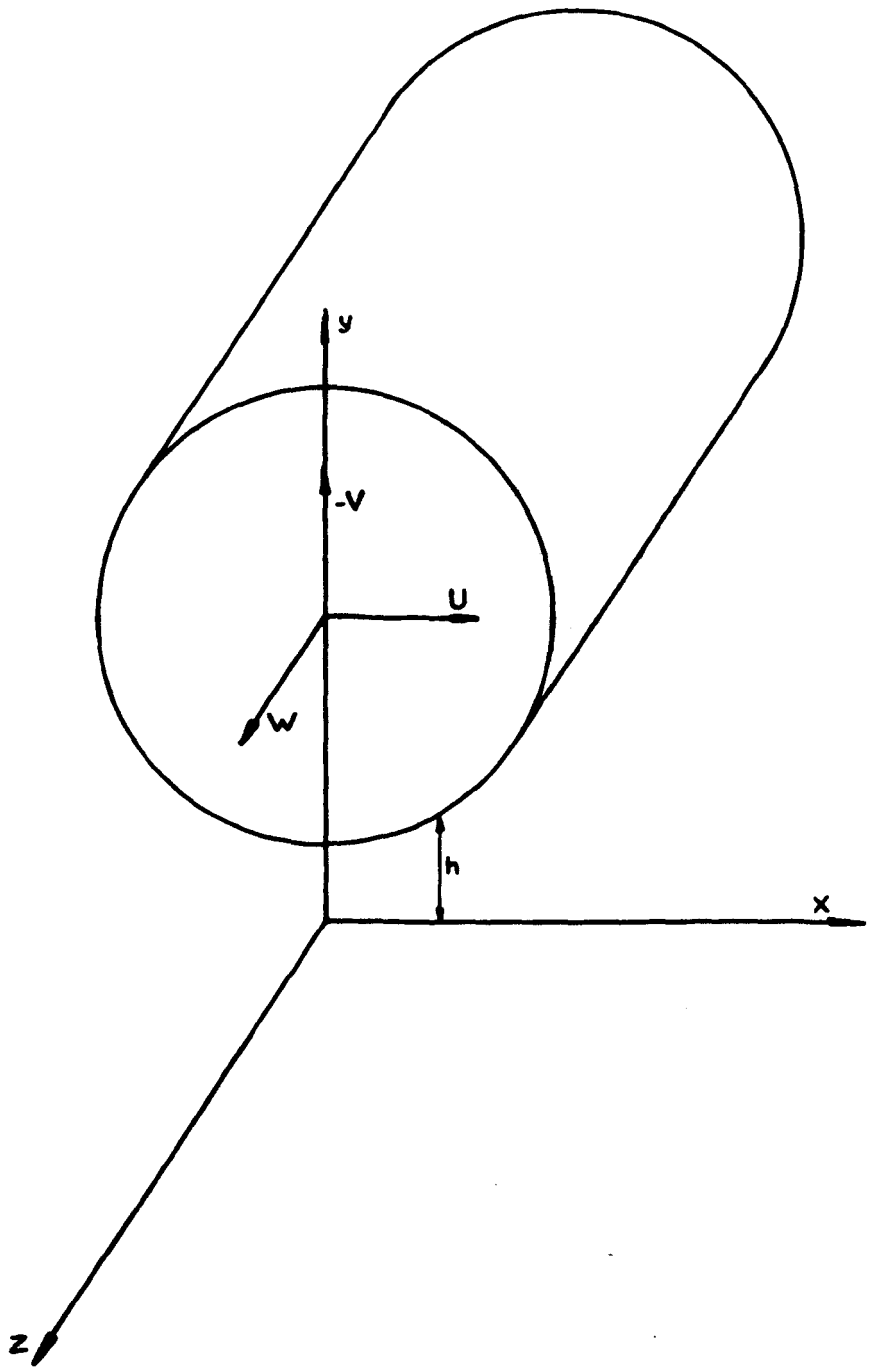

1.1.

Later, more complete theories, taking account of variable viscosity and tooth flattening, have been put forward by various writers: Grubin (2), Petrusevich (3), Poritsky (4), Weber and Saalfeld (5) and Dowson and Higginson (6). These writers have all attempted to solve numerically the equation 1.1.1. with the appropriate boundary conditions in one way or another.

All these theories consider the simplified problem of steady rolling and sliding of two circular cyclinders separated by a lubricating film, and the elasto-hydrodynamic problem of normal approach seems to have received little attention in the literature. In this problem the motion of the two cyclinders are along the line joining their centres. Such a motion is encountered in gears, rotating machine elements where vibrations are present etc.

1.2

Investigations described in this Thesis.

The problem investigated here is that of two circular cylinders in normal approach under some load. The problem had its origin in the more limited problem of evaluating the velocity of approach for various film thicknesses under constant load, since this had some interest in connection with gears. It was hoped that this solution could be used to estimate the thickness of the lubricating film separating the meshing teeth, and also give some indication as to the amount of tip relief needed.

In the preliminary attempts to solve this problem a film shape, which was taken to correspond to the deformed boundaries, was assumed and the hydrodynamics was thus solved using these assumed boundaries. E.g. it was assumed that the deformed geometry could still be represented by two cylinders, but with different radii than the original undeformed cylinders.

Apart from being arbitrary, it soon become clear that this process could not be expected to lead to a satisfactory solution, since this solution was very sensitive to film thickness.

Furthermore, it was discovered that under certain conditions, the pressure generated in the lubricating film might reach very high values. This high pressure might have some effect on the material boundary, and affect the wear characteristics of the gears

1.2

It was therefore decided to investigate the elasto-hydrodynamic problem of normal approach of cylindrical rollers in a more general way by a direct numerical attack on equ. 1.1.1.

Fortunately, the University's electronic, digital computer was available for this work.

Chapter 2

Theory

2.1 General Equations.

The system is in general governed by eight equations, together with the appropriate boundary and initial conditions, this being sufficient to determine the eight unknowns. These are the three velocity components, pressure, density, viscosity, temperature and the elastic deformation of the boundary solids.

Three of these equations are expressions for three conservation principles of physics, i.e. the conservation of mass, momentum and energy. Of the remaining three relations, two connects the fluid properties of viscosity and density to pressure and temperature, while the remaining equation connects the elastic displacements of the bounding solids with the fluid pressure.

For completeness these equations will be derived in convenient form in the following sections.

Before attempting to derive these equations, some basic assumptions regarding the fluid and the boundary solids must be laid down. It is consequently assumed that the fluid can be regarded as a continous, homogeneous medium and that any irregularities in the fluid or in the bounding solids are sufficiently small and can be ignored.

2.2 The General Equation of Motion.

Stresses in a fluid in motion.

Referring to fig.2.2.1, consider a small parallelepiped with centre P(x,y,z) and sides δx, δy, δz parallel to the axis of a fixed coordinate system situated in the moving fluid.

The stresses at the centre of the face $\delta y \delta z$ away from the origin are:

$$P_{xx} + \tfrac{1}{2}\frac{\partial P_{xx}}{\partial x}\delta x \; ; \; P_{xy} + \tfrac{1}{2}\frac{\partial P_{xy}}{\partial x}\delta x \; ; \; P_{xz} + \tfrac{1}{2}\frac{\partial P_{xz}}{\partial x}\partial x$$

where as usual the first suffix denotes the direction of the normal to the plane considered, and the second denotes the direction of the component stress.

At the centre of the opposite face the corresponding stresses are:

$$P_{xx} - \tfrac{1}{2}\frac{\partial P_{xx}}{\partial x}\delta x \; ; \; P_{xy} - \tfrac{1}{2}\frac{\partial P_{xy}}{\partial x}\delta x \; ; \; P_{xz} - \tfrac{1}{2}\frac{\partial P_{xz}}{\partial x}\delta x$$

The force arising from these stresses are:

$$\frac{\partial P_{xx}}{\partial x}\delta V \; ; \; \frac{\partial P_{xy}}{\partial x}\delta V \; ; \; \frac{\partial P_{xz}}{\partial x}\delta V \qquad 2.2.1$$

where $\delta V = \delta x \delta y \delta z$

and similarly for the other directions. Hence there are in all nine stress components at a point.

Considering the couples arising from the forces we have:

$$-P_{xz}\delta V + P_{xy}\delta V$$

about OY and OZ respectively.

STRESSES IN FLUID

FIG 2·2·1

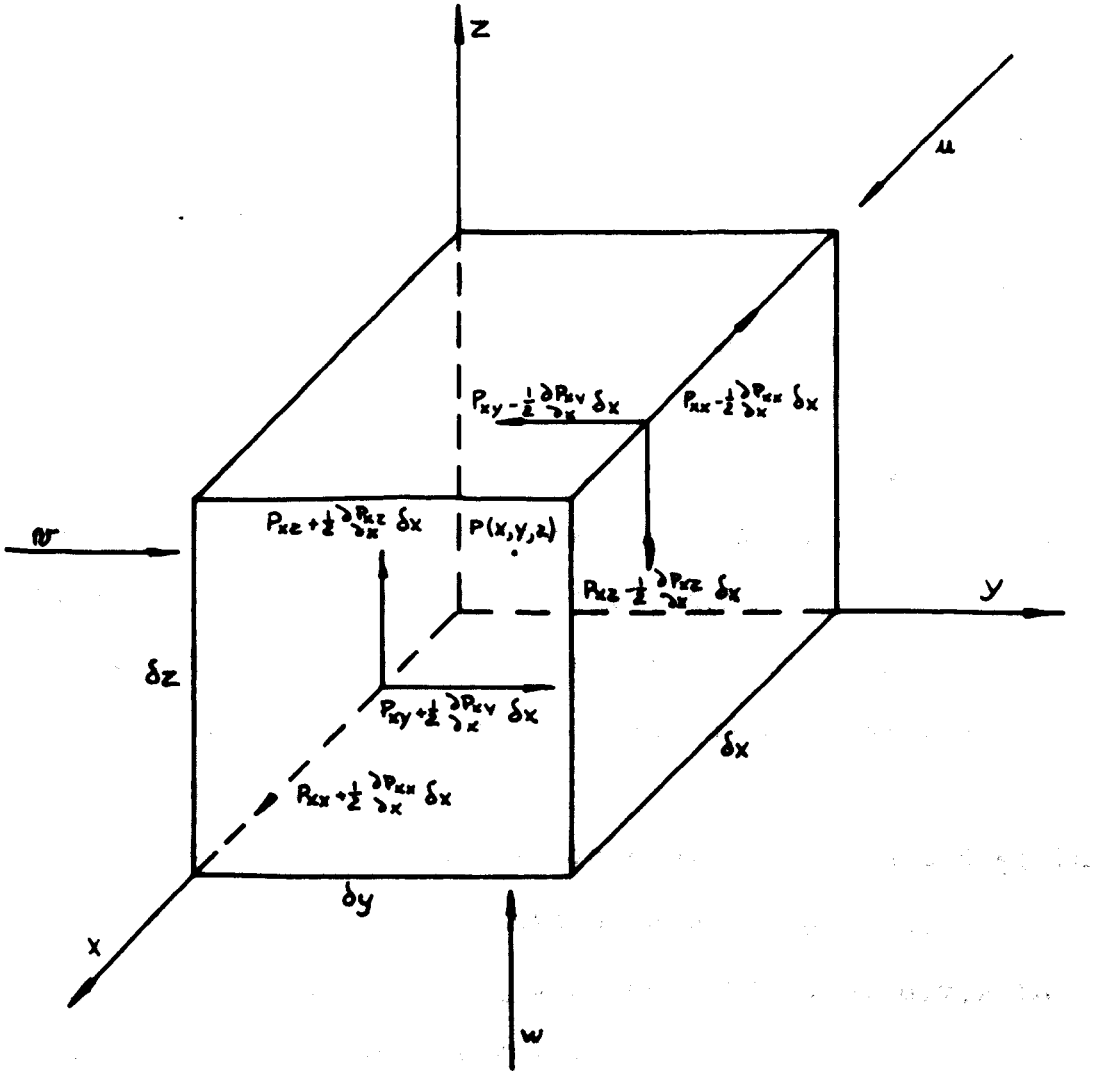

2.2

On considering the equlibrium of the parallelepiped under these forces and letting the edges diminish to zero we have

$$(-P_{xz} + P_{zx})\delta V = 0$$

$$\therefore P_{xz} = P_{zx}$$

and similarly for the other directions. Hence the nine stress-components are thus reduced to six.

Bodyforces and Inertiaforces.

In addition to the surface forces, the fluid may also be subjected to bodyforces such as gravitational forces and inertiaforces.

The bodyforce per unit volume acting on a fluid particle situated at a point P may be expressed as $\rho \underline{F}$ where ρ is the density and $\underline{F}$ the forcevector at the point.

The inertiaforce may be derived by considering the motion of a particle situated at a point P(x,y,z) at time t and having a velocity $\underline{u}$.

At time $t + \delta t$ the same fluidparticle will be situated at the point $P'(x+\delta x, y+\delta y, z+\delta z)$ and have a velocity $\underline{u} + \delta \underline{u}$.

The components of the vector $\underline{u}$ will be denoted by u,v,w in the x,y,z directions respectively.

Considering the x component of velocity, if we assume

$\underline{u} = \underline{u}(x,y,z,t)$

2.2

Taylors theorem gives

$$u + \delta u = u + \left[u\frac{\partial u}{\partial x} + v\frac{\partial u}{\partial y} + w\frac{\partial u}{\partial z} + \frac{\partial u}{\partial t} \right]\delta t + \text{higher terms in } \delta t$$

The component acceleration is now given by

$$\lim_{\delta t \to 0} \frac{\delta u}{\delta t} = \frac{Du}{Dt} = \frac{\partial u}{\partial t} + u\frac{\partial u}{\partial x} + v\frac{\partial u}{\partial y} + w\frac{\partial u}{\partial z} \qquad 2.2.2$$

where the operator $\frac{D}{Dt}$ defined above is known as the total derivative.

Similar expressions can be found for the component of acceleration in the other two directions.

Equating the components of surface- and bodyforces to the corresponding components of rate of change of momentum:

$$\rho\frac{Du}{Dt} = \rho X + \frac{\partial P_{xx}}{\partial x} + \frac{\partial P_{yx}}{\partial y} + \frac{\partial P_{zx}}{\partial z} \qquad 2.2.3$$

with similar expressions for the y and z directions.

Stresses and Velocitygradients.

Equation 2.2.3 is the equation of motion in terms of the stresses in the fluid. In general it is more convenient to have the stresses expressed in terms of the velocitygradients.

The stresses in a fluid are not, by definition, dependant upon its translation or rotation, but only upon the relative motion of its parts i.e. the rates of strain of the particle.

If a fluid particle is situated at a point P(x,y,z) and having a velocity $\underline{u}$ and a nearby particle is at a point

2.2

$P'(x+\delta x, y+\delta y, z+\delta z)$ at the same instant of time and moving with a velocity $\underline{u}+\delta\underline{u}$, the relative velocity between the two particles is:

$$\left.\begin{aligned} du &= \frac{\partial u}{\partial x}\delta x + \frac{\partial u}{\partial y}\delta y + \frac{\partial u}{\partial z}\delta z \\ dv &= \frac{\partial v}{\partial x}\delta x + \frac{\partial v}{\partial y}\delta y + \frac{\partial v}{\partial z}\delta z \\ dw &= \frac{\partial w}{\partial x}\delta x + \frac{\partial w}{\partial y}\delta y + \frac{\partial w}{\partial z}\delta z \end{aligned}\right\} \qquad 2.2.4$$

Defining now the rate of strain components:

$$\epsilon_x = 2\frac{\partial u}{\partial x} \;;\; \epsilon_y = 2\frac{\partial v}{\partial y} \;;\; \epsilon_z = 2\frac{\partial w}{\partial z} \qquad 2.2.5$$

$$\gamma_{xy} = \left(\frac{\partial v}{\partial x} + \frac{\partial u}{\partial y}\right) ; \gamma_{yz} = \left(\frac{\partial w}{\partial y} + \frac{\partial v}{\partial z}\right) ; \gamma_{xz} = \left(\frac{\partial w}{\partial x} + \frac{\partial u}{\partial z}\right)$$

and the components of vorticity:

$$\Omega_x = \left(\frac{\partial w}{\partial y} - \frac{\partial u}{\partial z}\right) ; \Omega_y = \left(\frac{\partial u}{\partial z} - \frac{\partial w}{\partial x}\right) ; \Omega_z = \left(\frac{\partial v}{\partial x} - \frac{\partial u}{\partial y}\right) \qquad 2.2.6$$

Substituting this into eqn. 2.2.4

$$2du = \epsilon_x dx + \gamma_{xy} dy + \gamma_{xz} dz + \Omega_y dz - \Omega_z dy \qquad 2.2.7$$

with similar expressions for dv and dw.

Erecting on the point P a new set of orthogonal axis x', y', z' orientated in such a way that the strains are parallel to these new axis, then the stresses on surfaces perpendicular to theseaxis will be normal stresses only. These new axis will be called principal axis and the normal stresses principal stresses and denoted by P_1, P_2, P_3.

Let the direction of the principal axis at a point P

2.2

relative to another set of rectangular axis be specified by directioncosines l_i, m_i, n_i ; $i = 1,2,3$ in the usual manner.

Also let

$$\epsilon_1' = 2\frac{\partial u'}{\partial x'} \quad ; \quad \epsilon_2' = 2\frac{\partial v'}{\partial y'} \quad ; \quad \epsilon_3' = 2\frac{\partial w'}{\partial z'} \qquad 2.2.8$$

where the primed quantities refer to the principal axis.

We then have:

$$\epsilon_x = l_1^2\epsilon_1' + l_2^2\epsilon_2' + l_3^2\epsilon_3' \qquad 2.2.9$$

and similarly for ϵ_y and ϵ_z

Also

$$\gamma_{xy} = l_1m_1\epsilon_1' + l_2m_2\epsilon_2' + l_3m_3\epsilon_3' \qquad 2.2.10$$

with similar expressions for γ_{yz} and γ_{xz}

Considering now the equilibrium of a small tetrahedron, neglecting inertia- and external forces of higher order of small quantities, we find

$$\left.\begin{aligned} P_{xx} &= P_1l_1^2 + P_2l_2^2 + P_3l_3^2 \\ P_{yy} &= P_1m_1^2 + P_2m_2^2 + P_3m_3^2 \\ P_{zz} &= P_1n_1^2 + P_2n_2^2 + P_3n_3^2 \end{aligned}\right\} \qquad 2.2.11$$

and similarly

$$P_{xy} = P_1l_1m_1 + P_2l_2m_2 + P_3l_3m_3$$

2.2

$$\left.\begin{aligned} P_{yz} &= P_1 m_1 n_1 + P_2 m_2 n_2 + P_3 m_3 n_3 \\ P_{zx} &= P_1 n_1 l_1 + P_2 n_2 l_2 + P_3 n_3 l_3 \end{aligned}\right\} \qquad 2.2.12$$

Hence, the six stresscomponents have been expressed in terms of the principal stresses.

Now, making the assumption that the principal stresses are linear functions of the rates of strain i.e.

$$\left.\begin{aligned} P_1 &= -P + \lambda(\epsilon_x' + \epsilon_y' + \epsilon_z') + 2\mu\epsilon_x' \\ P_2 &= -P + \lambda(\epsilon_x' + \epsilon_y' + \epsilon_z') + 2\mu\epsilon_y' \\ P_3 &= -P + \lambda(\epsilon_x' + \epsilon_y' + \epsilon_z') + 2\mu\epsilon_z' \end{aligned}\right\} \qquad 2.2.13$$

where $-P$ is the hydrostatic pressure

μ is the coefficient of viscosity

By addition, since $P_1 + P_2 + P_3 = -3P$, it follows that

$$3\lambda + 2\mu = 0$$

Hence, from 2.2.9; 2.2.11; 2.2.13 we find,

$$\left.\begin{aligned} P_{xx} &= -P - \tfrac{2}{3}\mu\left(\frac{\partial u}{\partial x} + \frac{\partial v}{\partial y} + \frac{\partial w}{\partial z}\right) + 2\mu\frac{\partial u}{\partial x} \\ P_{yy} &= -P - \tfrac{2}{3}\mu\left(\frac{\partial u}{\partial x} + \frac{\partial v}{\partial y} + \frac{\partial w}{\partial z}\right) + 2\mu\frac{\partial v}{\partial y} \\ P_{zz} &= -P - \tfrac{2}{3}\mu\left(\frac{\partial u}{\partial x} + \frac{\partial v}{\partial y} + \frac{\partial w}{\partial z}\right) + 2\mu\frac{\partial w}{\partial z} \end{aligned}\right\} \qquad 2.2.14$$

Now substituting the relations 2.2.14; 2.2.15 for the stress-components into eqn. 2.2.4 we obtain the equations of motion

2.2

in their most general form

$$\left.\begin{aligned}
\rho\frac{Du}{Dt} &= \rho X - \frac{\partial P}{\partial x} + \frac{2\partial}{3\partial x}\mu\left(\frac{\partial u}{\partial x} - \frac{\partial v}{\partial y}\right) + \frac{2\partial}{3\partial x}\mu\left(\frac{\partial u}{\partial x} - \frac{\partial w}{\partial z}\right) + \\
&\quad + \frac{\partial}{\partial y}\mu\left(\frac{\partial v}{\partial x} + \frac{\partial u}{\partial y}\right) + \frac{\partial}{\partial z}\mu\left(\frac{\partial u}{\partial z} + \frac{\partial w}{\partial x}\right) \\
\rho\frac{Dv}{Dt} &= \rho Y - \frac{\partial P}{\partial y} + \frac{2\partial}{3\partial y}\mu\left(\frac{\partial v}{\partial y} - \frac{\partial u}{\partial x}\right) + \frac{2\partial}{3\partial y}\mu\left(\frac{\partial v}{\partial y} - \frac{\partial w}{\partial z}\right) + \\
&\quad + \frac{\partial}{\partial x}\mu\left(\frac{\partial u}{\partial y} + \frac{\partial v}{\partial x}\right) + \frac{\partial}{\partial z}\mu\left(\frac{\partial v}{\partial z} + \frac{\partial w}{\partial y}\right) \\
\rho\frac{Dw}{Dt} &= \rho Z - \frac{\partial P}{\partial z} + \frac{2\partial}{3\partial z}\mu\left(\frac{\partial w}{\partial z} - \frac{\partial u}{\partial x}\right) + \frac{2\partial}{3\partial z}\mu\left(\frac{\partial w}{\partial z} - \frac{\partial v}{\partial y}\right) + \\
&\quad + \frac{\partial}{\partial y}\mu\left(\frac{\partial w}{\partial y} + \frac{\partial v}{\partial z}\right) + \frac{\partial}{\partial x}\mu\left(\frac{\partial w}{\partial x} + \frac{\partial u}{\partial z}\right)
\end{aligned}\right\} \quad 2.2.16$$

If one can justify the assumption that the terms arising from variable viscosity are small and can be neglected, (appendix A) the equations can be further reduced to the more familiar form:

$$\left.\begin{aligned}
\rho\frac{Du}{Dt} &= \rho X - \frac{\partial P}{\partial x} + \frac{1}{3}\mu\frac{\partial}{\partial x}\Delta + \mu\nabla^2 u \\
\rho\frac{Dv}{Dt} &= \rho Y - \frac{\partial P}{\partial y} + \frac{1}{3}\mu\frac{\partial}{\partial y}\Delta + \mu\nabla^2 v \\
\rho\frac{Dw}{Dz} &= \rho Z - \frac{\partial P}{\partial z} + \frac{1}{3}\mu\frac{\partial}{\partial z}\Delta + \mu\nabla^2 w
\end{aligned}\right\} \quad 2.2.17$$

where $\Delta = \frac{\partial u}{\partial x} + \frac{\partial v}{\partial y} + \frac{\partial w}{\partial z}$

2.2

$\nabla^2 = \frac{\partial^2}{\partial x^2} + \frac{\partial^2}{\partial y^2} + \frac{\partial^2}{\partial z^2}$, the Lapla cian operator.

The above equations are the well known Navier - Stokes equations of motion.

2.3 General Equation of Cont inuity.

This equation is the mathematical formulation of the principle of conservation of mass.

Referring again to fig. 2.2.1, let the fluid particle centred on P(x,y,z) be of density ρ and have a velocity $\underline{u}$. The flow into the parallelepiped in the x-direction in time δt is then given by

$$\left[\rho u - \tfrac{1}{2}\frac{\partial}{\partial x}(\rho u)\delta x \right]\delta y \delta z \delta t$$

Similarly the outflow through the opposite face is given by

$$\left[\rho u + \tfrac{1}{2}\frac{\partial}{\partial x}(\rho u)\delta x \right]\delta y \delta z \delta t$$

Hence the excess of outflow over inflow is

$$\frac{\partial}{\partial x}(\rho u)\delta x \delta y \delta z \delta t$$

with similar expressions for the other directions.

Now, the mass originally inside the volume is $\rho \delta x \delta y \delta z$, and equating the rate of change of this to the excess outflow gives

$$\left\{ \frac{\partial}{\partial x}(\rho u) + \frac{\partial}{\partial y}(\rho v) + \frac{\partial}{\partial z}(\rho w) \right\}\delta x \delta y \delta z \delta t = -\frac{\partial \rho}{\partial t}\delta x \delta y \delta z \delta t$$

2.3

$$\therefore \frac{\partial \rho}{\partial t} + \frac{\partial}{\partial x}(\rho u) + \frac{\partial}{\partial y}(\rho v) + \frac{\partial}{\partial z}(\rho w) = 0 \qquad 2.3.1$$

Performing the differentiation this can also be written as

$$\frac{D\rho}{Dt} + \rho \Delta = 0 \qquad 2.3.2$$

If the fluid is incompressible the equation of continuity takes the simpler form

$$\Delta = \frac{\partial u}{\partial x} + \frac{\partial v}{\partial y} + \frac{\partial w}{\partial z} = 0 \qquad 2.3.3$$

2.4 General Equation of State.

The equation of state is a relation between the density and the pressure and temperature at a point in a fluid, and may formally be indicated by

$$\rho = \rho(P,T)$$

In the case of an ideal gas the function $\rho(P,T)$ may be explicitly written as P/RT where R is the gas constant and which depends only upon the kind of gas.

In the case of most liquids ,however, no such simple mathematical form seems to exist and resort must therefore be made to various empirical relations. One way to do this is to assume that the density can be expressed as a polynomial in P and T, and determine the coefficients from measurements on the liquid.

Alternatively, the equation of state may be defined numerically by giving a table of ρ for various values of pressure and temperature obtained from measurements.

Many liquids are fairly incompressible and have a low expansioncoefficient. Then as a first approximation the density may be taken as being independant of pressure and temperature. In this case the equation of state reduce to the

2.5 General Equation connecting Viscosity with Pressure and Temperature.

This relation is analogous to the equation of state and may formally be indicated by

$\mu = \mu(P,T)$

where μ is the dynamic coefficient of viscosity.

no general theoretical expression for the viscosity of liquids seem to exist, although a number of empirical relations connecting viscosity with pressure and temperature have been proposed. A common feature of all these expressions is that they contain arbitrary coefficients which values must be determined from measurements made on the liquid in question.

The pressure and temperature range within which the expression used will yield reasonably accurate values depends to a large extent upon the liquid. At higher pressures a lubricating oil will tend to solidify, but this effect may be offset or reduced by increasing the lubricant temperature. Also the rate of shear the lubricant is subjected to may influence its properties to a large extent. At high rates of shear or shearstress the fluid may deviate from the newtonian, i.e. the shearstress may no longer be a linear function of velocity gradient. Various values for this critical shear-

2.5

stress are found in the literature, a typical value seems to be 500 000 dyn/cm^2 (7).

An equation that will be used in this work appears in (8), and is of the form

$$(\log_{10}\mu_{P,T})^2 = a(T)P + (\log_{10}\mu_{0,T})^2 \qquad 2.5.1$$

where

$\mu_{P,T}$ = viscosity at pressure P and temperature T, millipois

a(T) = function of temperature alone.

P = pressure above atmospheric, atm.

$\mu_{0,T}$ = viscosity at atm. pressure and temperature T, millipois

The above equation was found to be accurate to within a few percent for pressures less than 40 000 p.s.i. in the case of two lubricants supplied by the Thornton Research Centre (8). At higher pressures the equation tends to underestimate the viscosity.

If $(\log_{10}\mu_{P,T})^2$ is plotted against P, a family of straight lines is obtained, one line for each value of T. Furthermore, it is known (8) that all these lines will pass through one point, and hence the viscosity at any pressure and temperature may be obtained by drawing a straight line

2.5

through this point and the relevant value of $(\log_{10}\mu_{0,T})^2$ obtained from viscosity measurements on the lubricant at atmospheric pressure.

Under isothermal conditions a viscosity equation of the form

$$\mu = \mu_0 \exp(\alpha P) \qquad 2.5.2$$

will sometimes be used in the following, on account of its mathematical simplicity. The coefficients μ_0 and α are characteristics of the lubricant and must be determined by measurements.

The expression 2.5.2 agrees with eqn. 2.5.1 for small values of P, as can be seen from expanding the argument in a binomial series retaining only the first two terms.

2.6 The General Energyequation.

In a moving viscous fluid irreversible work will be done by the shearforces, and this work will appear in the fluid in the form of heat.

The energy equation express the energy balance, and is a formulation of the principle of conservation of energy.

Referring to fig. 2.2.1, consider the energy balance for the fluid element centred on P(x,y,z) moving with velocity components u,v,w in the x,y,z directions.

The rate at which work is done on the element by the bodyforces is

$$\rho\left[\, Xu + Yv + Zw \,\right] \qquad 2.6.1$$

Also, the rate at which work is being done by the surface stresses can be evaluated by considering the difference in the rate of work done on each of two parallel surfaces, neglecting small quantities of higher order.

Consider for the normal stress component in the x direction

$$-P_{xx}u\delta y\delta z + \left(P_{xx} + \frac{\partial P_{xx}}{\partial x}\delta x \right)\left(u + \frac{\partial u}{\partial x}\delta x \right)\delta y\delta z =$$

$$= \frac{\partial}{\partial x}\left(uP_{xx} \right)\delta x\delta y\delta z \qquad 2.6.2$$

and similarly for the other stresses.

2.6

Hence, the rate of work being done by the surface stresses becomes

$$\left\{ \frac{\partial}{\partial x}(uP_{xx} + vP_{xy} + wP_{xz}) + \frac{\partial}{\partial y}(uP_{yx} + vP_{yy} + wP_{yz}) + \right.$$

$$\left. + \frac{\partial}{\partial z}(uP_{zx} + vP_{zy} + wP_{zz}) \right\} \delta x \delta y \delta z \qquad 2.6.3$$

Expanding this and substituting for the stresses from eqn. 2.2.3

$$\left\{ -\rho(uX + vY + wZ) + \tfrac{1}{2}\rho \frac{D}{Dt}(u^2 + v^2 + w^2) - P\Delta + \right.$$

$$+ \mu \left[2(\frac{\partial u}{\partial x})^2 + 2(\frac{\partial v}{\partial y})^2 + 2(\frac{\partial w}{\partial z})^2 + (\frac{\partial u}{\partial y} + \frac{\partial v}{\partial x})^2 + (\frac{\partial v}{\partial z} + \frac{\partial w}{\partial y})^2 + \right.$$

$$\left. + (\frac{\partial u}{\partial z} + \frac{\partial w}{\partial x})^2 - \tfrac{2}{3}\Delta^2 \right] \delta x \delta y \delta z \qquad 2.6.4$$

The terms in the square bracket represent the irreversible friction work due to viscosity.

Defining a dissipation function

$$\Phi = \mu \left[2(\frac{\partial u}{\partial x})^2 + 2(\frac{\partial v}{\partial y})^2 + 2(\frac{\partial w}{\partial z})^2 + (\frac{\partial u}{\partial y} + \frac{\partial v}{\partial x})^2 + (\frac{\partial v}{\partial z} + \frac{\partial w}{\partial y})^2 + \right.$$

$$\left. + (\frac{\partial u}{\partial z} + \frac{\partial w}{\partial x})^2 - \tfrac{2}{3}\Delta^2 \right] \qquad 2.6.5$$

With this notation expression 2.6.4 becomes

$$\left\{ -\rho \underline{u} \cdot \underline{F} + \tfrac{1}{2}\rho \frac{D}{Dt}(\underline{u} \cdot \underline{u}) - P\Delta \right\} \delta V \qquad 2.6.6$$

2.6

where $\underline{u}$ is the velocity field

$\underline{F}$ is the force field due to the bodyforces.

In addition to energy supplied to the fluid element by work done upon it, energy is also supplied by conduction and convection neglecting radiation which is negligable exept for very high temperatures.

The rate of energy supplied by conduction is

$$K\nabla^2 T \delta V \qquad 2.6.7$$

where K is the coefficient of thermal conductivity.

Similarly the rate of convection of kinetic and internal energy is

$$-\left\{ \frac{\partial}{\partial x}[\ \rho u(\ KE + E\ )] + \frac{\partial}{\partial y}[\ \rho v(\ KE + E\ )] + \frac{\partial}{\partial z}[\ \rho w(\ KE + E)] \right\}\delta V \qquad 2.6.8$$

where

KE = kinetic energy/unit volume = $\frac{1}{2}(\ \underline{u}\cdot\underline{u})$

E = internal energy/unit volume = cT where c is the specific heat of the fluid.

Equating the rate of energy supplied to the element by 2.6.1, 2.6.6, 2.6.7, 2.6.8 to the rate of increase of kinetic and internal energy within the element:

2.6

$$\Big\{ \rho(Xu + Yv + Zw) - \rho(Xu + Yv + Zw) + \tfrac{1}{2}\rho\frac{D}{Dt}(u^2 + v^2 + w^2) -$$

$$-P\Delta + \Phi + K\nabla^2T - \Big[\frac{\partial}{\partial x}(\rho u(KE + E)] + \frac{\partial}{\partial y}[\rho v(KE + E)] +$$

$$+ \frac{\partial}{\partial z}[\rho w(KE + E)] \Big] \Big\} \delta V = \frac{\partial}{\partial t}[\rho(KE + E)] \delta V \qquad 2.6.9$$

Rearranging the terms and remembering that from continuity

$$\frac{\partial}{\partial x}(\rho u) + \frac{\partial}{\partial y}(\rho v) + \frac{\partial}{\partial z}(\rho w) = -\frac{\partial \rho}{\partial t}$$

the energy equation finally becomes

$$\rho\frac{DE}{Dt} = -P\Delta + K\nabla^2T + \Phi \qquad 2.6.10$$

Initial and boundary conditions to eqn. 2.6.10 are

$T = T_0 = f(x,y,z)$ at $t = 0$

Where the fluid meets up with another substance, and assuming that heat transfer across the boundary takes place by conduction only, and denoting the normal to the boundary at the point by n we have

$$K\frac{\partial T}{\partial n} = K_b\frac{\partial T_b}{\partial n}$$

where suffix b refer to substance on the other side of the boundary.

Two limiting conditions can here be recognized. One is

2.6

characterized by letting $K = K_b \to \infty$.˙. $T \to T_0$

$t > 0$. This is the isothermal condition.

The other is obtained by putting $K\frac{\partial T}{\partial n} = 0$; $t > 0$

This may be termed the adiabatic condition. All heat developed in the fluid stays there and goes to increase the temperature.

2.7 The General Elastic Equation.

The derivation of the equation of motion for a homogeneous, isotropic, elastic solid is completely analogous to that given for a fluid in section 1.2, and the equation of motion or equilibrium in the x direction is

$$\rho\frac{Du}{Dt} = \rho X + \frac{\partial P_{xx}}{\partial x} + \frac{\partial P_{yx}}{\partial y} + \frac{\partial P_{zx}}{\partial z} \qquad 2.7.1$$

where the symbols u, v, w have now been redefined to mean displacements in the x, y, z directions respectively.

As before a hypothesis connecting stresses and strains is needed and this is provided by Hookes law which states:

$$\left.\begin{aligned} \epsilon_x &= \frac{1}{E}[\, P_{xx} - \nu(\, P_{yy} + P_{zz}\,)] \\ \epsilon_y &= \frac{1}{E}[\, P_{yy} - \nu(\, P_{xx} + P_{zz}\,)] \\ \epsilon_z &= \frac{1}{E}[\, P_{zz} - \nu(\, P_{xx} + P_{yy}\,)] \end{aligned}\right\} \qquad 2.7.2$$

where

E = Youngs modulus for material

ν = Poissons ratio for material

and as previously

$$\epsilon_x = \frac{\partial u}{\partial x} \quad ; \quad \epsilon_y = \frac{\partial v}{\partial y} \quad ; \quad \epsilon_z = \frac{\partial w}{\partial z}$$

$$\gamma_{xy} = (\frac{\partial u}{\partial y} + \frac{\partial v}{\partial x}\,); \quad \gamma_{xz} = (\frac{\partial u}{\partial z} + \frac{\partial w}{\partial x}\,); \quad \gamma_{yz} = (\frac{\partial v}{\partial z} + \frac{\partial w}{\partial y}\,)$$

$$P_{xy} = G\gamma_{xy} \; ; \; P_{xz} = G\gamma_{xz} \; ; \; P_{yz} = G\gamma_{yz} \qquad 2.7.3$$

2.7

where

G = modulus of rigidity = $\frac{E}{2(1+\nu)}$

Eliminating the stress components in 2.7.1 by using Hookes lew and expressing the stress components in terms of displacements neglecting inertia- and bodyforces gives the equation of equilibrium in terms of displacements i.e.

$$\left.\begin{aligned}(\lambda + G)\frac{\partial \Delta}{\partial x} + G\nabla^2 u &= 0\\ (\lambda + G)\frac{\partial \Delta}{\partial y} + G\nabla^2 v &= 0\\ (\lambda + G)\frac{\partial \Delta}{\partial z} + G\nabla^2 w &= 0\end{aligned}\right\} \qquad 2.7.4$$

where

$$\lambda = \frac{\nu E}{(1+\nu)(1-2\nu)}$$

$$\Delta = \frac{\partial u}{\partial x} + \frac{\partial v}{\partial y} + \frac{\partial w}{\partial z}$$

A general solution to eqn. 2.7.4 is

$$\left.\begin{aligned}u &= \phi_1 - \frac{1}{4(1-\nu)}\frac{\partial}{\partial x}(\phi_0 + x\phi_1 + y\phi_2 + z\phi_3)\\ v &= \phi_2 - \frac{1}{4(1-\nu)}\frac{\partial}{\partial y}(\phi_0 + x\phi_1 + y\phi_2 + z\phi_3)\\ w &= \phi_3 - \frac{1}{4(1-\nu)}\frac{\partial}{\partial z}(\phi_0 + x\phi_1 + y\phi_2 + z\phi_3)\end{aligned}\right\} \qquad 2.7.5$$

where the ϕ_i are harmonic functions i.e. satisfies

$\nabla^2 \phi_i = 0$; $i = 0,1,2,3$

2.7

Suppose that a concentrated normal force F is applied at the origen of a semi infinite elastic body bounded by the plane z = 0.

Symmetry suggest that one can take $\phi_1 = \phi_2 = 0$, hence the solution to the equation of equilibrium becomes

$$\left.\begin{aligned} u &= -\frac{1}{4(1-\nu)}\frac{\partial}{\partial x}(\phi_0 + z\phi_3) \\ v &= -\frac{1}{4(1-\nu)}\frac{\partial}{\partial y}(\phi_0 + z\phi_3) \\ w &= -\frac{1}{4(1-\nu)}\frac{\partial}{\partial z}(\phi_0 + z\phi_3) + \phi_3 \end{aligned}\right\} \qquad 2.7.6$$

The associated stress pattern then becomes

$$P_{xx} = \frac{G}{2(1-\nu)}\left[2\nu\frac{\partial\phi_3}{\partial z} - \frac{\partial^2\phi_0}{\partial x^2} - z\frac{\partial^2\phi_3}{\partial x^2} \right] \qquad 2.7.7$$

with similar equations for P_{yy} and P_{zz}

$$\left.\begin{aligned} P_{xy} &= \frac{-G}{2(1-\nu)}\left[\frac{\partial^2\phi_0}{\partial x\partial y} + z\frac{\partial^2\phi_3}{\partial x\partial y} \right] \\ P_{xz} &= \frac{-G}{2(1-\nu)}\left[\frac{\partial^2\phi_0}{\partial x\partial z} + z\frac{\partial^2\phi_3}{\partial x\partial z} - (1-2\nu)\frac{\partial\phi_3}{\partial x} \right] \\ P_{zy} &= \frac{-G}{2(1-\nu)}\left[\frac{\partial^2\phi_0}{\partial y\partial z} + z\frac{\partial^2\phi_3}{\partial y\partial z} - (1-2\nu)\frac{\partial\phi_3}{\partial y} \right] \end{aligned}\right\} \qquad 2.7.8$$

Boundary conditions demand that on the surface

$z = 0 \; ; \; P_{zz} = P_{zx} = P_{zy} = 0$

2.7

Taking

$\frac{\partial \phi_0}{\partial z} = (1 - 2\nu) \phi_s$; P_{zx} and P_{zy} becomes zero at $z = 0$

Choosing for the function ϕ_s the harmonuc $\frac{A}{R}$, where $R^2 = x^2 + y^2 + z^2$; A constant, P_{zz} likewise vanish at $z = 0$ Hence the boundary conditions are satisfied.

In order to determine the constant A, consider the equilibrium of a small cylindrical disc having the z axis as its symmetry axis and of thickness c and radius a. The shear stresses vanish in the limit $c \to 0$, hence

$$F = -\int_0^a 2\pi r P_{zz} dr \quad ; \quad r^2 = x^2 + y^2 \qquad 2.7.9$$

$$\therefore F = -\int_0^a 2\pi \frac{Gr}{2(1-\nu)R^5} 3z^2 \, dr = \frac{A\pi G}{1-\nu}$$

$$\therefore A = \frac{1-\nu}{\pi G} F$$

Hence, the vertical displacement at the surface corresponding to this value of ϕ_s is

$$w_{z=0} = \frac{(1 - \nu^2) F}{\pi E r} \qquad 2.7.10$$

In the case where a distrubeted load or pressure is applied, the deformation of the surface is obtained from the a bove equation by superposition, and is given by

2.7

$$w_{z=0} = \delta = \frac{1-\nu^2}{\pi E}\int\int\frac{P(x,y)}{r}dydx \qquad 2.7.11$$

where the integration extends over the whole of the pressure distribution.

In a different coordinate system x',y', specified by the coordinate transform

$$x' = \xi + x$$

$$y' = \eta + y$$

$$z' = z$$

equation 2.7.11 becomes

$$\delta = \frac{1-\nu^2}{\pi E}\int\int\frac{P(x',y')dx'dy'}{\sqrt{(x'-\xi)^2+(y'-\eta)^2}} \qquad 2.7.12$$

where again the integration extends over the whole of the pressure distribution.

In the two dimensional case the pressure must be regarded as a function of x' only, and the deformation must be independant of the η coordinate.

Considering therefore the deformation due to a pressure distribution over a rectangle $x' = \pm\alpha$; $y' = \pm\beta$

we have

2.7

$$\delta = \frac{1 - \nu^2}{\pi E} \int_{-\alpha}^{\alpha} \int_{-\beta}^{\beta} \frac{P(x')\, dx'dy'}{\sqrt{(x'-\xi)^2 + y'^2}}$$

$$= \frac{2(1 - \nu^2)}{\pi E} \int_{-\alpha}^{\alpha} P(x') \ln \frac{\beta + \sqrt{(x' - \xi)^2 + \beta^2}}{(x' - \xi)} dx' \qquad 2.7.13$$

Assuming now that $\beta \gg |x - \xi|$ and that the term $(x - \xi/\beta)^2$ is negligable compared to unity, we have

$$\delta = \frac{2(1 - \nu^2)}{\pi E} \int_{-\alpha}^{\alpha} P(x') \ln \frac{2\beta}{(x-\xi)} dx'$$

$$= \frac{2(1 - \nu^2)}{\pi E} \ln 2\beta \int_{-\alpha}^{\alpha} P(x')dx' - \frac{2(1 - \nu^2)}{\pi E} \int_{-\alpha}^{\alpha} P(x') \ln|x' - \xi| dx' \qquad 2.7.14$$

The first integral is the total load on the material. Thus if W' denotes the total load and W the total load per unit length in the y' direction, we have

$$W = \frac{W'}{2\beta} = \int_{-\alpha}^{\alpha} P(x')dx'$$

If a positive pressure P(x') is applied, the integral can not vanish. Therefore if β is infinite W' must be infinite, but W may be finite. The whole term, however, is infinite due to the factor $\ln(2\beta)$. This result is not unexpected since the material was assumed to extend to infinity in the -z direction.

The change of shape of the surface z = 0 is due entirely to the second term in 2.7.14. Discarding the infinite constant

2.7

we have

$$\delta = -\frac{2(1-\nu^2)}{\pi E}\int_{-\infty}^{\infty} P(x')\ln|x'-\xi|dx' \qquad 2.7.15$$

and this will be denoted the local deformation.

Writing $x' - \xi = r$, we have

$$\delta = -\frac{2(1-\nu^2)}{\pi E}\int_{\Omega} P \ln(r)dr \qquad 2.7.16$$

If the undeformed filmshape is given by the equation

$$h = f(x) + h_o$$

then after undergoing deformation the filmshape is specified by

$$h = H + f(x) + \lambda\int_{\Omega} P(x')\ln|x'-x|dx' \qquad 2.7.17$$

where H is an arbitrary consta nt which is so chosen that the filmthickness at some given point has a specified value. Eg. if the central filmthickness shall have the value h_o then clearly

$$H = h_o - \lambda\int_{\Omega} P(x')\ln(x')dx'$$

If both the boundary surfaces are deformed, and the materials are specified by the elastic properties E_1, ν_1 and E_2, ν_2, then

2.7

$$\lambda = -\frac{2}{\pi}\left[\frac{1-\nu_1^2}{E_1} + \frac{1-\nu_2^2}{E_2}\right] \qquad 2.7.18$$

The calculation of filmthickness is based on eqn. 2.7.17.

2.8 Additional Assumptions and Simplified Equations of Motion.

The equations governing the motion of the fluid derived in the preceding sections are much too general to be solved directly.

In order to simplify and reduce these equations to a more manageable form, additional assumptions are introduced. The purpose of this section is to state these assumptions and give some justification for introducing them.

A1 The motion will be considered to take place in a two dimensional space only.

A2 The terms arising from the inertia of the fluid in the momentum equation are small compared to the viscous terms and may be neglected.

A3 The terms due to external bodyforces acting on the fluid are small compared to the viscous terms and may be neglected.

A4 No temperature gradient exists across the film.

Mathematically the assumption A1 means that with the previous definition of the coordinate system one may put

2.8

$$w = \frac{\partial^n}{\partial z^n} = 0$$

The physical interpretation is that no velocities nor any gradients exists in the z direction, or as an approximation that these gradients are small and can be neglected compared with corresponding gradients in other coordinate directions. This condition is fulfilled if the dimensions in the z direction are large compared with the x and y dimensions. This condition may not be met in the present problem and hence solutions obtained using A1 may not give a true description of the flow.

The component of the inertia force in the x direction is given by

$$\rho\frac{Du}{Dt} = \rho\left\{ \frac{\partial u}{\partial t} + u\frac{\partial u}{\partial x} + v\frac{\partial u}{\partial y} \right\}$$

and this is of order of magnitude $\frac{\rho V^2 x}{h^2}\left\{ 1 - \frac{x}{2h}\frac{\partial h}{\partial x} \right\}$

where V is the velocity of approach.

The corresponding viscous forces are

$$\mu\nabla^2 u = \mu\left\{ \frac{\partial^2 u}{\partial x^2} + \frac{\partial^2 u}{\partial y^2} \right\}$$

and this is of the order of $12\mu\frac{Vx}{h^2}$.

The ratio of the inertia forces to the viscous forces known as the Reynolds number R_e then becomes

2.8

$$R_e \geq \frac{\rho V h}{12\mu}\left(1 - \frac{x}{2h}\frac{\partial h}{\partial x}\right)$$

Under conditions where we have $R_e \ll 1$ the introduction of assumption A2 may not cause great error on the solutions.

Similarly the influence of the bodyforces may be investigated. The only bodyforce assumed present is gravity acting in the -y direction. The order of magnitude of the ratio of the bodyforce to the viscous forces is

$$\frac{\rho g h^2}{12\mu V x}$$

and if the order of magnitude of this quantity is small compared with unity, bodyforces may be neglected.

Taking account of A1, A2 and A3 the momentum equation 2.2.17 reduce to

$$\left.\begin{aligned} \frac{\partial P}{\partial x} &= \tfrac{1}{3}\mu\frac{\partial}{\partial x}\Delta + \mu\nabla^2 u \\ \frac{\partial P}{\partial y} &= \tfrac{1}{3}\mu\frac{\partial}{\partial y}\Delta + \mu\nabla^2 v \end{aligned}\right\} \qquad 2.8.1$$

2.9 Solution of the Equations of Motion in Bipolar Coordinates.

Investigating the case of motion of an incompressible fluid of constant viscosity, bounded by rigid surfaces, the momentum equation takes the form (fig. 2.9.1)

$$\frac{\partial P}{\partial x} = \frac{1}{3}\mu\frac{\partial}{\partial x}\Delta + \mu\nabla^2 u \qquad 2.9.1$$

$$\frac{\partial P}{\partial y} = \frac{1}{3}\mu\frac{\partial}{\partial y}\Delta + \mu\nabla^2 v \qquad 2.9.2$$

and the equation of continuity becomes

$$\frac{\partial u}{\partial x} + \frac{\partial v}{\partial y} = 0 \qquad 2.9.3$$

Now introducing the Lagrangian streamfunction ψ defined in the usual way by

$$u = -\frac{\partial \psi}{\partial y} \; ; \quad v = \frac{\partial \psi}{\partial x} \qquad 2.9.4$$

the continuity equation is satisfied.

Differentiating .1 and .2 by y and x respectively, subtracting and substituting the relation .4, we obtain

$$\nabla^4 \psi = 0 \qquad 2.9.5$$

i.e. the streamfunction is a solution of the biharmonic equation.

Differentiating .1 and .2 by x and y respectively and adding

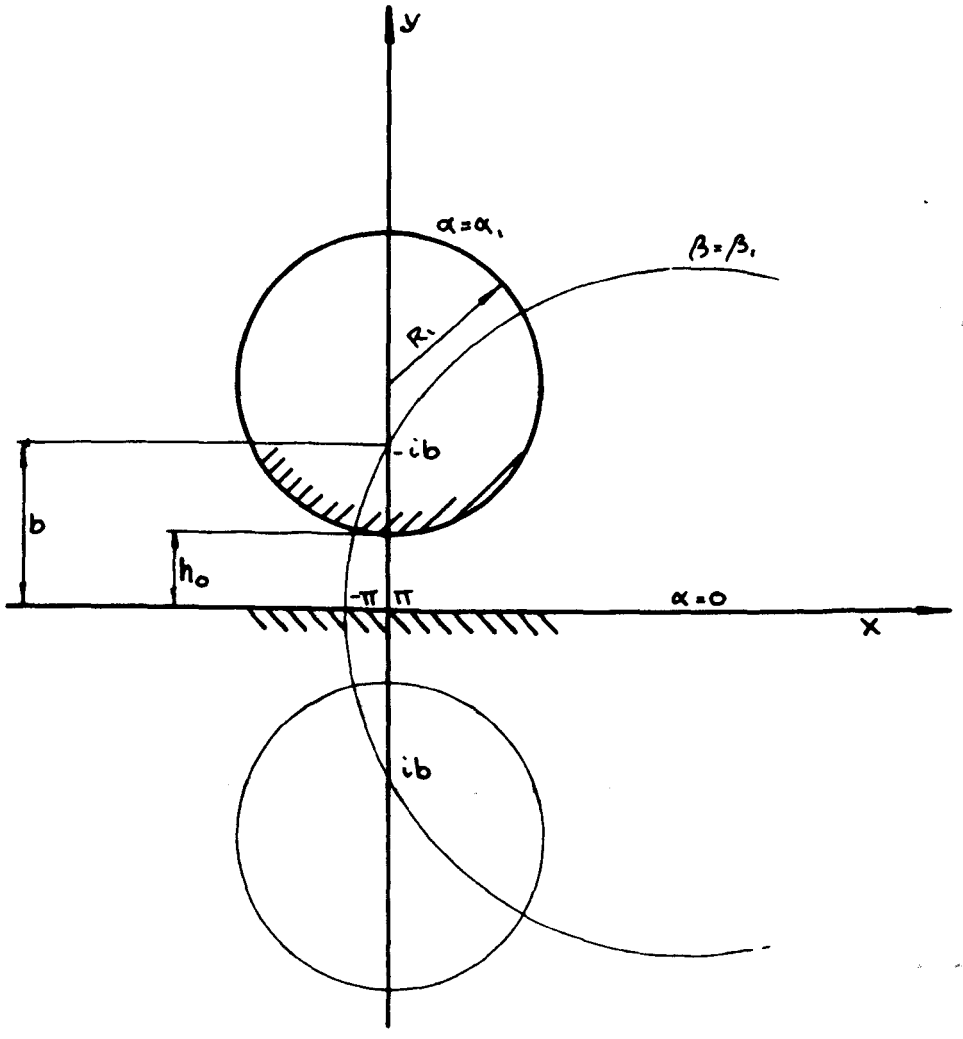

BIPOLAR COORDINATES

FIG 2·9·1

2.9

we get on account of .4

$$\nabla^2 P = 0 \qquad 2.9.6$$

Defining the vorticity

$$\zeta = \frac{\partial v}{\partial x} - \frac{\partial u}{\partial y} = \nabla^2 \psi \qquad 2.9.7$$

we have

$$\nabla^2 \zeta = 0 \qquad 2.9.8$$

i.e. the pressure and vorticity are conjugate harmonic functions.

The problem is now reduced to finding solutions of .5 satisfying the boundary conditions.

For the geometry in this problemit will be convenient to employ bipolar coordinates defined by

$$z = ib \operatorname{cath}\tfrac{1}{2}\xi \qquad 2.9.9$$

$$z = x + iy \; ; \quad \xi = \alpha + i\beta \qquad 2.9.10$$

Solving for ξ

$$\xi = \ln \frac{z + ib}{z - ib} \qquad 2.9.11$$

and separating real and imaginary parts

$$x = \frac{b \sin\beta}{\cosh\alpha - \cos\beta} \qquad 2.9.12$$

$$y = \frac{b \sinh\beta}{\cosh\alpha - \cos\beta} \qquad 2.9.13$$

2.9

and defining the transformation parameter

$$bK = \cosh\alpha - \cos\beta \qquad 2.9.14$$

Now, let one cylinder be represented by the equation

$\alpha = \alpha_1$

and the other cylinder by $\alpha = \alpha_2 = 0$

Then if R_1 and R_2 is the radius of the first and second cylinder respectively and D_1 and D_2 the distance of their centres from the origin, we have

$$R_1 = \frac{b}{\sinh\alpha_1} \; ; \qquad R_2 = \frac{b}{\sinh\alpha_2} = \infty \qquad 2.9.15$$

$$D_1 = R_1 + h_0 = \frac{b}{\tanh\alpha_1} ; \qquad D_2 = \frac{b}{\tanh\alpha_2} = \infty \qquad 2.9.16$$

Now, in bipolar coordinates the Laplacian becomes

$$\nabla^2 = K^2\left(\frac{\partial^2}{\partial\alpha^2} + \frac{\partial^2}{\partial\beta^2}\right) \qquad 2.9.17$$

and on changing the dependant variable from ψ to $K\psi$ we have

$$b\nabla^2\psi = \left\{ K\left(\frac{\partial^2}{\partial\alpha^2} + \frac{\partial^2}{\partial\beta^2}\right) - 2\sinh\alpha\frac{\partial}{\partial\alpha} - 2\sin\beta\frac{\partial}{\partial\beta} + \right.$$

$$\left. + \cosh\alpha + \cos\beta \right\}(K\psi) \qquad 2.9.18$$

Applying the operator again we get for the biharmonic

$$\nabla^4\psi = \left\{ \frac{\partial^4}{\partial\alpha^4} + 2\frac{\partial^4}{\partial\alpha^2\partial\beta^2} - 2\frac{\partial^2}{\partial\alpha^2} + 2\frac{\partial^2}{\partial\beta^2} + \frac{\partial^4}{\partial\beta^4} + 1 \right\}(K\psi) = 0 \qquad 2.9.19$$

2.9

which is a linear equation with constant coefficients.

The coordinate β has a finite discontinuity of 2π on the line $x = 0$. The pressure, however, is a continous function and moreover must be symmetrical about $x = 0$. Seeking solutions that are periodic in 2π and which will give a symmetric pressure distribution, we are interested in solutions of the form

$$K\psi = f(\alpha)\sin(n\beta) \qquad 2.9.20$$

Assuming a solution of this form, the equation for $f(\alpha)$ becomes

$$\left\{ \frac{\partial^4}{\partial\alpha^4} - 2(n^2 + 1)\frac{\partial^2}{\partial\alpha^2} + (n^2 - 1)^2 \right\} f(\alpha) = 0 \qquad 2.9.21$$

Assuming solutions of the form $f(\alpha) = e^{n\alpha}$ we obtain

$$f(\alpha) = A_n\cosh(n+1)\alpha + B_n\cosh(n-1)\alpha + C_n\sinh(n+1)\alpha + D_n\sinh h(n-1)\alpha \qquad n \geqslant 2 \qquad 2.9.22$$

For $n = 1$ the solution becomes

$$f(\alpha) = A_1\cosh 2\alpha + B_1 + C_1\sinh 2\alpha + D_1\alpha \qquad 2.9.23$$

and for $n = 0$

$$f(\alpha) = A_0\cosh\alpha + B_0\alpha\cosh\alpha + C_0\sinh\alpha + D_0\alpha\sinh\alpha \qquad 2.9.24$$

Hence the complete solution is given by

$$K\psi = (A_o + B_o\alpha)\cosh\alpha + (C_o + D_o\alpha)\sinh\alpha +$$
$$+ \left\{ A_1\cosh 2\alpha + B_1 + C_1\sinh 2\alpha + D_1\alpha \right\}\sin\beta +$$
$$+ \sum_{n=2}\sin(n\beta) \left\{ A_n\cosh(n+1)\alpha + B_n\cosh(n-1)\alpha + \right.$$
$$\left. + C_n\sinh(n+1)\alpha + D_n\sinh(n-1)\alpha \right\} \qquad 2.9.25$$

The vorticity is given by

$$b\zeta = \left\{ (\cosh\alpha - \cos\beta)\left(\frac{\partial^2}{\partial\alpha^2} + \frac{\partial^2}{\partial\beta^2} \right) - 2\sinh\alpha\frac{\partial}{\partial\alpha} - \right.$$
$$\left. - 2\sin\beta\frac{\partial}{\partial\beta} + \cosh\alpha + \cos\beta \right\}(K\psi) \qquad 2.9.26$$

Now, from reasons of symmetry it will be seen that terms arising from n = 0 must vanish. Furthermore we will assume that a solution can be obtained using only the terms arising from n = 1. Thus we have

$$K\psi = \left\{ A_1\cosh 2\alpha + B_1 + C_1\sinh 2\alpha + D_1\alpha \right\}\sin\beta \qquad 2.9.27$$

$$b\zeta = 4(C_1\sinh\alpha + A_1\cosh\alpha)\sin\beta -$$
$$- (C_1\sinh 2\alpha + A_1\cosh 2\alpha)\sin 2\beta \qquad 2.9.28.$$

The pressure can now be determined with the aid of the Ca uchy - Riemann equations, since pressure and vorticity are conjugate functions.

$$bP = b\int\frac{\partial\zeta}{\partial\alpha}d\beta + C$$

$$\therefore bP = C - 4(C_1\cosh\alpha + A_1\sinh\alpha)\cos\beta + $$

$$+ (C_1\cosh 2\alpha + A_1\sinh 2\alpha)\cos 2\beta \qquad 2.9.29$$

where C is an arbitrary constant .

Now, if v_α and u_β are the component velocities of the fluid in the positive direction of α and β(fig. 2.9.2) we have

$$\left.\begin{aligned} v_\alpha &= -K\frac{\partial\psi}{\partial\beta} = -\frac{\partial}{\partial\beta}(K\psi) + \frac{(K\psi)}{bK}\sin\beta \\ u_\beta &= K\frac{\partial\psi}{\partial\alpha} = \frac{\partial}{\partial\alpha}(K\psi) - \frac{(K\psi)}{bK}\sinh\alpha \end{aligned}\right\}$$

$$v_\alpha = (A_1\cosh 2\alpha + B_1 + C_1\sinh 2\alpha + D_1\alpha) \frac{1 - \cosh\alpha\cos\beta}{\cosh\alpha - \cos\beta}$$

$$u_\beta = \left\{(2A_1\sinh 2\alpha + 2C_1\cosh 2\alpha + D_1) - \right. \qquad 2.9.30$$

$$\left. - (A_1\cosh 2\alpha + B_1 + C_1\sinh 2\alpha + D_1\alpha) \frac{\sinh\alpha}{\cosh\alpha - \cos\beta}\right\}\sin\beta$$

Consider the system at an instant when the surface $\alpha = 0$ coincide with the x axis as shown in fig. 2.9.1.

The boundary conditions are:

1. On $\alpha = 0$, $u_\beta = 0$
2. On $\alpha = \alpha_1$, $u_\beta = 0$

} Hypothesis of no slip

3. The relative velocity of approach of the two surfaces $\alpha = \alpha_1$ and $\alpha = 0$ is V

Substituting B.C.1. gives $2C_1 + D_1 = 0$

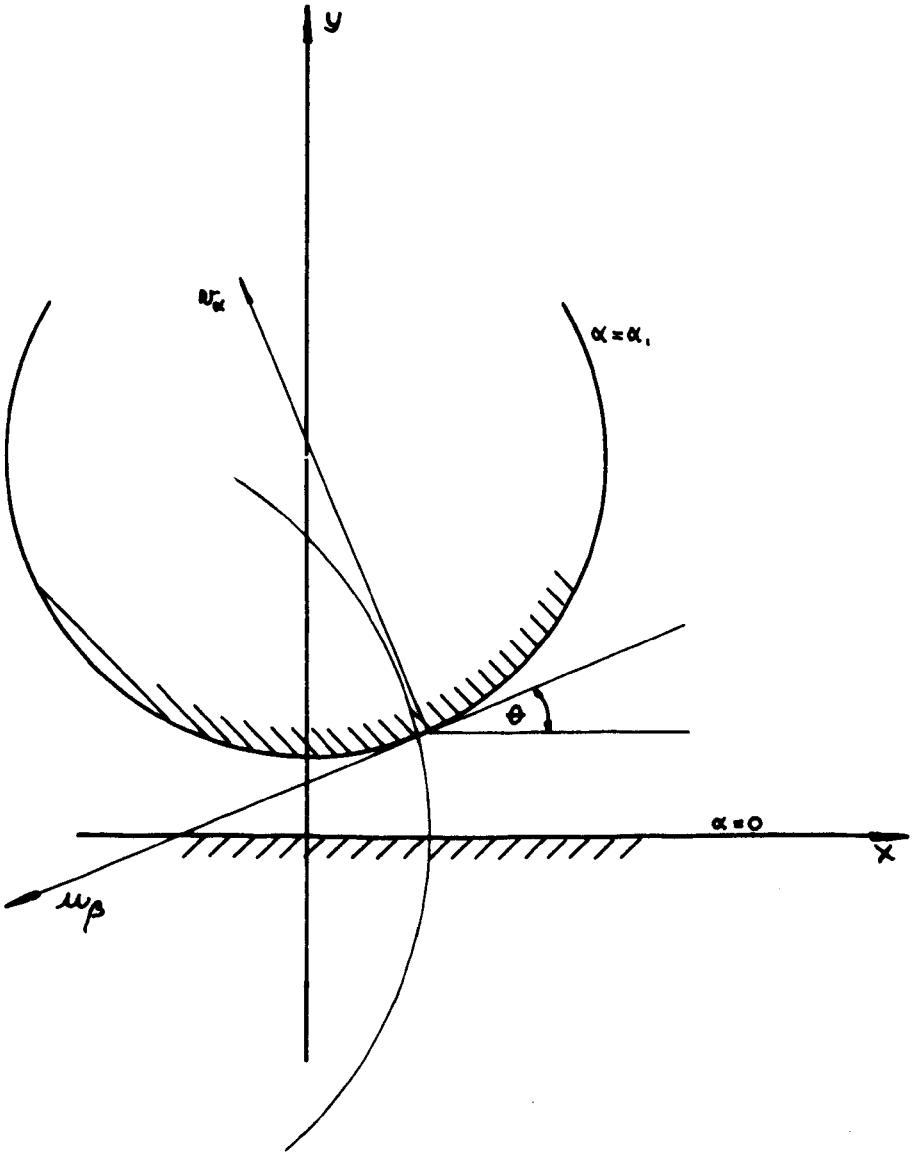

FIG 2·9·2

2.9

B.C.2 gives two relations for the constants, namely

$$(2A_1\sinh 2\alpha_1 + 2C_1\cosh 2\alpha_1 - 2C_1)\cosh\alpha_1 -$$

$$- (A_1\cosh 2\alpha_1 + B_1 + C_1\sinh 2\alpha_1 - 2C_1\alpha_1)\sinh\alpha_1 = 0$$

$$2A_1\sinh 2\alpha_1 + 2C_1\cosh 2\alpha_1 - 2C_1 = 0$$

$$\therefore A_1 = C_1\frac{1 - \cosh 2\alpha_1}{\sinh 2\alpha_1} \qquad 2.9.31$$

$$B_1 = C_1\left[\frac{1 - \cosh 2\alpha_1}{\sinh 2\alpha_1} + 2\alpha_1\right] \qquad 2.9.32$$

The velocity of the lower cylinder $\alpha = 0$ is

$$v_{\alpha=0} = A_1 + B_1 = 2C_1\left[\frac{1 - \cosh 2\alpha_1}{\sinh 2\alpha_1} + \alpha_1\right]$$

At the top surface $\alpha = \alpha_1$ we get

$$v_{\alpha=\alpha_1} = 0$$

and since we also have $u_\beta = 0$, the fluid velocity at this surface is zero. Hence, in order to satisfy B.C.3 we must take $v_{\alpha=0} = V$.

$$\therefore C_1 = \tfrac{1}{2}V\frac{\sinh 2\alpha_1}{1 - \cosh 2\alpha_1 + \alpha_1\sinh 2\alpha_1} \qquad 2.9.33$$

Now, from previous we have the relations

$$\sinh\alpha_1 = \frac{b}{R_1} \; ; \quad \tanh\alpha_1 = \frac{b}{R_1 + h_0}$$

$$\therefore \cosh\alpha_1 = 1 + \frac{h_0}{R_1}$$

2.9

Expanding the cosh, we have

$$\cosh\alpha_1 = 1 + \frac{\alpha_1^2}{2!} + \frac{\alpha_1^4}{4!} + \cdots + = 1 + \frac{h_0}{R_1}$$

Since $\frac{h_0}{R_1}$ is small, the value of $\cosh\alpha_1$ will be nearly 1. Taking therefore only the first two terms in the expansion we get

$$\alpha_1^2 \sim \frac{2h_0}{R_1} \quad ; \therefore \alpha_1 = \sqrt{\frac{2h_0}{R_1}}$$

Similarly ex panding the sinh, and neglecting terms of α_1^2 and higher

$$b = R\alpha_1 = \sqrt{2h_0R_1}$$

and to the same approximation

$$\cosh 2\alpha_1 = 1 + \frac{4h_0}{R_1}$$

In this work the order of magnitude of the parameter h_0/R_1 is $2\cdot10^{-4}$

Hence we have the inequalities

$$1.0000 \leqslant \cosh\alpha \leqslant 1.0002 \qquad \alpha \leqslant \alpha_1$$

Hence, by taking $\cosh\alpha \sim 1$, errors of less than 0.1% are introduced.

To the same order of approximation we also have

2.9

$A_1 = - C_1\alpha_1$

and since $\sinh\alpha \leqslant \alpha_1$ we have for terms such as $A_1\sinh\alpha \sim C_1\alpha_1^2$ which are small and may be neglected in comparison with terms of the form $C_1\cosh\alpha$.

Similarly, for the coefficient C_1, we get

$$C_1 \sim \frac{3V}{2\alpha_1^3}$$

Taking account of this and also determining the constant C such that the pressure will va nish at infinity, the expression for the pressure becomes

$$bP = \frac{3V}{\alpha_1^3}\left[\ 3 + \cos2\beta - 4\cos\beta\ \right]$$

$$\therefore\ P = \frac{3VR\mu}{2h\delta^2}(\ \cos\beta - 1\ )^2 \qquad 2.9.34$$

The load supported by the film is the integral over the pressure distribution.

$$\therefore\ W = \frac{3VR\mu}{h\delta^2} b \int_{\pi}^{0} (\ \cos\beta - 1\ )d\beta$$

$$= \frac{3\pi\sqrt{2}\mu VR^{3/2}}{h\delta^{3/2}} \qquad 2.9.35$$

Now, we previously had

$$x = \frac{b\ \sin\beta}{\cosh\alpha - \cos\beta}$$

and to the same approximation as previously this may be written as

2.9

$$\cos\beta - 1 \sim -\frac{2b^2}{x^2 + b^2}$$

Sub stituting this into eqn. 2.9.34, the pressure is transformed (approximately) into cartesian coordinates

$$\therefore\ P = \frac{6\mu VR}{(h_0 + x^2/2R)^2} = \frac{6\mu VR}{h^2} \qquad 2.9.36$$

This result shows that to the given approximation the pressure is constant across the film. Furthermore, it is seen tha t the pressure has an appreciable value only on a narrow zone centred on the line x = 0, and that within this zone the approximation to the geometry $h = h_0 + x^2/2R$ is acceptable. Geometrically this is equivalent to replacing the circular cylinder with part of a parabolic cylinder.

By calculating the cartesian approximations to the velocity components u and v, and then differentiating these twice w.r.t. x and y, we may show that

$$\frac{\partial^2 u}{\partial x^2} \simeq 0 \simeq \frac{\partial^2 v}{\partial x^2} \simeq 0 \simeq \frac{\partial^2 v}{\partial y^2} < \frac{\partial^2 u}{\partial y^2}$$

confirming a result obtained by means of a order ofmagnitude analysis.

2.10 Solution of the Equations of Motion of a Compressible Fluid with Variable Viscosity.

The solution arrived at in the previous section is only valid for an incompressible fluid having a constant viscosity and confined within rigid boundaries. In this section the restrictions on the physical properties of the fluid will be removed.

If we assume that the general conclusions drawn at the end of the previous section, i.e. that the terms $\partial^2u/\partial x^2$; $\partial^2v/\partial x^2$; $\partial^2v/\partial y^2$ are sufficiently small to be neglected in comparison with $\partial^2u/\partial y^2$, that the main pressures are confined to a narrow strip at the centre and that the pressure does not vary appreciably across the film, then in view of the assumption that temperatures are not varying across the film, the fluid properties, density and viscosity will not be functions of y.

The momentum equation in cartesian coordinates then take the form (fig. 2.10.1)

$$\frac{\partial P}{\partial x} = \frac{1}{3}\mu\frac{\partial}{\partial x}\Delta + \mu\frac{\partial^2 u}{\partial y^2} \qquad 2.10.1$$

where Δ is a term arising from compressibility and is given by

$$\Delta = \frac{\partial u}{\partial x} + \frac{\partial v}{\partial y}$$

$$\therefore \frac{\partial}{\partial x}\Delta = \frac{\partial^2 u}{\partial x^2} + \frac{\partial^2 v}{\partial x \partial y}$$

and this is of the order of magnitude of terms previously

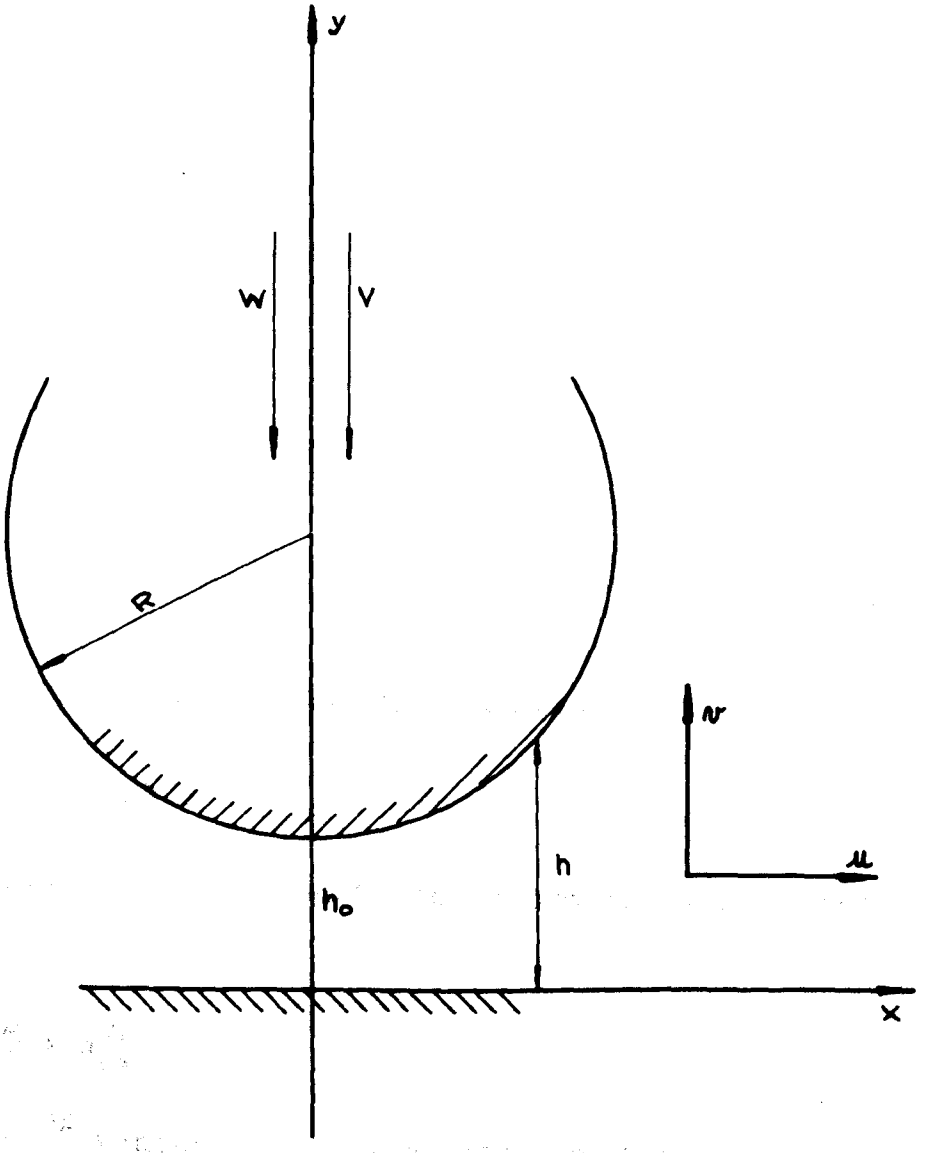

COORDINATES

FIG 2·10·1

2.10

neglected. Neglecting these terms does not mean that compressibility effects are ignored, since these will arise again in the continuity equation.

Thus,

$$\frac{\partial P}{\partial x} = \mu \frac{\partial^2 u}{\partial y^2} \qquad 2.10.2$$

Integrating twice w.r.t. y

$$\mu u = \frac{\partial P}{\partial x} \frac{y^2}{2} + C_1 y + C_2$$

and applying the boundary conditions of no slip

$$\left.\begin{aligned} u(x,0) &= 0 \\ u(x,h) &= 0 \end{aligned}\right\}$$

Substituting these boundary conditions:

$$u = \frac{1}{2\mu} \frac{\partial P}{\partial x} (y^2 - yh) \qquad 2.10.3$$

The equation of continuity for a compressible fluid is

$$\Delta = -\frac{1}{\rho}\left[\frac{\partial \rho}{\partial t} + u\frac{\partial \rho}{\partial x} + v\frac{\partial \rho}{\partial y} \right]$$

and the term $\frac{\partial \rho}{\partial y}$ vanish from the assumption that the properties do not vary with y.

Integrating w.r.t. y, taking account of the fact that v = 0 on the lower surface and - $\partial h/\partial t$ on the upper:

$$\frac{\partial h}{\partial t} = -\int_0^h \left\{ \frac{1}{\rho}\left(\frac{\partial \rho}{\partial t} + u\frac{\partial \rho}{\partial x} \right) + \frac{\partial u}{\partial x} \right\} dy \qquad 2.10.4$$

Substituting for u from 2.10.3, we get after

2.10

rearrangement

$$\frac{\partial}{\partial t}(\rho h) = \frac{\partial}{\partial x}\left[\frac{\rho h^3}{12\mu}\frac{\partial P}{\partial x}\right] \qquad 2.10.5$$

This equation may be termed the Reynolds Equation for the motion and may be solved numerically if required. Before attempting to do so, it may be profitable to investigate closer any possibility of simplifying it further.

It has previously (2.7.17) been shown that the equation for the filmshape can be written

$$h(x,t) = h_o(t) + f(x) + g(x,t)$$

where the last term arises from deformation of the boundary material. Hence,

$$\frac{\partial h}{\partial t} = \frac{\partial h_o}{\partial t} + \frac{\partial}{\partial t}(g)$$

It is thus seen that the velocity of approach consists of two terms. The first $\partial h_o/\partial t$ is the motion of the cylinder as a whole, the second term is the contribut ion from the rate of deformation and varies along the film. If the rate of deformation is small we may introduce an average velocity for the surface as a whole and use this in eqn. 2.10.5. Adopting this procedure and defining

$$\frac{\partial h}{\partial t} = - V$$

where V is regarded as being a function of time only.

We then have

2.10

$$\frac{\partial}{\partial t} = \frac{\partial h}{\partial t}\frac{\partial}{\partial h} = - V \frac{\partial}{\partial h}$$

and eqn. 2.10.5 becomes

$$- V \frac{\partial}{\partial h}(\rho h) = \frac{\partial}{\partial x}\left[\frac{\rho h^3}{12\mu} \frac{\partial P}{\partial x} \right] \qquad 2.10.6$$

If the fluid is regarded as incompressible, the equat ion reduces to

$$P = \int_{\infty}^{x} \frac{12\mu V x}{h^3}\, dx \qquad 2.10.7$$

after two integrations and substitution of the boundary conditions

$$\frac{\partial P}{\partial x} = 0 \; ; \quad x = 0 \, , \; t \geqslant 0$$

$$\lim_{x \to \infty} P = 0 \; ; \; t \geqslant 0$$

It is thus seen tha t the simplification arising from the assumption of incompressibility is considerable.

The compressibility effects are represented in the eqn. 2.10.5 mainly by the term

$$\frac{\partial}{\partial h}(\rho h) = \rho + h\frac{\partial \rho}{\partial h}$$

Now, if for purposes of investigating more closely the influence of compressibility it is assumed that density is a function of pressure only, then for liquids such as lubricating oils which are fairly incompressible, the first term predominates. The second term in addition to being smaller is also of opposite sign, at least in the most interesting

2.10

range near the centre.For this reason, retaining only the first term, equation 2.10.6 integrated once gives

$$\frac{\rho h^3}{12\mu}\frac{\partial P}{\partial x} = -V\int_0^x \rho\, dx \qquad 2.10.8$$

Defining:

$$\left.\begin{aligned} Q_x &= \frac{1}{\rho x}\int_0^x \rho\ dx \quad ; \quad x \neq 0 \\ Q_x &= 1 \qquad\qquad\quad ; \quad x = 0 \end{aligned}\right\} \qquad 2.10.9$$

and integrating again:

$$P = \int_{\infty}^{x} \frac{12\mu V x}{h^3} Q_x dx \qquad 2.10.10$$

Now, assuming that density is a linear function of pressure

$$\rho = \rho_0(1 + \alpha P)$$

$$q = \alpha P_m = \frac{\rho_m - \rho_0}{\rho_0}$$

where ρ_m is density corresponding to maximum pressure P_m

ρ_0 is density at atmospheric conditions.

With this 2.10.9 becomes:

$$Q_x = \frac{\rho_0}{\rho x}\int_0^x (1 + \alpha P)\, dx = \frac{\rho_0}{\rho}\left\{ 1 + \frac{q}{x}\int_0^x \frac{P}{P_m}\, dx \right\} \qquad 2.10.11$$

Expanding ρ^{-1} in a binomial series retaining only the first two terms

$$Q_x = 1 + \frac{q}{x}\int_0^x \frac{P}{P_m}\, dx - q\frac{P}{P_m} = 1 + q\left[\frac{1}{x}\int_0^x \frac{P}{P_m}\, dx - \frac{P}{P_m} \right] \qquad 2.10.11$$

2.10

The term

$$\beta(x) = \frac{1}{x}\int_{o}^{x}\frac{P}{P_m}\,dx - \frac{P}{P_m}$$ has the approximate value

$$0 \leqslant \beta \leqslant 0.5 \quad \text{for } 0 \leqslant x \leqslant \infty$$

depending upon the shape of the pressure distribution. The value of β computed for some typical pressure distributions are shown in fig. 2.10.2.

Substituting the result 2.10.11 into the expression for the pressure eqn. 2.10.10:

$$P = \int_{\infty}^{x}\frac{12\mu Vx}{h^3}\,dx + q\int_{\infty}^{x}\frac{12\mu Vx}{h^3}\beta(x)dx \qquad 2.10.12$$

The first integral represent the incompressible case, the second is the contribution to pressure from compressibility. Since β varies from about 0 - 0.5 and the value of q may be taken t o be about 0.10 - 0.15 for some lubricating oils, it seems that the influence of density variation on pressure will only be of the order of a few percent. One may therefore be justified in calculating the pressure from the simpler eqn. 2.10.7 rather than from the complicated but more accurate eqn. 2.10.6.

The total load carried by the film is given by

$$W = \int_{-\infty}^{\infty} P\,dx = 2\int_{o}^{\infty} P\,dx$$

Denoting the integral

$$R(x) = \int_{\infty}^{x}\frac{\mu x\,dx}{h^3} \qquad 2.10.13$$

COMPRESSIBILITY
β/β_{MAX}
FOR TWO PRESSUREDISTR.

FIG 2·10·2

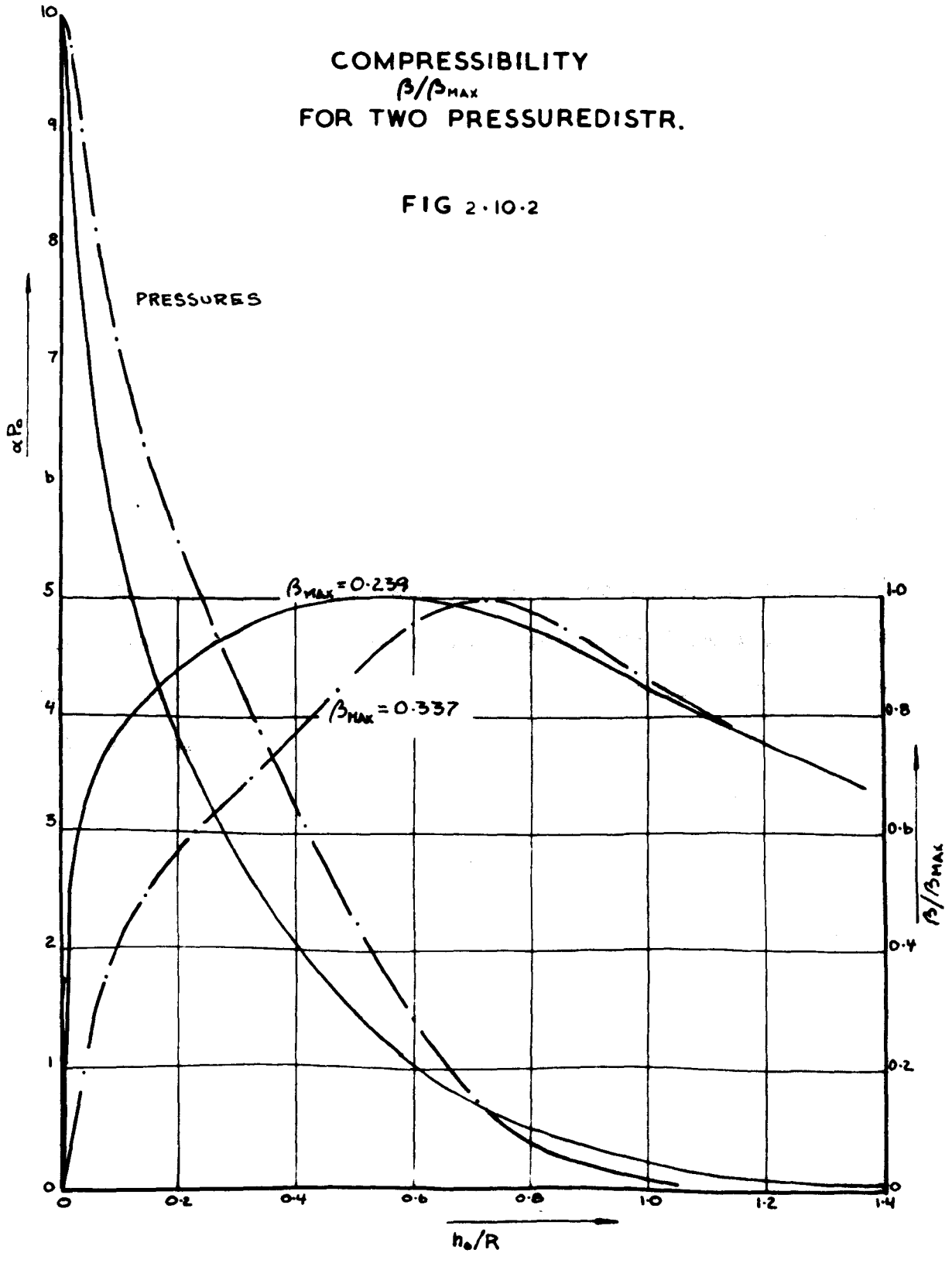

2.10

we have

$$W = 24V \int_{c}^{\infty} R(x)dx \qquad 2.10.14$$

Hence the velocity of approach becomes

$$V = \frac{W}{24S} \qquad 2.10.15$$

$$S = \int_{\delta}^{\infty} R(x)dx \qquad 2.10.16$$

In this notation the relation for the pressure becomes

$$P = \frac{W}{2}\frac{R(x)}{S} \qquad 2.10.17$$

The integrals R(x) and S can be obtained by numerical integration using a convenient quadrature formula, once the appropriate values of viscosity and filmthickness have been determined.

2.11 The Energy Equation.

The general energy equation as derived in section 2.6 was

$$\rho\frac{DE}{Dt} = -P\Delta + KV^2T + \Phi \qquad 2.11.1$$

where Φ is the source function.

Taking account of the additional assumptions this becomes

$$c\rho\left[\frac{\partial T}{\partial t} + u\frac{\partial T}{\partial x}\right] = -P\left[\frac{\partial u}{\partial x} + \frac{\partial v}{\partial y}\right] + K\frac{\partial^2 T}{\partial x^2} + \Phi \qquad 2.11.2$$

and Φ is now given by

$$\Phi = \mu\left[2\left(\frac{\partial u}{\partial x}\right)^2 + 2\left(\frac{\partial v}{\partial y}\right)^2 + \left(\frac{\partial u}{\partial y} + \frac{\partial v}{\partial x}\right)^2 - \frac{2}{3}\left(\frac{\partial u}{\partial x} + \frac{\partial v}{\partial y}\right)^2\right] \qquad 2.11.3$$

Substituting for u from eqn 2.10.3 and integrating w.r.t. y from 0 to h, writing $\partial/\partial t = -V\,\partial/\partial h$, we get

$$c\rho\left[Vx\frac{\partial T}{\partial x} - Vh\frac{\partial T}{\partial h}\right] = -\int_0^h P\Delta dy + Kh\frac{\partial^2 T}{\partial x^2} + \int_0^h \Phi dy$$

$$\therefore \frac{K}{c\rho V}\frac{\partial^2 T}{\partial x^2} - \frac{x}{h}\frac{\partial T}{\partial x} + \frac{\partial T}{\partial h} - \frac{1}{c\rho Vh}\int_0^h \Phi dy + \Omega(x,h) = 0 \qquad 2.11.4$$

where

$$\Omega(x,h) = \frac{P}{c\rho Vh}\int_0^h \Delta dy$$

Now for liquids such as lubricating oils with small heatconduction coefficients, it appears that the conduction term is small compared with the other terms in the equation and can be neglected.

The term $\Omega(x,h)$ is entirely due to variation in density.

2.11

In the previous section it was concluded that the influence of compressibility on the solution of the momentum equation was relatively slight, a few percent, and this was disregarded so as to obtain a considerable simplification of the equation. A similar argument is not available in the case of the energy equation, for although the factor Δ is small it is multiplied by the pressure which may be large, and hence the complete term may contribute significantly to the temperature rise.

Making use of the same argument that was employed in section 2.10 for the derivation of the pressure, the function $\Omega(x,h)$ may be written:

$$\Omega(x,h) = -\frac{P}{c\rho^2}\left[\frac{x}{h}\frac{\partial\rho}{\partial x}-\frac{\partial\rho}{\partial h}\right] \qquad 2.11.5$$

Previously it was shown that the order of magnitude of the velocity gradients $\partial u/\partial x$, $\partial v/\partial x$, $\partial v/\partial y$ were all small compared to the value of $\partial u/\partial y$.
If this is made use of the source function becomes

$$\Phi = \mu\left(\frac{\partial u}{\partial y}\right)^2$$

The argument breaks down, however, near the axis $0 \leqslant x \leqslant h_o$, since within this narrow range $\partial u/\partial y$ is very small, and $\partial u/\partial x$ and $\partial v/\partial y$ may well be the dominating terms. It seems therefore desirable to include the effects of $\partial u/\partial x$ and $\partial v/\partial y$ in this range.

$$\frac{\partial u}{\partial x} = -\frac{6Vy}{h^3}\left[\, h\,(\,y-h\,) + x\frac{\partial h}{\partial x}\,(\,2h-3y\,)\,\right]$$

2.11

From symmetry it is apparent that in the range $0 \leqslant x \leqslant h_o$, $\partial h/\partial x$ will be small. Neglecting the term containing this factor we have

$$\frac{\partial u}{\partial x} = -\frac{6Vy}{h^3}(y - h) \qquad -h_o \leqslant x \leqslant h_o \qquad 2.11.6$$

Similarly

$$\frac{\partial v}{\partial y} = \frac{6Vy}{h^3}(y - h)$$

Substituting this into 2.11.3, we get

$$\Phi = \mu \left[4\left(\frac{\partial u}{\partial x}\right)^2 + \left(\frac{\partial u}{\partial y}\right)^2 \right]$$

$$\frac{1}{c\rho Vh}\int_o^h \Phi dy = \frac{12\mu V}{c\rho h^2}\left(\frac{x^2}{h^2} + 0.4\right) \qquad 2.11.7$$

The term 0.4 is that due to the gradients $\partial u/\partial x$ and $\partial v/\partial y$.

Substituting into eqn. 2.11.4 we obtain

$$\frac{x}{h}\frac{\partial T}{\partial x} - \frac{\partial T}{\partial h} - \frac{12V\mu}{c\rho h^2}\left(\frac{x^2}{h^2} + 0.4\right) - \Omega(x,h) = 0 \qquad 2.11.8$$

It was mentioned previously that the limiting cases of the boundary conditions were:

1. Adiabatic conditions, $\partial T/\partial n = 0$ where n is the normal at the boundary. This condition implies that all heat developed in the film stays there and increases the flu id temperature.

2. Isothermal condition, $T(x,t) = T(x,0)$ i.e. all the heat developed is imediately removed and no temperature rise takes pla ce in the fluid.

probably in between the two limiting cases, but as the properties eg. viscosity, may be critically dependant upon temperature, it will be of interest to see which of the two limiting cases gives the best approximation, and to obtain some measure of the closeness of this approximation.

Instead of attempting to solve eqn. 2.11.8, the much simpler problem of linea r heatconduction in a composite solid will be solved, and it is believed that this solution will give some indication as to what is happening in the fluid.

Consider a composite solid consisting of a finite medium $-1 \leqslant x \leqslant 0$ of temperature T_1 with heatconduction coefficient K_1, and thermal diffusivity α_1 etc. in contact with a semi infinite medium $x \geqslant 0$ of temperature T_2 and properties K_2, α_2 etc.

The equations governing the flow of heat are:

$$\left.\begin{aligned} \frac{\partial^2 T_1}{\partial y^2} - \frac{1}{\alpha_1}\frac{\partial T_1}{\partial t} &= -\frac{\Phi t^{\frac{m}{2}-1}}{K_1} \\ \frac{\partial^2 T_2}{\partial y^2} - \frac{1}{\alpha_2}\frac{\partial T_2}{\partial t} &= 0 \end{aligned}\right\} \quad \begin{aligned} -1 \leqslant x \leqslant 0 \\ x \geqslant 0 \end{aligned} \qquad 2.11.9$$

The initial and boundary conditions may be taken as

$$\left.\begin{aligned} K_1 \frac{\partial T_1}{\partial y} &= K_2 \frac{\partial T_2}{\partial y} \\ T_1 &= T_2 \end{aligned}\right\} \quad x = 0 \; ; \; t \geqslant 0$$

$$K_1 \frac{\partial T}{\partial y} = 0 \qquad x = -1 \; ; \; t > 0$$

$$\lim_{y \to \infty} T_2 = 0 \qquad t > 0$$

2.11

$$T_1(x,0) = T_2(x,0) = 0 \qquad t = 0$$

The solution to this system is given by (see appendix B)

$$\frac{\bar{T}_1}{T_1} = 1 - \frac{\sigma}{\sigma+1} \sum_{n=0}^{\infty} (-1)^n \beta^n i \left(\operatorname{erfc} \frac{2n-\xi}{2\chi} + \operatorname{erfc} \frac{2(n+1)+\xi}{2\chi} \right) \qquad 2.11.10$$

where

$\bar{T}_1$ is the average adiabatic temperature of the finite medium.

$\xi = y/l \qquad \chi^2 = \alpha_1 t/l^2$

$K = \sqrt{\alpha_1/\alpha_2} \qquad \sigma = \frac{K_2}{K_1} K \qquad \beta = \frac{\sigma-1}{\sigma+1}$

and where i is an integral operator operating on the erfc functions and defined by

$$i \operatorname{erfc} x = \int_x^{\infty} \operatorname{erfc} \zeta \, d\zeta$$

Equation 2.11.10 was solved on the computer for four different values of $l = h/2$, corresponding to x-stations 2, 6, 10 a nd 14×10^{-2} cm from the centre of the cylinder. For each x-station six different values of $\xi = y/l$ were used i.e. $\xi = 0,\ 0.2,\ 0.4,\ 0.6,\ 0.8$ a nd 1.0
In each case six timesteps were taken: $t = \frac{1}{2},\ 1,\ 1\frac{1}{2},\ 2,\ 2\frac{1}{2}$ a nd 3 milliseconds.

The solutions are shown in figs. 2.11.1 to 2.11.4, one figure for each value of l. These show $T_1/\bar{T}_1$ % as a funct ion of ξ, one curve for each value of the timeinterval.

The analysis takes no account of the fact that the bou ndaries are moving i.e. that l is a function of time. Some allowance can be made for this effect by making y_{max}

a function of time, the appropriate function being determined from filmthickness/time relationship available for the motion in question. These values of $\xi_{max} = y_{max}/l$ are dra wn in on the graphs of $T_1/\overline{T}_1$, and only values of ξ to the left of this line for a ny value of t have any meaning.

In order to find the actual temperature in the fluid the adiabatic temperatures must be made available. The analysis demands that these must be calculated from an expression of the form $\overline{T} = K\sqrt{t}$, where K is an appropriate constant. If now the adiabatic temperatures are taken from the computer solution of the case a, constant viscosity, rigid materials, these temperatures for any given x-station approximately follows the above law. These temperatures are given in fig. 2.11.5.

True filmtemperatures taking account of heatconduction can now be computed as functions of ξ and t by:

$$T_1 = (T_1/\overline{T}_1 \times 100\%) \times \overline{T}_1$$

The ma ximum values at any x-station are reached at $\xi = \xi_{max}$. These maximum temperatures are plotted in fig. 2.11.6 as a function of time.

These curves show that the maximum temperature in the film occur at the x-station of about 10×10^{-2}cm, and has the value of about 6%. The maximum adiabatic temperature on the other hand is of the order of 40°C. It is thus clear that a large amount of the heat generated in the film is conducted away, and into the metal boundaries, and that the

LINEAR HEATCONDUCTION

AT PT. $x = 2 \cdot 10^{-2}$ cm FROM ℄

FIG 2·11·1

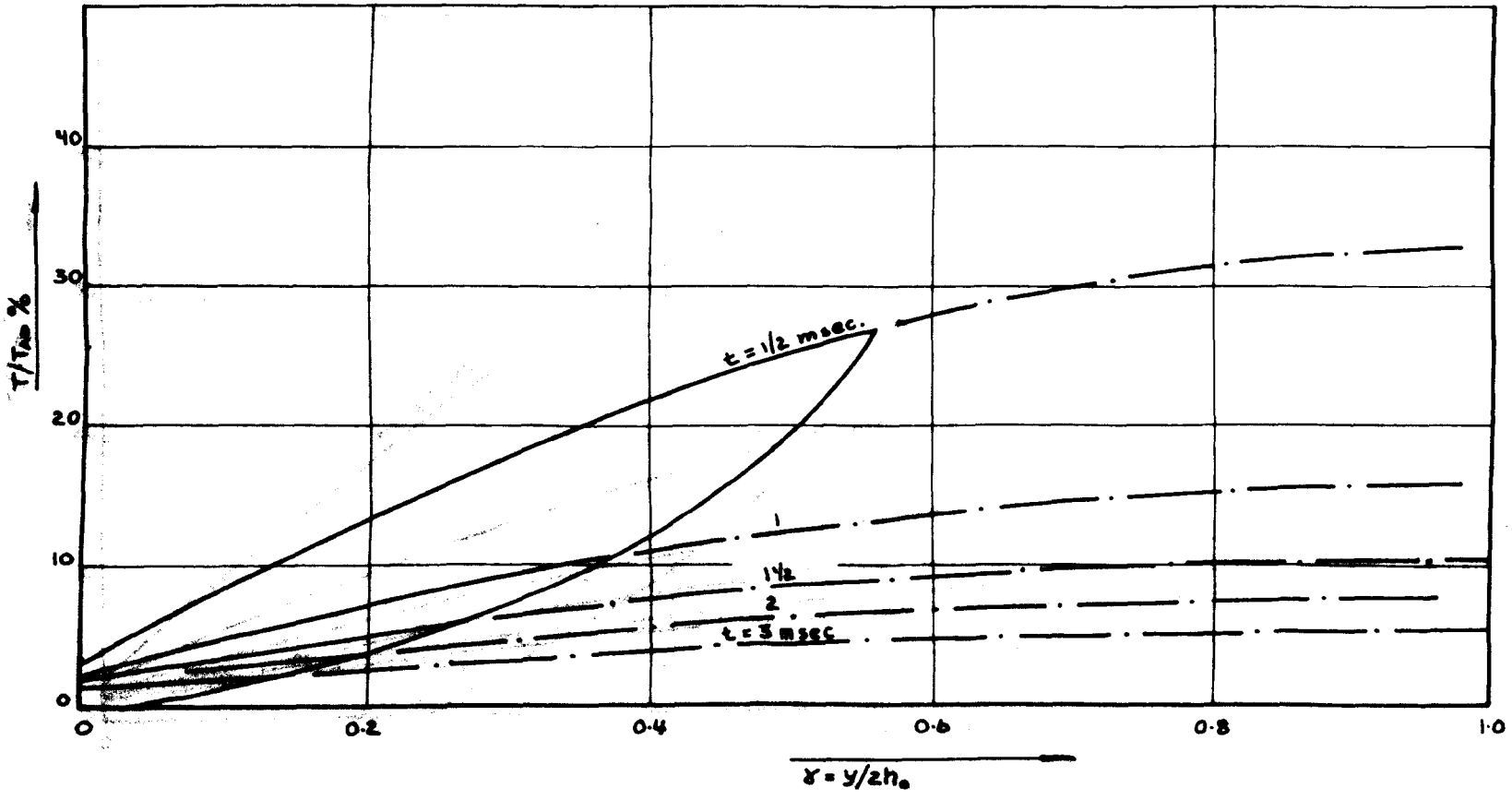

LINEAR HEATCONDUCTION

AT PT. $x = 6 \cdot 10^{-2}$ cm FROM ℄

FIG 2·11·2

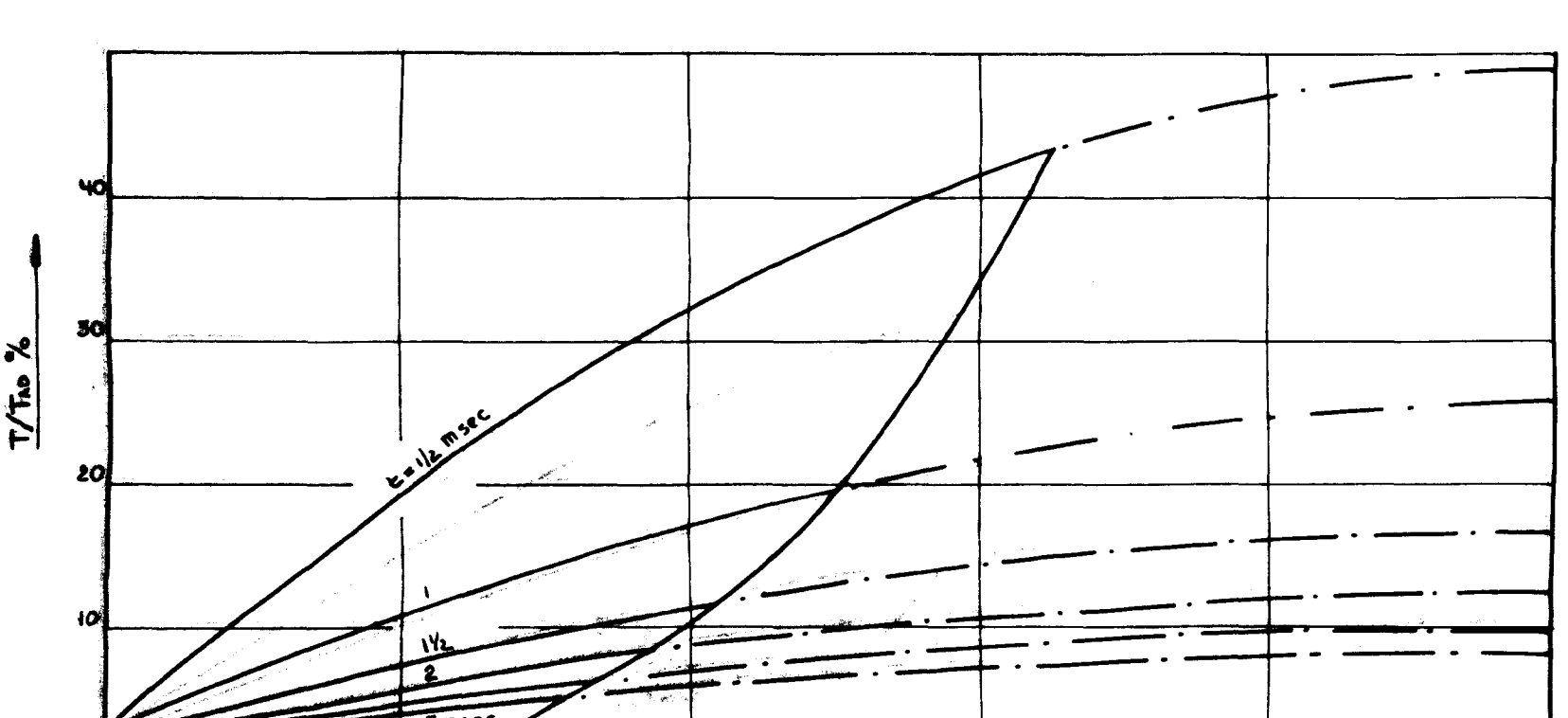

LINEAR HEATCONDUCTION

AT PT. $X = 10 \cdot 10^{-2}$ cm FROM ℄

FIG 2·11·3

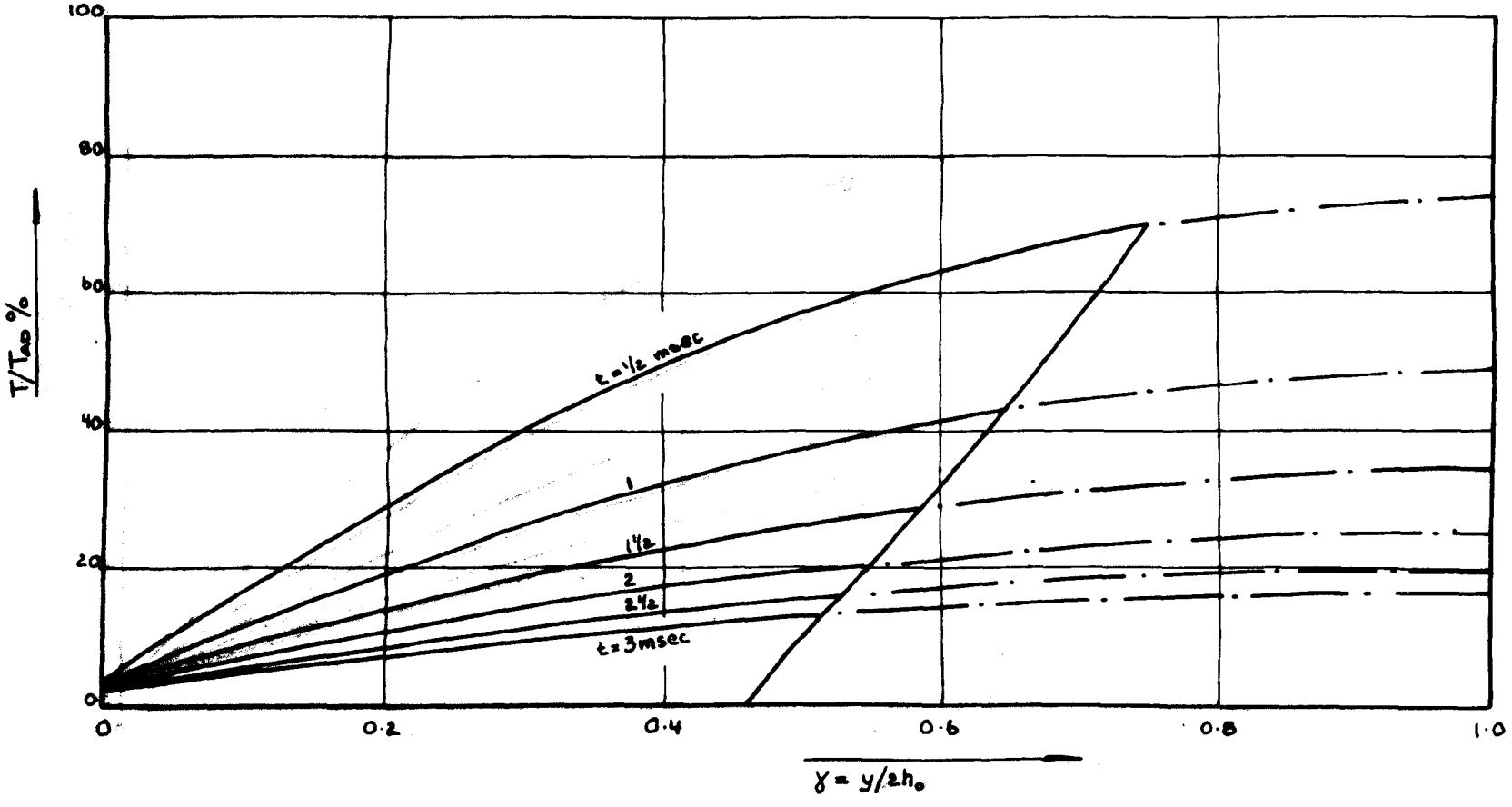

LINEAR HEATCONDUCTION

AT PT. $x = 14 \cdot 10^{-2}$ cm FROM $\mathbb{C}$

FIG 2·11·4

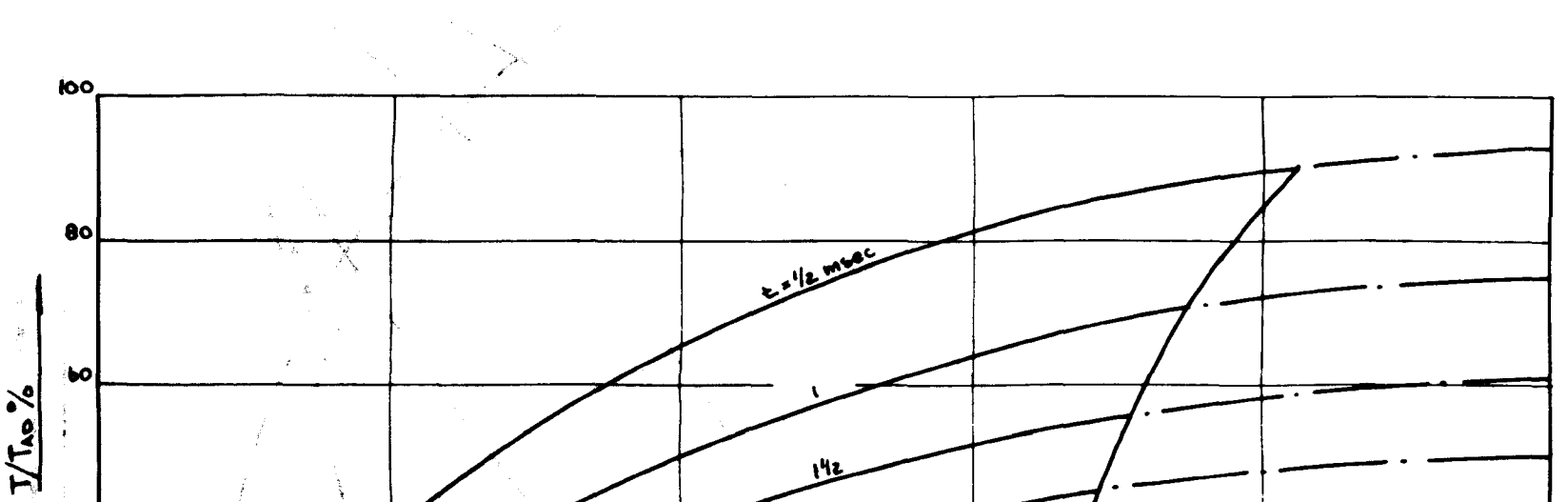

LINEAR HEATCONDUCTION

ADIABATIC FILMTEMPERATURES

MOTION OF BOUNDARY

CASE 0: CONST. VISC; RIGID BOUNDARIES

FIG 2·11·5

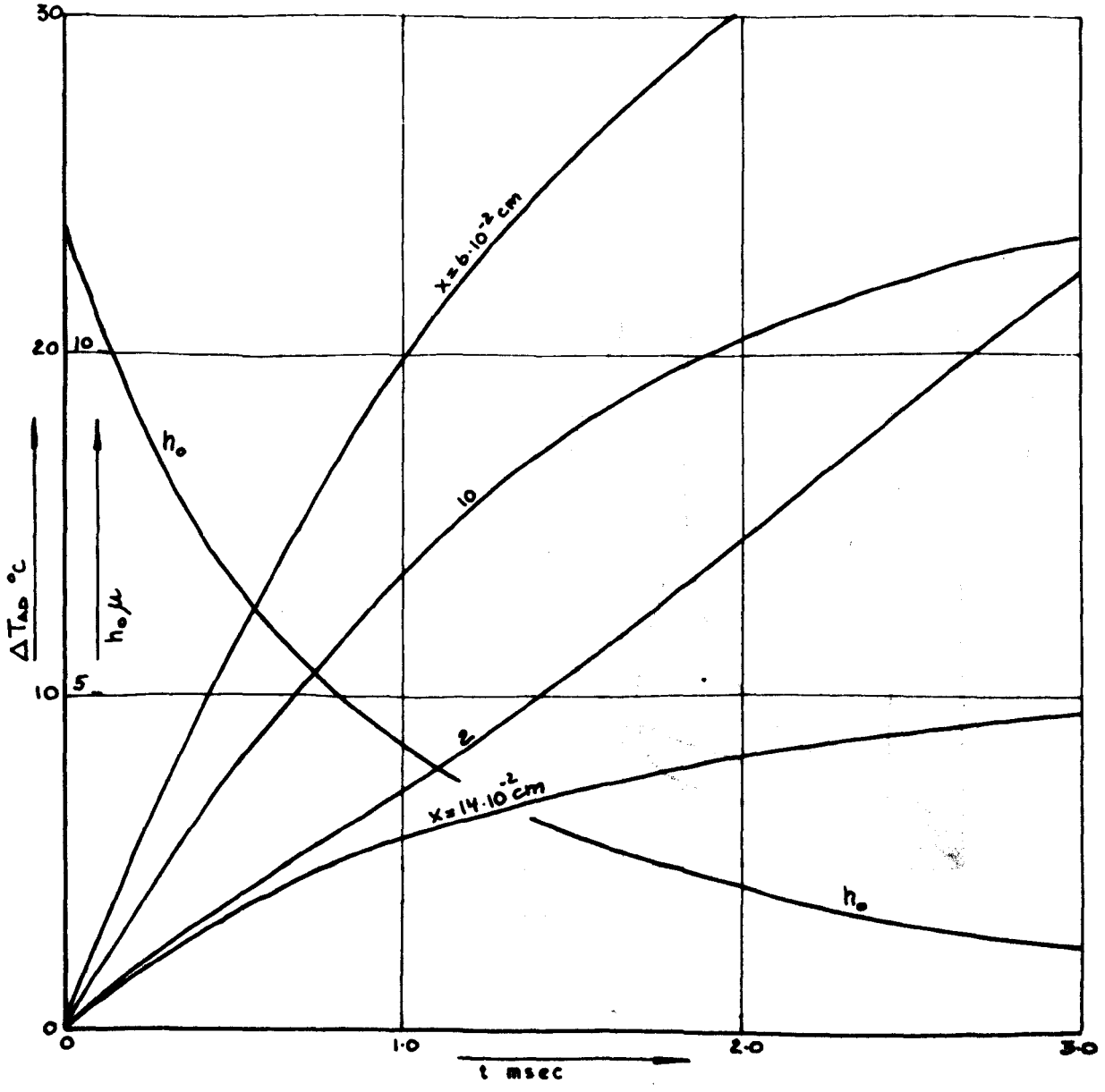

LINEAR HEATCONDUCTION

MAX. FILMTEMPERATURES AT
VARIOUS X-STATIONS

FIG 2·11·6

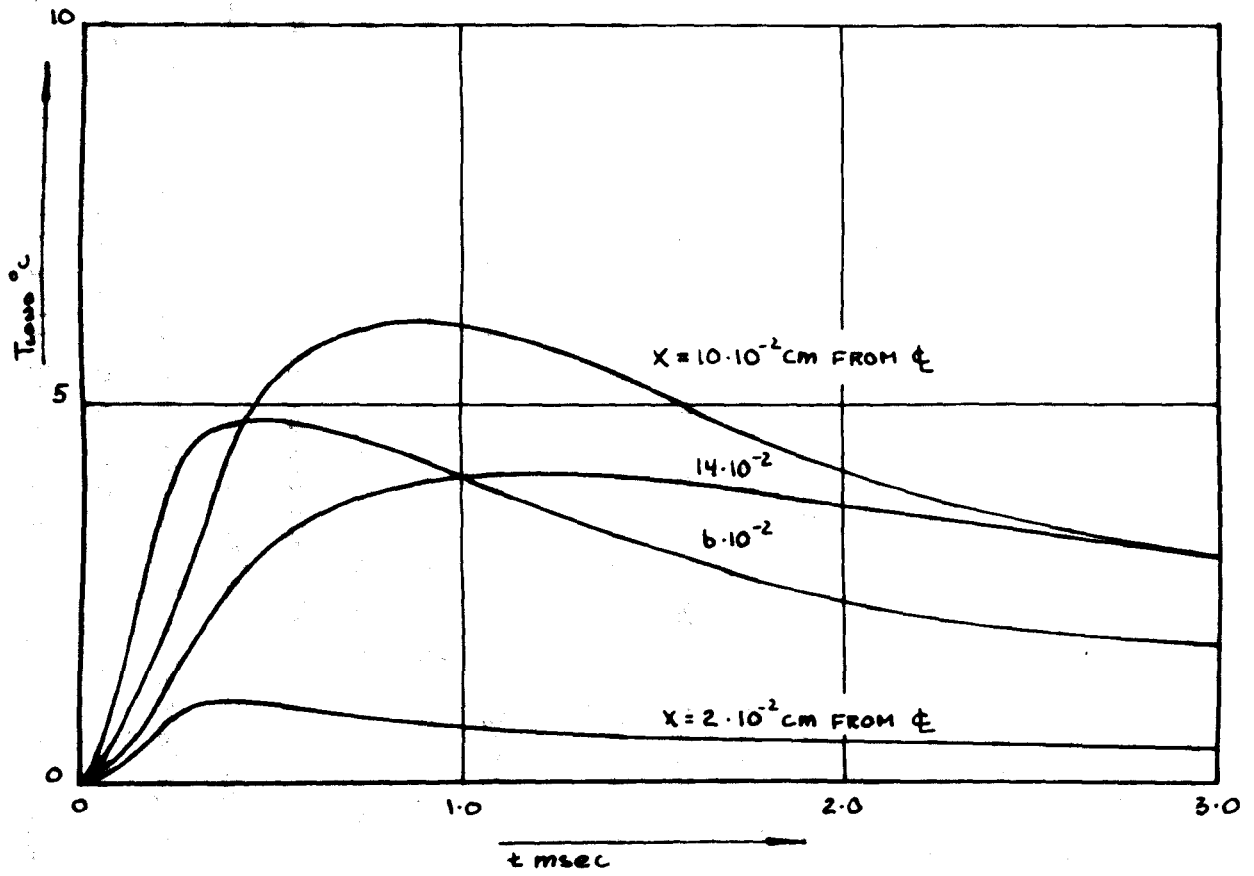

true fluid temperatures are very much lower than those predicted by the adiabatic hypothesis.

The minimum filmtemperatures occur, as expected, on the metal boundary, and are of the order less than 1% for all x-stations for all times. It thus appear that the average temperature across the film will only be a few degrees.

The above analysis is only a crude approximation of the physical case since it fails to account for the two-dimensional aspect of the latter, does not account properly for the motion of the boundaries, assumes that heat is generated evenly across the film, and neglecting convection entirely. These effects properly accounted for would, it is believed, give lower maximum temperatures than the ones calculated here, hence the present analysis provides upper limits for the fluid temperatures.

From this it seems clear that of the two available working hypothesis the isothermal hypothesis provides the best approximation to the physical case and should be used under conditions such as these investigated here.

This conclusion depends to a large extent upon the thermal properties of the fluid and boundary materials, as well as other factors. Thus under other conditions, a different conclusion might well have been reached, and the adiabatic hypothesis might have proved to give the best approximation.

2.12 Viscosity and Density.

Viscosity.

The general relation was stated in section 2.5, and was written as:

$$(\log_{10}\mu_{P,T})^2 = a\cdot(T)P + (\log_{10}\mu_{0,T})^2 \qquad 2.12.1$$

Let P_1, T_1 and P_2, T_2 be two sets of pressures and temperatures, we then have

$$\left.\begin{aligned} (\log_{10}\mu_{P_1,T_1})^2 &= a(T_1)P_1 + (\log_{10}\mu_{0,T_1})^2 \\ (\log_{10}\mu_{P_2,T_2})^2 &= a(T_2)P_2 + (\log_{10}\mu_{0,T_2})^2 \end{aligned}\right\} \qquad 2.12.2$$

These equations represent straight lines, and intersect at a point $P_k, (\log_{10}\mu_k)^2$

At the point of intersection we must have

$$\left.\begin{aligned} &(\log_{10}\mu_{P_1,T_1})^2 = (\log_{10}\mu_{P_2,T_2})^2 = (\log_{10}\mu_k)^2 \\ &P_1 = P_2 = P_k \end{aligned}\right\} \qquad 2.12.3$$

Hence

$$\left.\begin{aligned} P_k &= \frac{(\log_{10}\mu_{0,T_2})^2 - (\log_{10}\mu_{0,T_1})^2}{a(T_1) - a(T_2)} \\ (\log_{10}\mu_k)^2 &= a(T_1)P_k + (\log_{10}\mu_{0,T_1})^2 = \\ &= a(T_2)P_k + (\log_{10}\mu_{0,T_2})^2 \end{aligned}\right\} \qquad 2.12.4$$

The constants $a(T_1)$, $a(T_2)$, $(\log_{10}\mu_{0,T_1})^2$ and $(\log_{10}\mu_{0,T_2})^2$ can be determined from viscosity measurements made on the lubricant and hence the characteristic pa rameters may be determined.

Hence, we have for any temperature

$$a(T) = \frac{(\log_{10}\mu_k)^2 - (\log_{10}\mu_{0,T})^2}{P_k} \qquad 2.12.5$$

The viscosity at any pressure and temperature may now be determined provided values of $\log_{10}\mu_{0,T}$, the viscosity at atmospheric pressure is available. These values may be obtained from standard viscosity mea surements for various values of the temperature.

From a computational point of view, however, it is more convenient to have the viscosity expressed by an equation than by a table of values.

Assuming that $(\log_{10}\mu_{0,T})^2$ is adequately expressed by an equation of the form

$$(\log_{10}\mu_{0,T})^2 = K_1 \exp(-\gamma T) \qquad 2.12.6$$

where the constants K_1 and γ may be chosen so that the values obtained give a sufficiently close agreement with the measured values.

Substituting 2.12.6 into 2.12.1, taking the square root and inverting the log gives

$$\mu_{P,T} = \exp\left[\frac{\sqrt{a(T)P + K_1 e^{-\gamma T}}}{\log_{10} e}\right] \text{ millipois} \qquad 2.12.7$$

where a(T) is given by 2.12.5

Multiplying by $10^{-3} = \exp(-6.90776)$, substituting 2.12.5 gives finally in pois:

2.12

$$\mu_{P,T} = \exp\left[\frac{\sqrt{(\log_{10}\mu_k)^2\frac{P}{P_k} + K_1 e^{-\gamma T}\left[1-\frac{P}{P_k}\right]} - 6.90776\ \log_{10}e}{\log_{10}e}\right]$$

2.12.8

Density

The equation of state was discussed in section 2.4 and it was suggested that the density could be expressed as a polynomial in pressure and temperature.

Adopting this suggestion we may write

$$\rho = [\ aP + b\ ]T + [\ cP + d\ ] \qquad 2.12.9$$

where the constants a, b, c, d must be so chosen that the values obtained give a sufficiently close agreement with the measured values over the whole range of pressure and temperature.

2.13 Equations of Motion under Isothermal Conditions.

If the motion is assumed to take place under isothermal conditions, the equations governing the motion are capable of further simplification.

The viscosity may then be given with sufficient accuracy by an expression of the form

$$\mu = \mu_0 e^{\alpha P}$$

Equation 2.10.10 then becomes after integrating once

$$\frac{\partial P}{\partial x} = - \frac{12\mu_0 \exp(\alpha P) V x}{h^3} \qquad 2.13.1$$

$$\therefore \exp(-\alpha P)\, dP = - \frac{12\mu_0 V x\, dx}{h^3}$$

Integrating:

$$\frac{1}{\alpha}[\, 1 - \exp(-\alpha P)\,] = -\int_{\infty}^{x} \frac{12\mu_0 V x\, dx}{h^3} \qquad 2.13.2$$

Now define,

$$I(x) = \int_{\infty}^{x} \frac{x\, dx}{h^3} \qquad 2.13.3$$

$$J = I(0) = \int_{\infty}^{0} \frac{x\, dx}{h^3} \qquad 2.13.4$$

Then,

$$\alpha P = - \ln [\, 1 - 12\mu_0 \alpha V I(x)\,] \qquad 2.13.5$$

At the center $x = 0$, the pressure becomes P_0, the maximum pressure. For this station:

$$1 - \exp(-\alpha P_0) = 6\mu_0 V \alpha J$$

2.13

$$\therefore\ 6\mu_0 V\alpha = \frac{1 - \exp(-\alpha P_0)}{J} \qquad 2.13.6$$

and hence,

$$\alpha P = -\ln\left[\ 1 - \left(\ 1 - \exp(-\alpha P_0)\right)\frac{I}{J}\ \right] \qquad 2.13.7$$

The load is again given by

$$\alpha W = 2\int_0^{\infty} (\alpha P)dx \qquad 2.13.8$$

If the boundaries are rigid, eqn. 2.13.7 is capable of analytic solution. In this case the filmthickness is given by

$$h = h_0 + \frac{x^2}{2R}$$

and the function I(x) becomes

$$I(x) = \int_0^{x} \frac{x\ dx}{h^3} = \frac{R}{2h^2} \qquad 2.13.9$$

$$J = \frac{R}{2h_0^2} \qquad 2.13.10$$

Thus,

$$\alpha P = -\ln\{\ 1 - [\ 1 - \exp(-\alpha P_0)][\ \frac{h_0}{h}]^2\ \} \qquad 2.13.11$$

Expanding the log in a Taylor series, writing

$$\xi = [\ 1 - \exp(-\alpha P_0)]h_0^2$$

$$\alpha P = -\ln[\ 1 - \frac{\xi}{h^2}\ ] = \sum_{n=0}^{\infty} \frac{\xi^{n+1}}{(n+1)\ h^{2n+2}} \qquad 2.13.12$$

This series converges uniformly for

2.13

$\frac{\xi}{h^2} < 1 \quad \therefore P_o < \infty$

for all values of $h \geqslant h_o$

The load now becomes:

$$\alpha W = 2 \int_0^\infty (\alpha P) dx = 2 \int_0^\infty \sum_{n=0}^{\infty} \frac{\xi^{n+1}}{(n+1)\, h^{2n+2}} dx \qquad 2.13.13$$

Interchanging the order of integration and summation, performing the integratiom and expressing the summation in terms of the gammafunction:

$$\alpha W = 2\sqrt{\pi}\,\sqrt{2Rh_o} \sum_{n=0}^{\infty} [\,1 - \exp(-\alpha P_o)]^{n+1} \frac{\Gamma(2n+3/2)}{\Gamma(2n+3)} \qquad 2.13.14$$

The sum of the series depends only upon the value of αP_o, the central pressure, hence the above equation defines load as a function of central filmthickness h_o for a specified maximum pressure.

For $P_o = \infty$ we have

$$\alpha W = 2\sqrt{2Rh_o}\,(2 - \sqrt{2})\pi \qquad 2.13.15$$

Summing the series in eqn. 2.13.14 with 180 terms on the computer for various values of the parameter αP_o, gave the result shown in the following table.

Since $1 - \exp(-30) \sim 1 - 10^{-13} \sim 1 \sim 1 - \exp(-\infty)$ the sum for $\alpha P_o = 30$ should have been very near $(2 - \sqrt{2})\sqrt{\pi} = 1.04$ i.e. the value obtained is about 5% small. This is due to the very poor convergence of the series for values of $1 - \exp(-\alpha P_o)$ near 1.

Summation of the series

$$\sum_{n=0} \left(1 - e^{-\alpha P_o} \right) \frac{\Gamma(2n + 3/2)}{\Gamma(2n + 3)}$$

αP_o	Σ
30	0.9858
10	.9854
8	.9827
7	.9776
6	.9646
5	.9341
4	.8738
3	.7727
2	.6132
1	.3678
$\frac{1}{2}$	0.2018

Table 2.13.1

2.14 Summary of Theory.

Although it has previously been concluded that the isothermal hypothesis probably gives the best description of the conditions under which the motion will take place, it will never the less be of interest to see the influence of temperature on the solution.

For this case the motion is described by the simultaneous solution of the system of equations:

$$P = \int_{\infty}^{x} \frac{12\mu V x}{h^3}\, dx \qquad 2.10.7$$

$$h = H + f(x) + \lambda \int_{\Omega} P(x') \ln|x' - x|\, dx' \qquad 2.7.17$$

$$\frac{x}{h}\frac{\partial T}{\partial x} - \frac{\partial T}{\partial h} - \frac{12\mu V}{c\rho h^2}\left[\frac{x^2}{h^2} + 0.4\right] - \Omega(x,h) = 0 \qquad 2.11.8$$

$$\mu_{P,T} = \exp\left[\frac{\sqrt{(\log_{10}\mu_k)^2 \frac{P}{P_k} + K_1 e^{-\gamma T}\left(1-\frac{P}{P_k}\right)}}{\log_{10} e} - 6.90776\right] \qquad 2.12.8$$

$$\rho = [\, aP + b \,]T + [\, cP + d \,] \qquad 2.12.9$$

$$W = 2\int_{0}^{\infty} P\, dx$$

The various constants in these equations must be empirically determined from tests done on the actual fluid, and from boundary and initial conditions.

If the motion is assumed to take place under isothermal conditions the system may be reduced to the simultaneous solution of two non-linear integral equations.

2.14

$$\alpha P = - \ln\{ 1 - [1 - \exp(-\alpha P_o)] \frac{I(x)}{J}\{ \qquad 2.13.7$$

$$h = H + f(x) + \lambda \int_{\Omega} P(x')\ln|x'-x|dx' \qquad 2.7.17$$

$$\alpha W = 2 \int_{\delta}^{\infty} (\alpha P)\, dx \qquad 2.13.8$$

It has not been possible to find an analytic solution to this system of equations and numerical methods have been used.

CHAPTER III

COMPUTATION

3.1 Computation

The solution of the system of equations given in the previous chapter was effected with the help of a Ferranti Pegasus computer. It was therefore necessary to re-arrange these equations so that they would be in a form suitable for numerical solution.

For this reason the domain will be covered by a grid (fig. 3.1.1). The interval size in the x - direction being Δx and in the h (or - t) direction by Δh. A general point in this grid will be denoted by ϕ i, j, where the subscript i refer to the x - coordinate and j to the h coordinate.

The value of the definite integrals can now be obtained for each grid point by ordinary quadrature, after the appropriate values of μ and h have previously been made available.

Similarly, the values of viscosities and densities may be found for each grid point from the equation in which the various parameters now have been replaced by an appropriate number.

The film thicknesses can be computed from equation 2.7.17 once the value of the pressure is known at each grid point. The function of F (x) being known from undeformed geometry.

The integrand has a singularity at $x = x'$ and although the integral converges, direct quadrature cannot be employed.

This difficulty can be surmounted in a number of ways, of which two will be described here and used in this work.

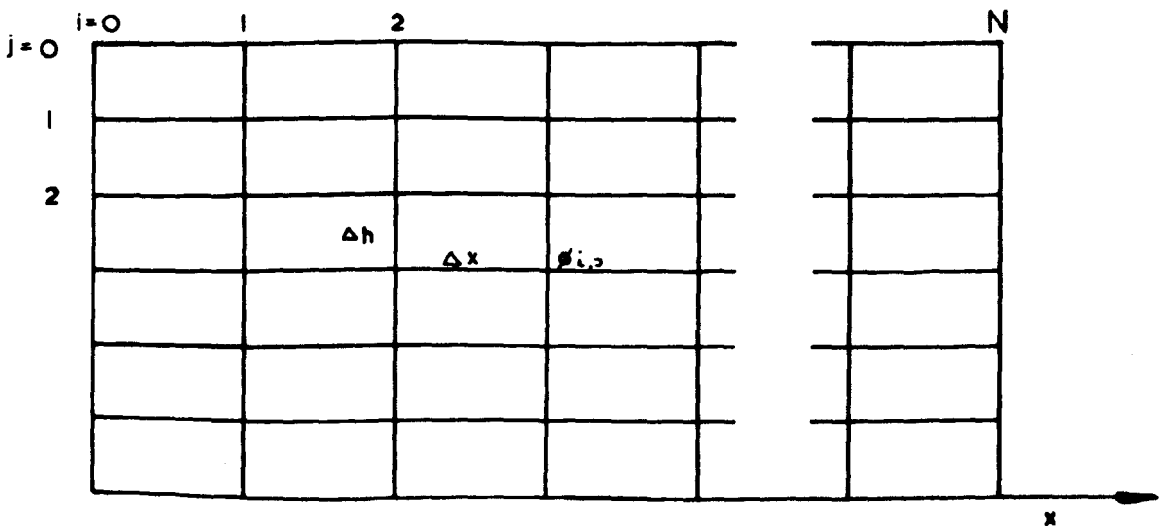

NUMERICAL INTEGRATION MESH

fig 3·1·1

3.1

If the singularity occurs for $x = x' = n\Delta x$, then no difficulty is encountered in the range $0 - (n - 1)\Delta x$ and $(n + 1)\Delta x - N\Delta x$, where N is number of points, and direct quadrature may be used for this range. To obtain the contribution from the pressures P_{n-1}, P_n and P_{n+1} corresponding to $x' = (n - 1)\Delta x$, $n\Delta x$, and $(n + 1)\Delta x$, a parabola may now be fitted through the three points.

The parabola is given by

$$P = \alpha x^2 + \beta x + \gamma$$

Hence for the contribution from this portion

$$\delta^x = -\frac{2}{\pi E}\int_{-\Delta x}^{\Delta x} [\, \alpha x^2 + \beta x + \gamma \,] \ln x \, dx$$

The coefficients are given by

$$\left.\begin{aligned} \alpha &= \frac{P_{i+1} + P_{i-1} - 2P_i}{2\Delta x^2} \\ \beta &= \frac{P_{i+1} - P_{i-1}}{2\Delta x} \\ \gamma &= P_i \end{aligned}\right\}$$

Substituting this and the limits:

3.1

$$\delta^x = -\frac{2\Delta x}{3\pi E}\left\{ [\, P_{i+1} + P_{i-1} + 4P_i \,][\, \ln\Delta x - \tfrac{1}{3} \,] - 4P_i \right\}$$

Hence the local deformation at x_i is

$$\delta = Q_o^{i-1} + Q_{i+1}^{\infty} + \delta^x$$

where

Q_o^{i-1} denotes quadrature from o to $(i-1)\,\Delta x$

Q_{i+1}^{N} denotes quadrature from $(i+1)\,\Delta x$ to $N\Delta x$

The above procedure is quite involved from the point of view of coding it for an automatic computer, and is fairly time consuming in execution. In order to have a simpler and faster routine, the following procedure was adopted for the solution of the isothermal system.

The discontinuity in the integrand at $x = x'$ may be avoided by, instead of taking the value of $\ln\Delta$ to be $-\infty$ as it should be, to give it an arbitrary finite value. This is equivalent to computing the integral not at $x' = i\Delta x$, but at $x' = i\Delta x + \varepsilon$, where ε is some arbitrary small quantity.

3.1

Since ε is small, the integrand will be very unsmooth in the vicinity of $x' = i\Delta x$ and a quadrature formula will generally not be able to follow, but will give a too large value. This tendency is partly offset by the fact that the parts of the contribution of the integral between $i\Delta x$ and $i\Delta x + \varepsilon$ will be ignored.

By judicious selection of ε, therefore, the resulting total error incurred may be made a minimum, and sufficiently small to be neglected.

The routine resulting from this procedure is much more straight forward and less time consuming than the previous described method, although of less accuracy.

In the solution of the equations described so far, it has not been necessary to refer to the time history of the motion, i.e., the equations are solved along a line only. The energy equation being a partial differential equation with independent variables x and h, this is not so any longer, and the solution must be effected on a surface.

The temperature at a point (i, j) may be obtained by expansion in a Taylor Series.

i.e.

$$\left.\begin{aligned} T_{i+1,j} &= T_{i,j} + \Delta x \frac{\partial T_{i,j}}{\partial x} + O(\Delta x^2) \\ T_{i-1,j} &= T_{i,j} - \Delta x \frac{\partial T_{i,j}}{\partial x} + O(\Delta x^2) \end{aligned}\right\}$$

3.1

Subtracting, a finite difference approximation to the partial derivative

$\partial T_{i,j}/\partial x$ is obtained

$$\frac{\partial T_{i,j}}{\partial x} = \frac{T_{i+1,j} - T_{i-1,j}}{2\Delta x} + O(\Delta x^3) \qquad 3.1.1$$

Similarly

$$\frac{\partial T_{i,j}}{\partial h} = -\frac{T_{i,j+1} - T_{i,j}}{\Delta h} \qquad 3.1.2$$

The forward difference approximation used for $\frac{\partial T}{\partial h}$ is not the best available. It leads, however, to an explicit equation in $T_{i,j+1}$ and is therefore simple to handle.

The use of the more accurate central difference approximation would lead to a set of simultaneous equations for the solution of the $T_{i,j+1}$'s.

Substituting 3.1.1, 3.1.2 into equation 2.11.8 and rearranging.

$$T_{i,j+1} = T_{i,j} + \Delta h \frac{12\mu V x^2}{c\rho h^4}\Big|_{i,j} - \frac{\Delta h}{2\Delta x}\frac{x}{h}\Big|_{i,j}\left(T_{i+1,j} - T_{i-1,j} \right) -$$

$$- \Delta h \Omega_{i,j} \qquad 3.1.3$$

3.1

The correction for compressibility Ω in terms of finite differences becomes

$$\Delta h \Omega_{i,j} = \frac{P}{c\rho^2}\Big|_{i,j}\left(\frac{\Delta h}{2\Delta x}\frac{x}{h}\Big|_{i,j}(\rho_{i+1,j} - \rho_{i-1,j}) - \right. \qquad 3.1.4$$

$$\left. - (\rho_{i,j+1} - \rho_{i,j}) \right)$$

The temperatures along the line (j + 1) may now be computed in terms of previous temperatures on the $j^{\underline{th}}$ line, and the appropriate values are provided by the boundary condition along the lines j = 0 and i = 0.

3.2 Programming.

a. The adiabatic case.

The program was organized in the normal way used with digital computers, i.e. it consists of a number of sub-routines doing the actual operations indicated, and the whole being under control of a master program.

Nine sub-routines were written:

a. Pressure and velocity

b. Viscosity.

c. Density.

d. Temperature.

e. Temperature corrections for compressibility.

f. Deformation and film thicknesses.

g. Test.

h. Simpson Quadrature.

i. Output.

The first six of these are solving the equations, using the Simpson routine when indicated. The test routine would determine when the iterations had been taken far enough, and then pass control to the output routine which would punch out the final iterated answer.

For starting values in the zero iteration cycle at any line j, the final iterated values of the previous line was used, with

appropriate changes as for film thickness where the previous values $h - \Delta h$ were used. On the first j = 0 line, the starting values were partly determined from boundary conditions, and partly assumed.

The cycle is started by the master program setting the appropriate starting values for the first order iteration of the pressure, and the velocity and the first sub-routine is entered. This then will calculate the pressure at the gridpoints, the load corresponding to this pressure distribution, and also the corresponding velocity and store these away in the backing store.

Next, the viscosities were computed, using the currently calculated pressures and the temperatures obtained from the last iteration cycle of the previous line, and store these.

In a similar way the densities were computed.

In the case of the temperatures, it should be noted that it is not values on the current $j^{\underline{th}}$ line that is computed, but those belonging to the next, $j + 1^{\underline{th}}$ line. This is evident from eqn. 3.1.3.

Finally, the first order iteration of the deformations and film thicknesses on the current line is computed. The sub-routine uses the first of the two previously described processes.

The decision whether the so far iterated values are a close enough approximation to the solution of the equations is determined by the Test routine.

Not only the values of the current $n^{\underline{th}}$ iteration are stored, but also those of the previous (n - 1) iteration. The Test routine extracts an appropriate pair from the store, examines their difference, and compares this with a pre set acceptable tolerance. If the difference is within this tolerance, the test is said to be passed, and the routine then passes on to test the next pair etc. If the whole test is passed, control is taken by the master program, which arranges for printing out the solution via the output routine, and then makes ready for starting of iteration on the next $(j + 1^{\underline{th}})$ line.

In the case that any one of the individual examinations fail, the whole test is said to have failed and the master program then arranges for a new (n + 1) iteration on the current $j^{\underline{th}}$ line. This procedure is kept up until the test is passed.

The test was applied to the velocity, load pressure distribution and deformation, in this order.

The program proved, not unexpectedly, to be very time consuming.

A flow diagram is shown in fig. 3.2.1.

b. <u>The isothermal case</u>.

The organization of the program for this case followed the same lines as for the previous case, but owing to the simple system of equations to be solved, only three routines were now written:

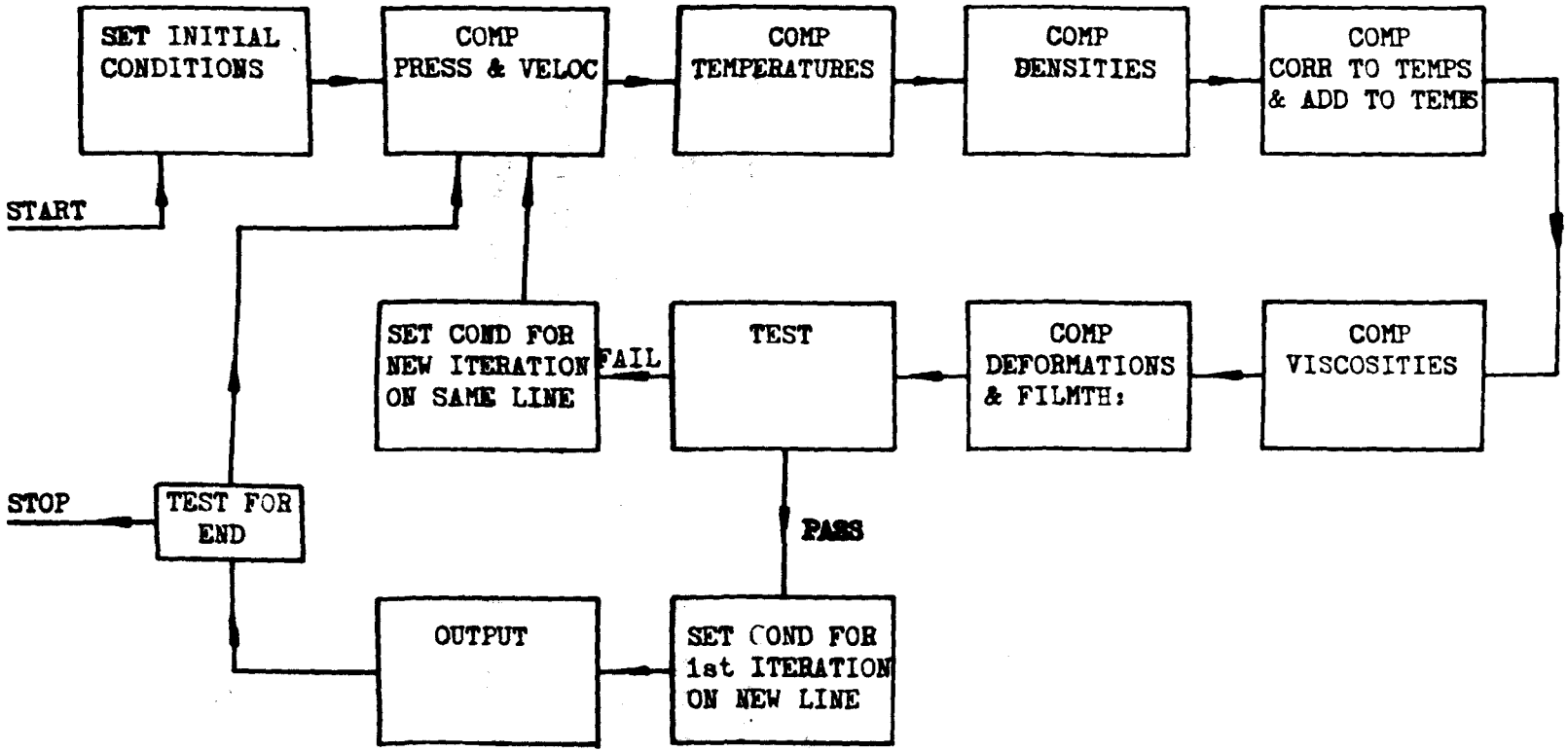

SIMPLIFIED FLOWDIAGRAM
ADIABATIC CASE

fig 3·2·1

3.2

a. Hydrodynamics

b. Elasticity

c. Output.

Endeavour was made to make the program as fast as possible. For this reason, the second of the two methods of integrating the elasticity equation was used. It was also found that for various reasons the trapezoidal rule of integration gave better results than Simpson, and hence the simpler quadrature formula was used.

The test was applied only to the load in this case, and was taken care of by the master program. A special sub-routine was therefore not needed for this operation.

The program proved very much faster in operation than the one for the previous case.

The flow diagram is given in fig. 3.2.2.

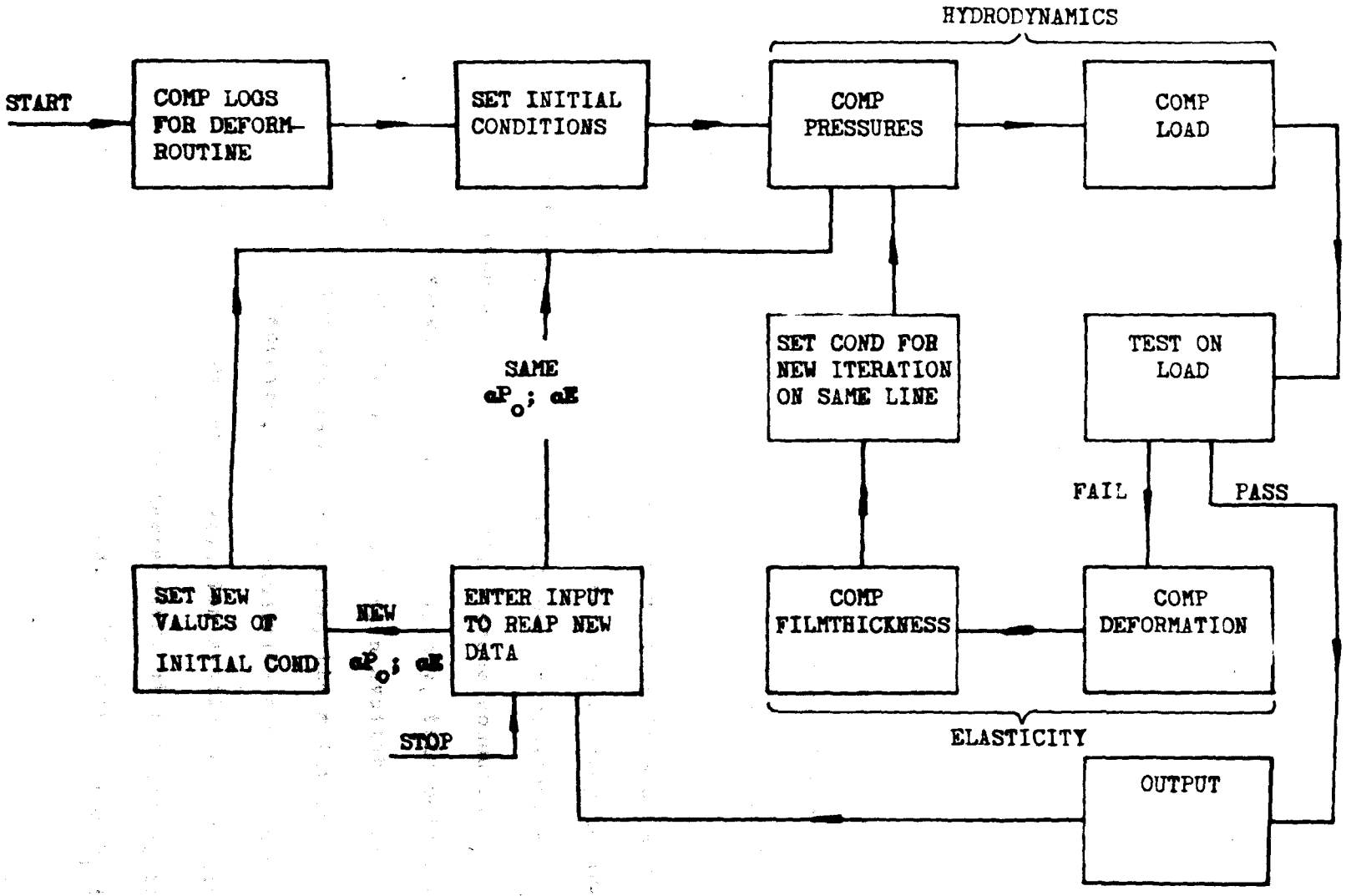

SIMPLIFIED FLOWDIAGRAM
ISOTHERMAL CASE

fig. 3·2·2

3.3 Checks

Mistakes in a calculation may be due to three different reasons:

1. Slip in the algebra or numercal analysis
2. Slip in programming.
3. Mistakes due to computer fault.

Case 3 is rare in practise, the computer usually being able to detect if it has made a mistake, and give appropriate warning.

In order to guard against the cases 1 and 2, checks were incorporated into the program, or performed in the computed results afterwards.

The general programs were written in such a way that by simple alterations they could be made to compute more special solutions, i.e., get the solution for constant viscosity or for rigid boundary materials etc. Hence computing the solution for constant viscosity and rigid boundary, this solution could be compared with the analytic solution available for this case. Similarly for the isothermal case, the solution for pressure dependant viscosity, rigid boundaries could be computed and compared with the series solution available for this case.

In the case of the temperature distribution, this could be checked by a different method. In moving from h_1 to h_2 under the

constant load W, the work done is given by W $(h_1 - h_2)$. For adiabatic conditions and for rigid boundaries, this work is nearly all spent into increasing the temperatures of the lubricant.

The increase in heat content of the lubricant is given by

$$\int_V c\rho T \, dV$$

where T is the increase in temperature from $h_1 \rightarrow h_2$ and V the volume of the lubricant. This temperature increase can be for instance obtained from the computed temperature distribution for the case constant viscosity, rigid boundaries, and from this case the value of the above integral could be estimated. This should be approximately the same as the work done. Approximately only, since the computed temperatures are approximate, and secondly even though T approaches zero as x increases, the product $T\Delta V$ may be large even though T may be diminishingly small, and this makes estimation of the integral difficult.

However, when this check was applied, agreement to within a few percent was obtained.

The routines calculating the elastic displacements were checked by feeding into the computer values of Hertzian pressure

3.3

obtained from the relation

$$\alpha P_h = \alpha P_o \sqrt{1 + \left(\frac{x}{b}\right)^2}$$

$$b = \frac{2R}{\alpha E} \alpha P_o$$

The elasticity routine was then made to operate on this pressure distribution, the resulting deformations should then be the Hertzian, i.e. a flat surface over the loaded zone. Deviations from the flat would indicate errors.

This method was also used to determine the best value of the parameter ε described in the second process for calculating displacements. ε was in fact adjusted so that the deviation from the Hertzian flat was as small as possible, and negligable in comparison with the film thicknesses considered in this work.

Chapter 4

Results

4.1 Adiabatic case.

The results for this case were related to an apparatus planned to be built for the purpose of checking some of the conclusions reached from the theoretical treatment. This apparatus was to consist of a cylindrical steel roller of radius 5 cm. and width 1 cm, and a flat steel plate. The roller was to be restrained, so as to move normal to the plate under a constant load applied by a spring. The lubricant planned to be used was HVI. 1074, supplied by Shell, and data on this oil was obtained from Thornton Research Centre (8). In addition to these data, it was also necessary to obtain values for the viscosity for various temperatures at atmospheric pressures. Viscosity measurements were therefore made on the oil, using a standard U-tube viscometer, and the tests were made according to British Standard.

The values of the viscosity at atmospheric pressure are given in fig. 4.1.1. In fig. 4.1.3, is shown the viscosity as a function of pressure at various temperatures. These curves were made partly from the data supplied from Thornton Research Centre and partly from the data obtained in the standard viscosity test performed.

From these viscosity values, the parameters in eqn. 2.12.8 were calculated. The following values were found:

4.1

$$K_1 = 24{\cdot}71$$

$$\gamma = 0{\cdot}01534$$

$$P_k = -1620{\cdot}5 \text{ atm}$$

$$\log_{10} \mu_k = -0{\cdot}611$$

The variation of density as a function of pressure and temperature was calculated from data given in (8) and is shown in fig. 4.1.2.

From this, the parameters in eqn. 2.12.9 were calculated and found to be:

$$a = 0{\cdot}07 \times 10^{-6}$$

$$b = -0{\cdot}505 \times 10^{-3}$$

$$c = 0{\cdot}024 \times 10^{-3}$$

$$d = 0{\cdot}919$$

No measurements were available for the specific heat or thermal conductivity of the lubricant. These parameters were calculated from the usually accepted formula (8), giving the results;

Specific heat $C = 0{\cdot}424$ cal/g^{o}c

Thermal conductivity $K = 0{\cdot}311 \times 10^{-3}$ cal/o_c sec cm.

measured

KINEMATIC VISCOSITY

of OIL T. 1074

at atmospheric press.

FIG 4.1.1

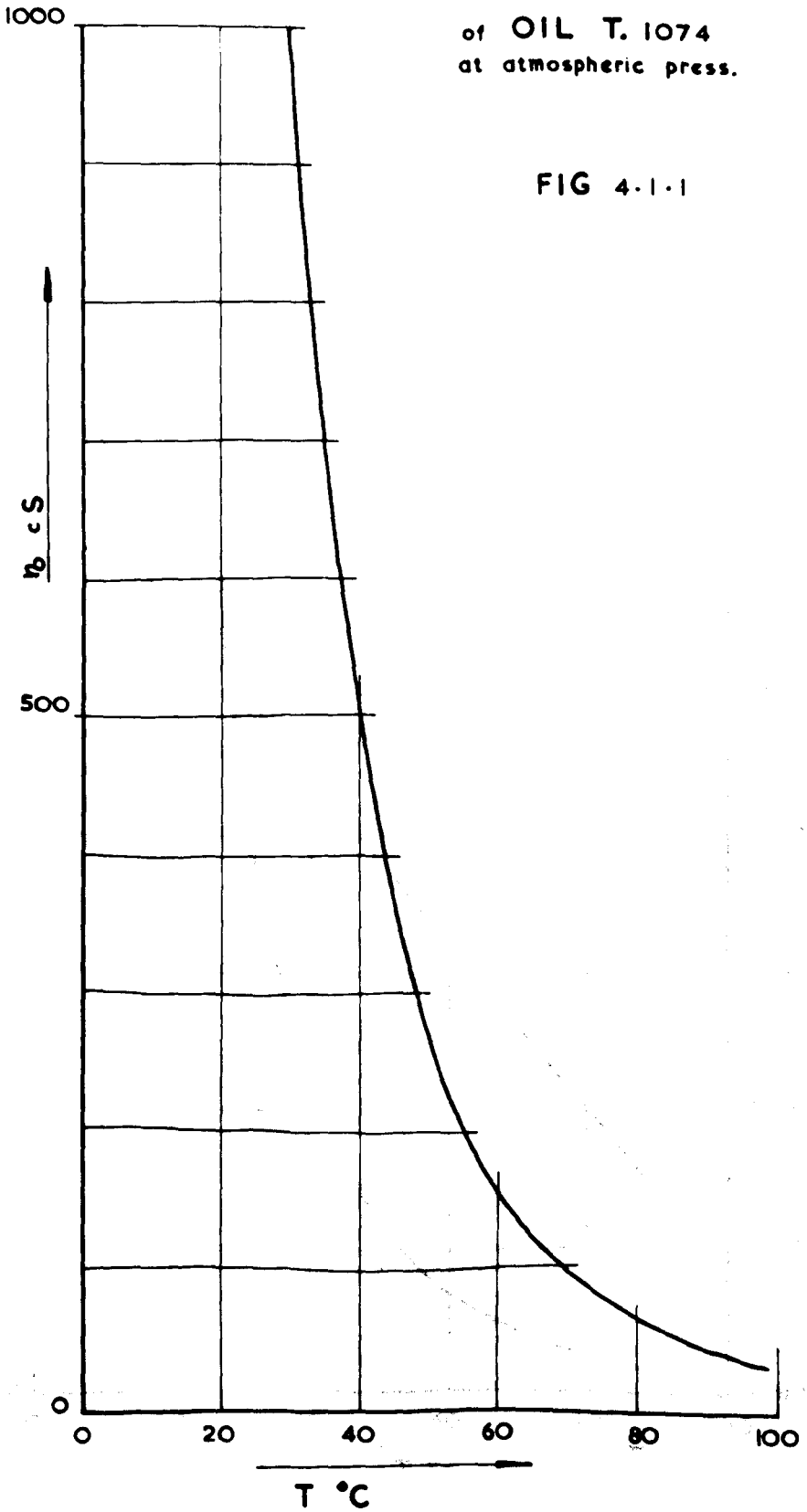

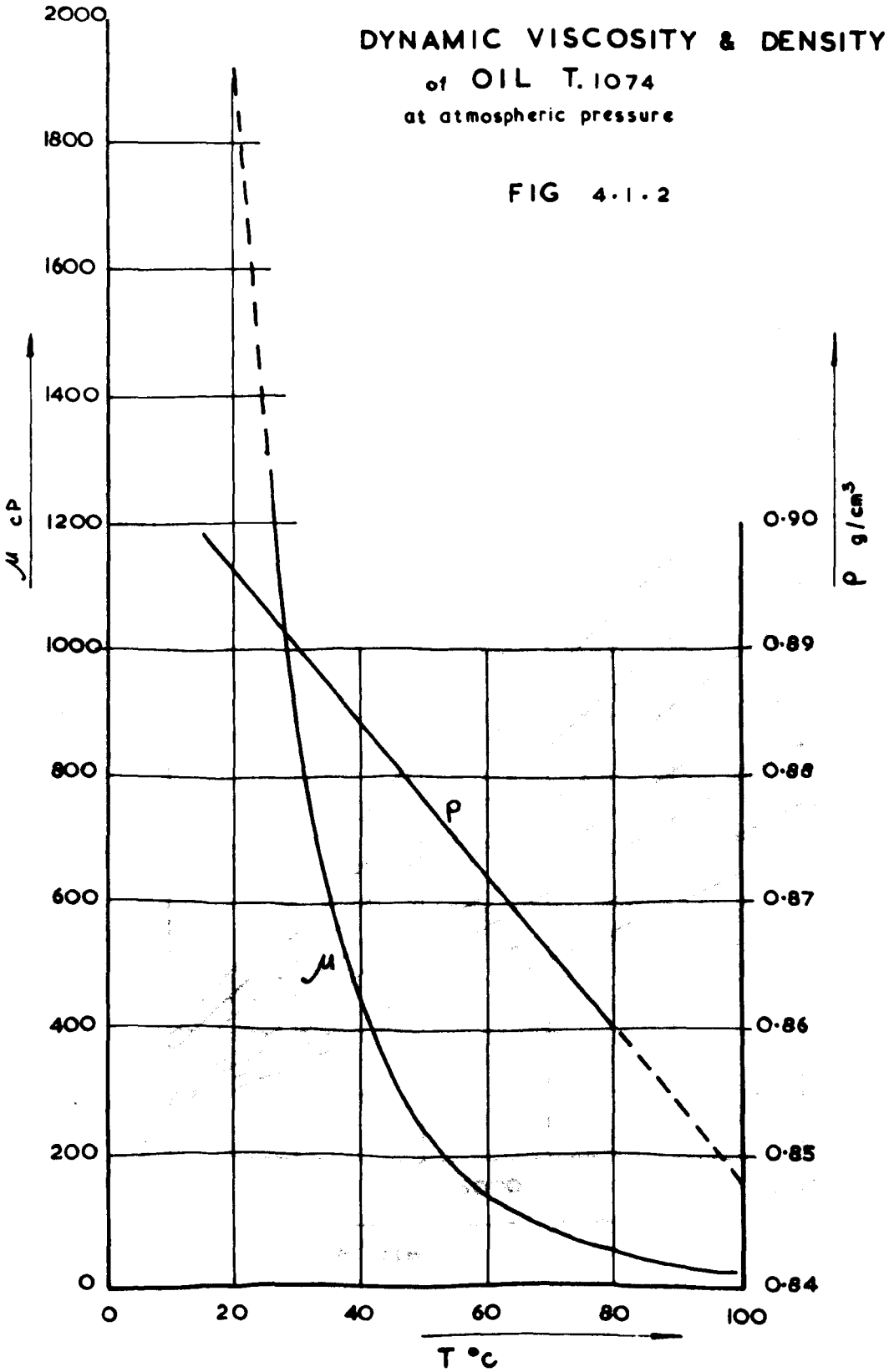
DYNAMIC VISCOSITY & DENSITY
of OIL T. 1074
at atmospheric pressure
FIG 4.1.2
μ cP
ρ g/cm³
2000
1800
1600
1400
1200
1000
800
600
400
200
0
0.90
0.89
0.88
0.87
0.86
0.85
0.84
ρ
μ
0
20
40
60
80
100
T °c

VISCOSITY
OIL T. 1074

FIG 4·1·3

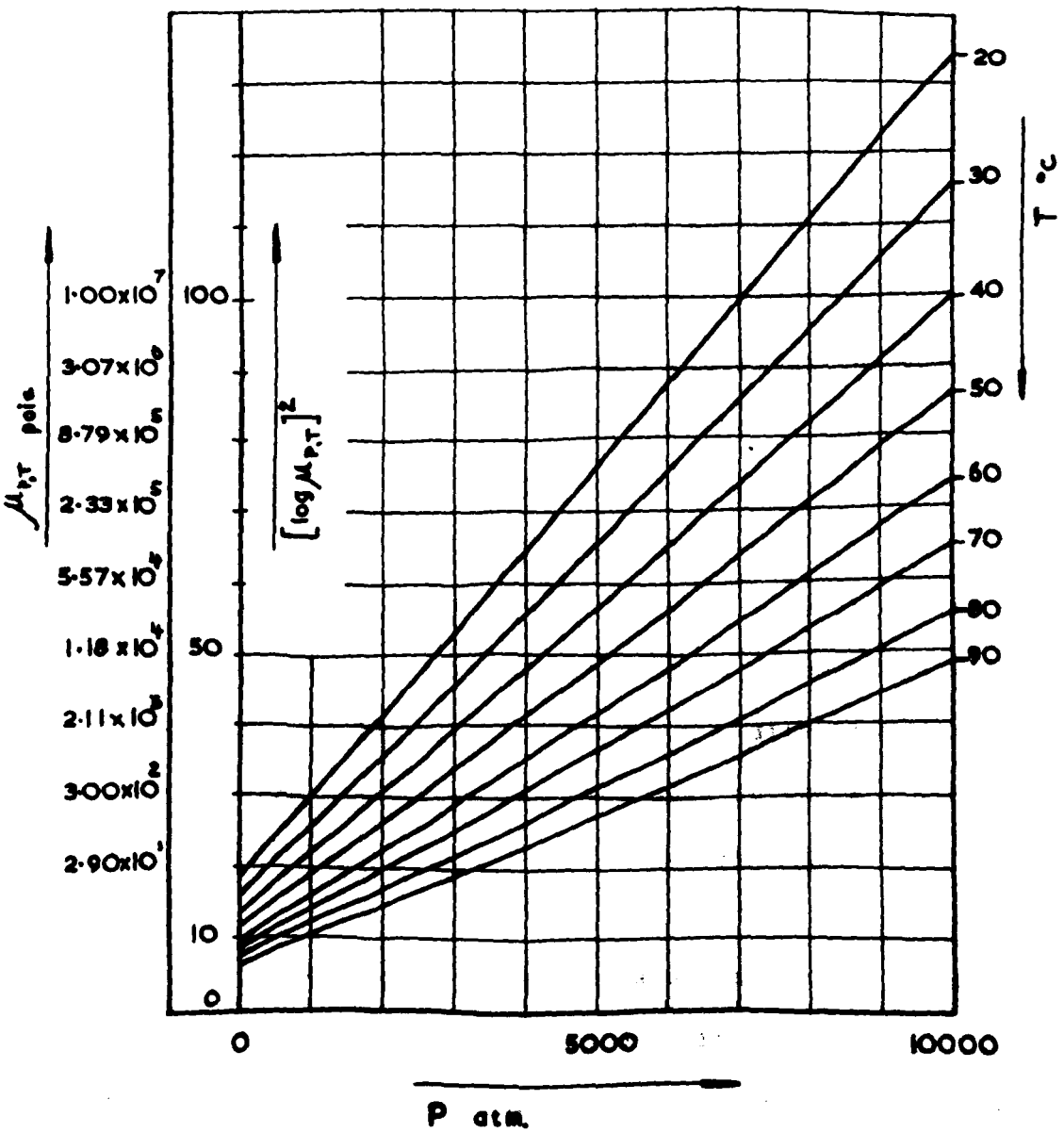

4.1

The elastic constants were taken to be:

$$E = 2{\cdot}1 \times 10 \text{ dyn/cm}^2$$

$$\nu = 0{\cdot}3$$

The constant applied load was taken as $120{\cdot}10^6$ dyn/cm.

Three different special cases were calculated:

a) Constant viscosity, rigid boundaries.

b) Variable viscosity, rigid boundaries.

c) variable viscosity, elastic boundaries.

In all three cases, pressure distribution, velocity of approach, temperature distribution were found. In addition, in case b and c, the viscosity distribution was also calculated; in case c, also the film thickness.

In all cases, the initial central film thickness h_o was taken as $h_o = 12\mu$ and the calculation proceded in steps of $\Delta h = 1\mu$. The interval in the x - direction was kept constant $\Delta x = 100\mu$ and 32 points were used in the x - direction. The initial temperature distribution was taken as $T(x, h_{o\,init}) = 20^o$.

The test was set to accept a difference of 1% or less, and it was found that in general 3 or 4 iterations were necessary to achieve this. That the accuracy of the iteration process is 1% does not mean that the final answer is obtained to this

4.1

accuracy. The accuracy of the final answer depends upon the accuracy of the various numerical processes, such as quadratures etc., and is the sum of all these individual contributions.

4.2 Case a, Constant viscosity, rigid boundaries

The main interest in this case is its use in checking the working of the computer program, as the pressures and velocity of approach can easily be obtained by analytical means for this case.

However, when it comes to the temperature distribution, this is not readily available, since even for this comparatively simple case, the energy equation is not easily solved analytically.

Since in this case all the functions are well behaved and reasonably smooth, no particular numerical difficulties were met and the solution proceeded smoothly all the way down to $h_o = 1\mu$, the last value computed for.

The obtained pressure distribution for 4 values of h_o is plotted in fig. 4.2.1. The corresponding temperature distribution is shown in fig. 4.2.2.

PRESSURE DISTRIBUTION

constant visc.

rigid boundaries.

FIG 4·2·1

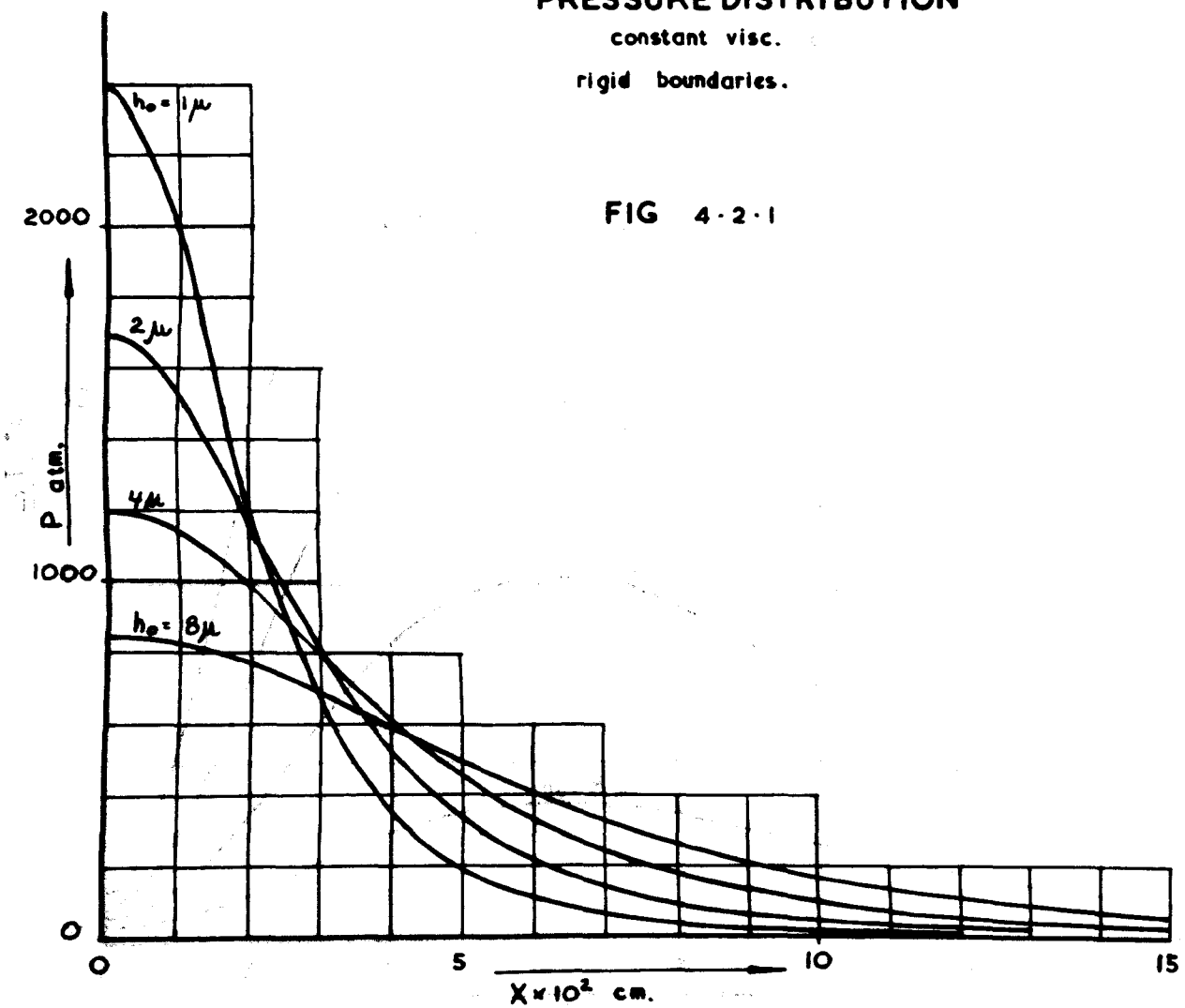

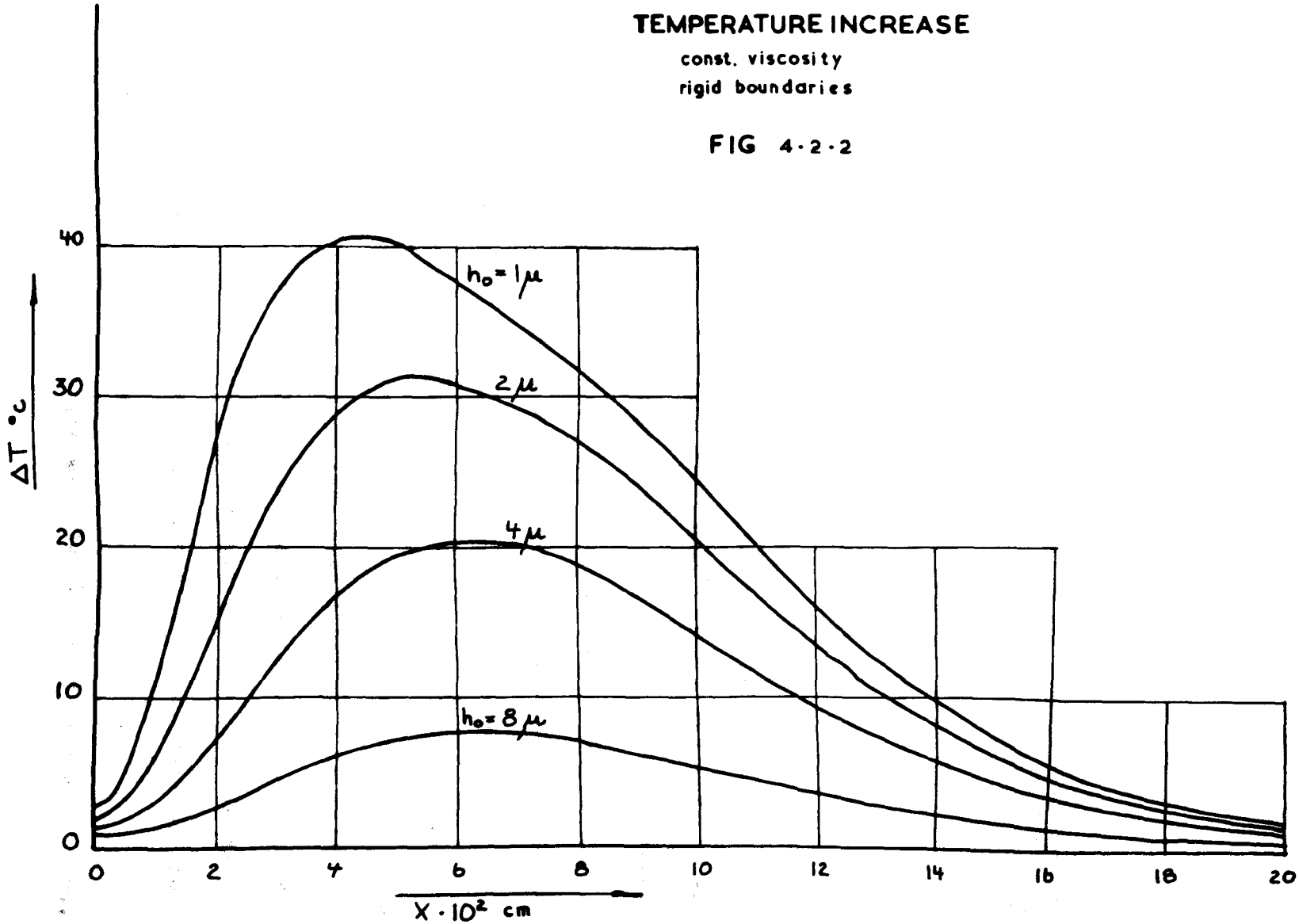
TEMPERATURE INCREASE
const. viscosity
rigid boundaries
FIG 4·2·2
ΔT °c
40
30
20
10
0
$h_o = 1\mu$
2μ
4μ
$h_o = 8\mu$
0
2
4
6
8
10
12
14
16
18
20
X · 10² cm

4.3 Case b, Variable viscosity, rigid boundaries

This case is of more interest than the preceding one in that an analytic solution is not easily available. Also, due to the variation of viscosity with pressure and temperature, some of the functions involved were far from smooth in parts of the range, and very steep gradients were involved. The consequence of this is that the accuracy of an integration process is expected to fall off, and now fundamental difficulties may arise in handling numbers in the machine.

The Pegasus computer is a fixed print machine, i.e., it can only handle numbers within the range $-1 \leq n \leq 1 - 2^{-38}$ with a maximum accuracy of about 11 decimal digits. In general, therefore, numbers must be scaled so as to be within the above range. In particular, this applies to viscosity values, which have to be computed explicitly at each grid point. It can be seen from fig. 4.3.2, that the variation of viscosity is very great for small values of $^{ho}/R$; it ranges from several thousand poise at the centre line to less than 1 poise. In order to scale this so that the highest value is within range, significant figures are lost for the lower viscosities and this leads to large errors. In general, two techniques are available for avoiding this difficulty.

First, one can operate with double length numbers, i.e.,

each number is represented to about 23 decimal digits in the machine. To do this would require much extra programming, which would greatly reduce the speed of the computation, and since the program was already slow it was not thought advisable to make it slower.

The same objection is leveled against the second technique available, that of floating point representation. In this scheme, a number is represented as a $\cdot 2^{b}$ where "a" is a fraction within range, and "b" and integer. All the ordinary arithmetic operations can be performed on such a number. However, such a representation is not natural to a Pegasus computer and would greatly reduce the speed of a program.

To avoid slowing down the program, the solution attempted was that of placing an arbitrary ceiling to the viscosities. This would mainly affect the viscosities near the centre line and would therefore result in reduction in maximum pressure. Since the error is confined to a narrow band, it would not greatly influence the accuracy of the load, or on quantities mainly dependant upon load. The pressure distribution is plotted in fig. 4.3.1. The corresponding viscosity and temperature distributions are shown in fig. 4.3.2, and 4.3.3 respectively.

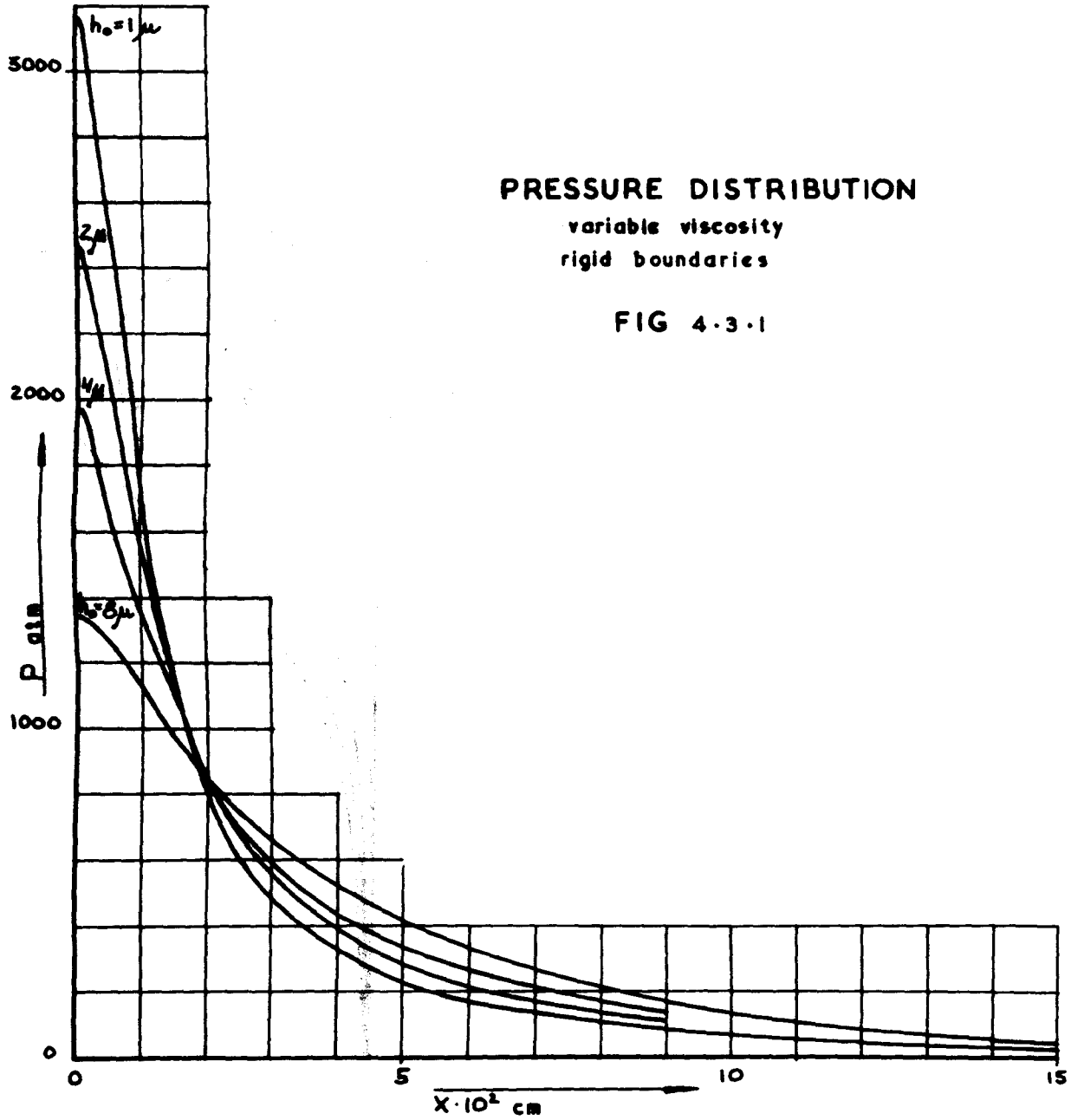

PRESSURE DISTRIBUTION

variable viscosity

rigid boundaries

FIG 4·3·1

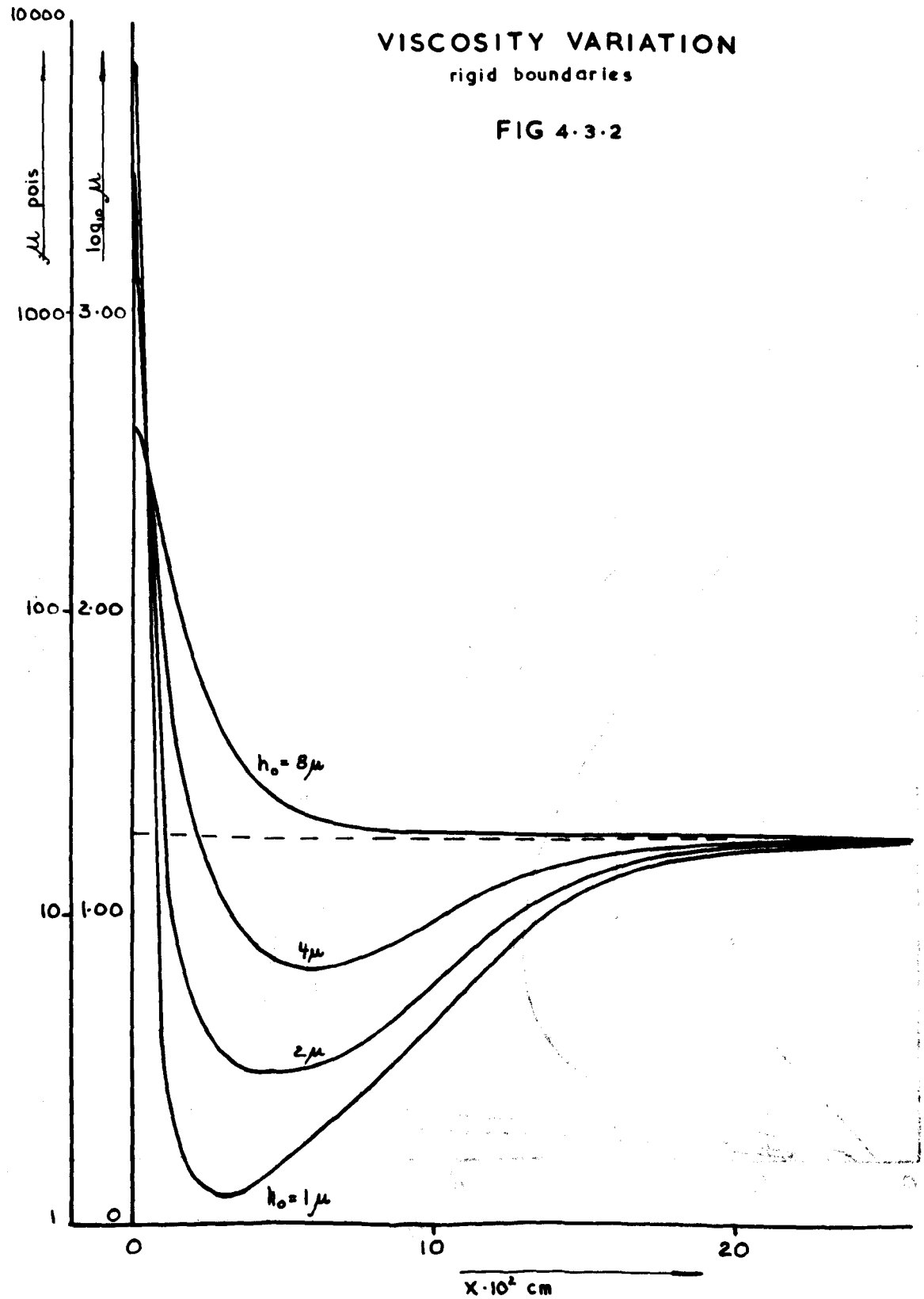
VISCOSITY VARIATION
rigid boundaries
FIG 4·3·2
μ poise
log₁₀ μ
10000
1000
100
10
1
3·00
2·00
1·00
0
$h_0 = 8\mu$
4μ
2μ
$h_0 = 1\mu$
0
10
20
X·10² cm

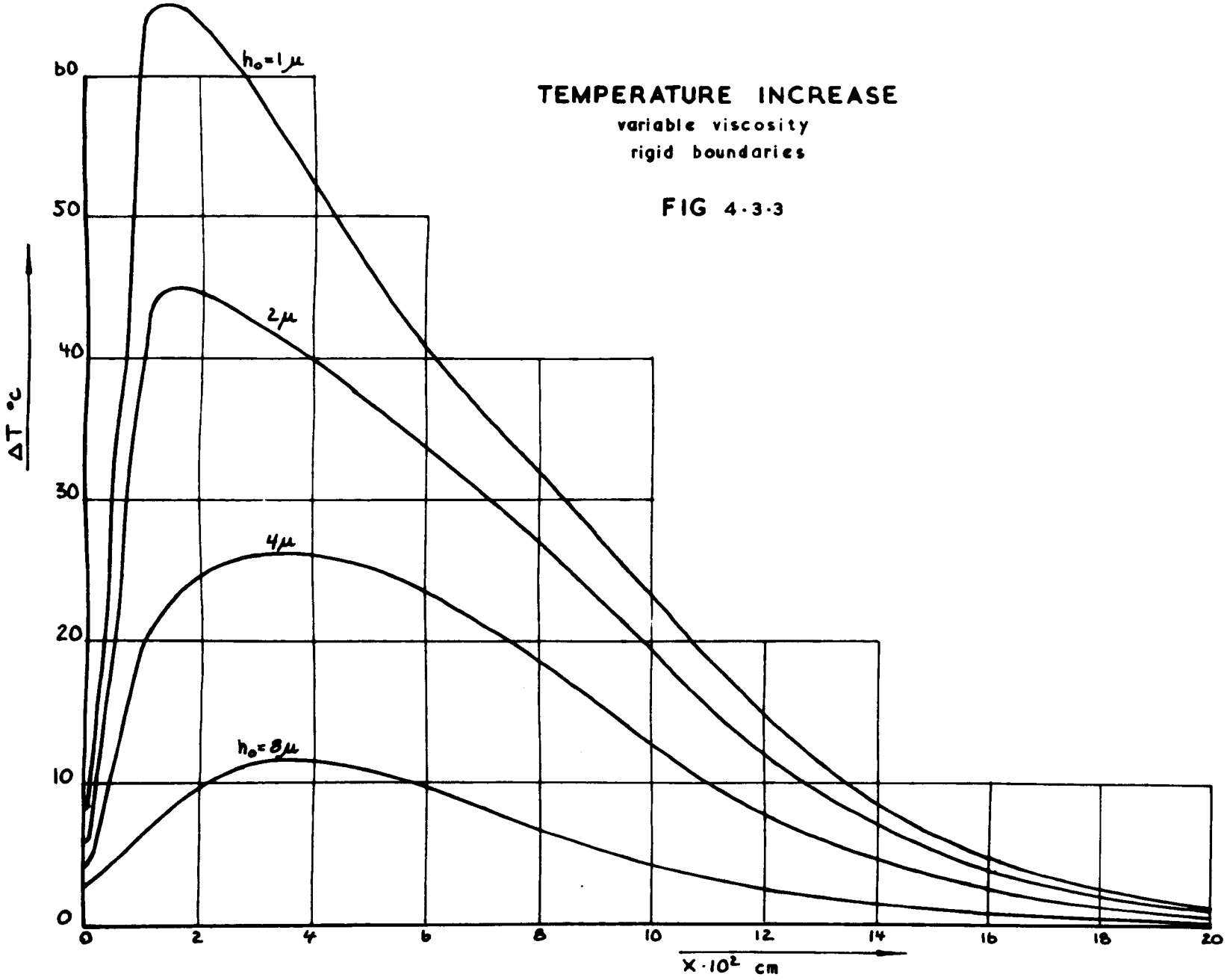
TEMPERATURE INCREASE
variable viscosity
rigid boundaries
FIG 4·3·3
$h_o = 1\mu$
2μ
4μ
$h_o = 8\mu$
ΔT °c
60
50
40
30
20
10
0
0
2
4
6
8
10
12
14
16
18
20
X·10² cm

4.4 Case c, Variable viscosity, elastic boundaries

This is the most general of the various cases treated. The numerical difficulties connected with variable viscosity also arise in this case, and in addition, the irregularities due to the deformation of the boundaries are beginning to be apparent at smaller values of film thickness. For these reasons, it was not possible to take the solution below $h_o = 2\mu$. For values of h_o below this, the convergance of the iteration process becomes poor, and it was evident that errors were building up.

As for the previous two cases, the pressure distribution, viscosity and temperature distributions were plotted, and are shown in figs. 4.4.1, 4.4.2 and 4.4.3.

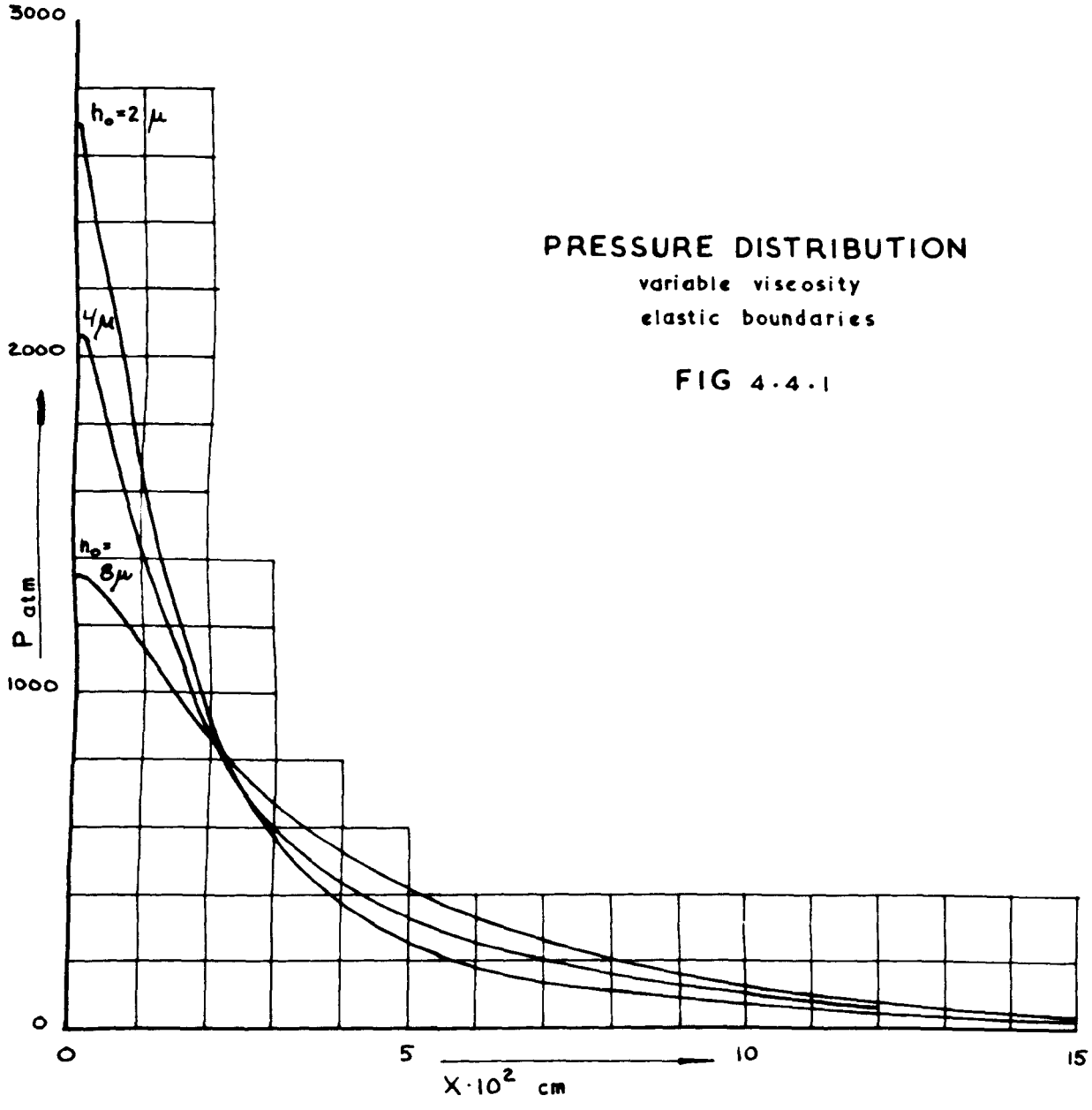

PRESSURE DISTRIBUTION

variable viscosity

elastic boundaries

FIG 4.4.1

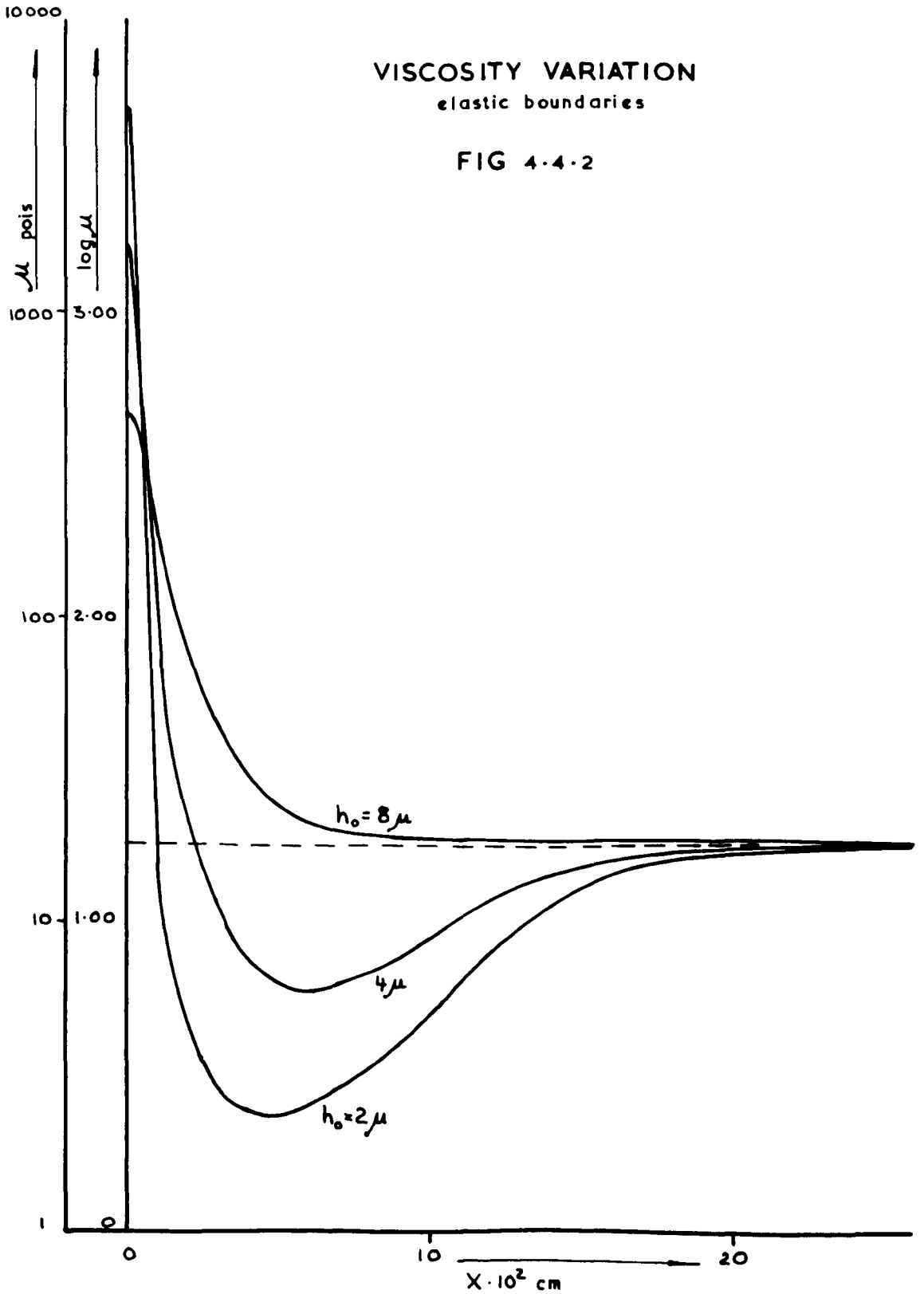
VISCOSITY VARIATION
elastic boundaries
FIG 4·4·2
μ poise
log μ
10000
1000
100
10
1
3·00
2·00
1·00
0
$h_o = 8\mu$
4μ
$h_o = 2\mu$
0
10
20
X · 10² cm

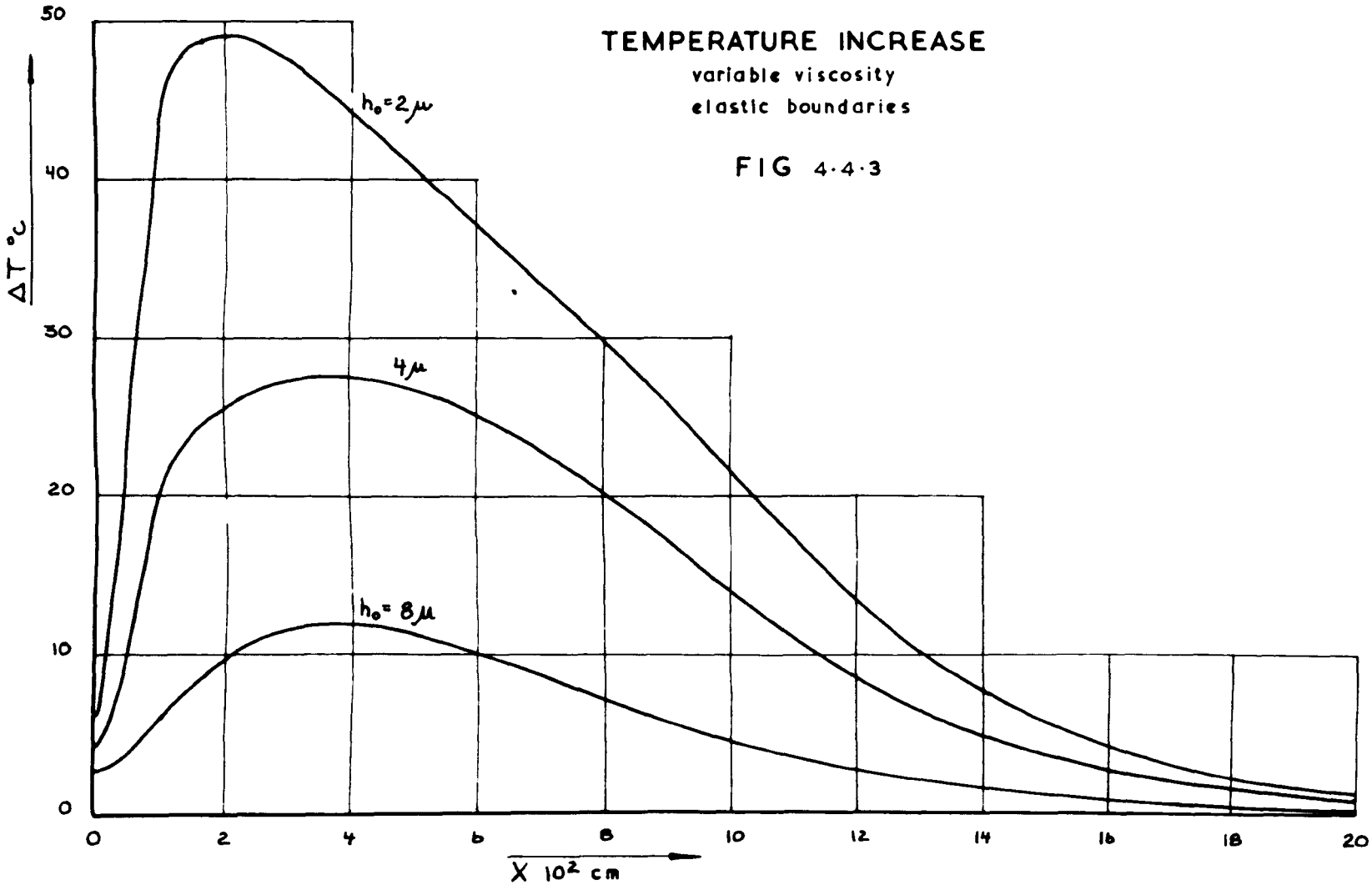
TEMPERATURE INCREASE
variable viscosity
elastic boundaries
FIG 4·4·3
ΔT °C
50
40
30
20
10
0
$h_o = 2\mu$
4μ
$h_o = 8\mu$
0
2
4
6
8
10
12
14
16
18
20
X 10^2 cm

4.5 Velocity of approach

In addition to the pressures etc., the velocity of approach was also calculated for the above cases as function of central film thickness h_o.

The variation of velocity of approach is shown in fig. 4.5.1.

FIG 4.5.1

VELOCITY of APPROACH

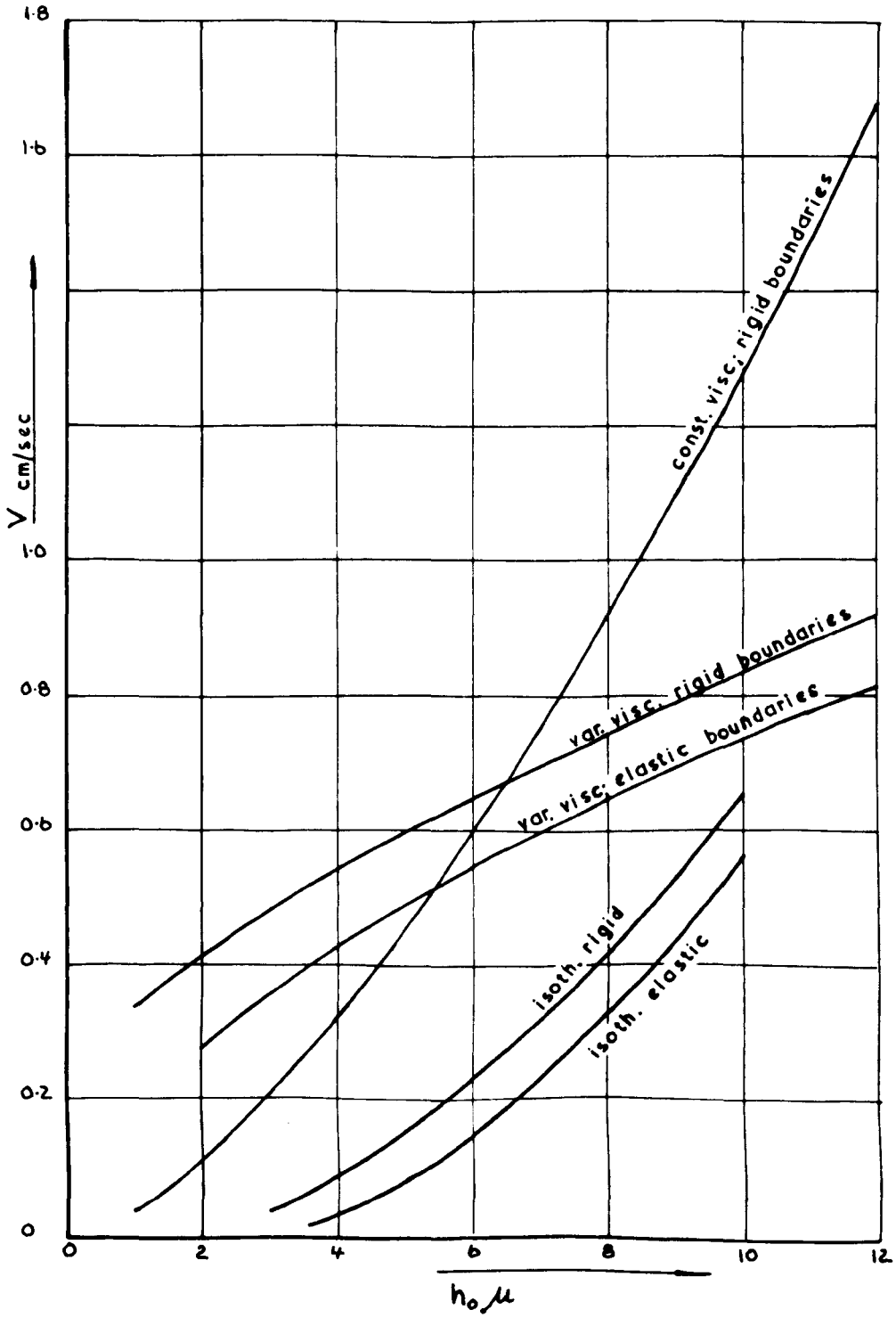

4.6 Isothermal case

In distinction to the previous case which had to be related to a physical apparatus, no such restrictions have been made in this case.

An immediate consequence of this is that a more natural way of solving the system of equations can be attempted. In particular, instead of solving for a constant load W, the more natural condition of keeping the maximum pressure constant, and then computing the corresponding load could be used.

Furthermore, it seemed advantageous to use dimensionless quantities in the computation. A dimensional analysis reveals as possible dimensionless forms:

$$\text{Dimensionalless load} = \frac{\alpha W}{R}$$

$$\text{Dimensionalless pressure} = \alpha P$$

$$\text{Dimensionalless velocity} = \frac{\alpha \mu_o V}{R}$$

$$\text{Dimensionalless film thickness} = \frac{h}{R}$$

Dimensionless pressure distribution, film thickness and loads were computed for values of constant maximum pressure ranging from $\alpha P_o = 10$ down to $\alpha P_o = 1$, as functions of dimensionless central film thickness.

This was done for three different values of the parameter αE, namely:

4.6

$$(\alpha E)_1 = 700$$

$$(\alpha E)_2 = 1{,}000$$

$$(\alpha E)_3 = 1{,}400$$

Since explicit values of viscosity are never required, but are always represented by its pressure coefficient, the difficulty arising in the adiabatic case was never encountered in the case of constant temperature.

However, the difficulty connected with the deformation of the boundaries is more serious in this case, since the solutions are carried to smaller values of film thickness. As can be seen in fig. 4.6.5, the deformation will cause "bumps" in the film shape at some finite distance away from the centre. This will cause the integrands in the I and J integrals to be very unsmooth in the vicinity of this bump, and the higher derivatives (or differences) entering into the remainder of a quadrature formula will be large. Because of this, a simple quadrature formula which does not make use of the higher differences may be found to give the best results. This was found to be so in the present case, and for this reason the trapezoidal rule, rather than Simpsons rule was used in the integrations.

In order to increase the accuracy of the solution, the number of prints used in the integration were increased to N = 40

throughout. In order to best utilize these points, three different interval sizes were used, i.e., $\Delta x = 0{\cdot}01$, $0{\cdot}005$ and $0{\cdot}0025$. The changeover from one interval to the next was not automatic, but had to be decided in each case by looking at the output. The changeover was then effected by feeding into the computer a tape, containing the necessary corrections.

Values of non-dimensional load as function of central film thickness h_o/R for each value of the parameter αE are shown in figs. 4.6.1 - 4.6.4, and film shapes corresponding to $\alpha E = 1{,}000$, $\alpha P_o = 4$ are shown in fig. 4.6.5.

Finally, fig. 4.6.6 - 4.6.8, shows estimated values of the velocity parameter $\frac{\mu_o \alpha V}{R}$

LOAD
$\alpha E = 700$

FIG 4·6·1

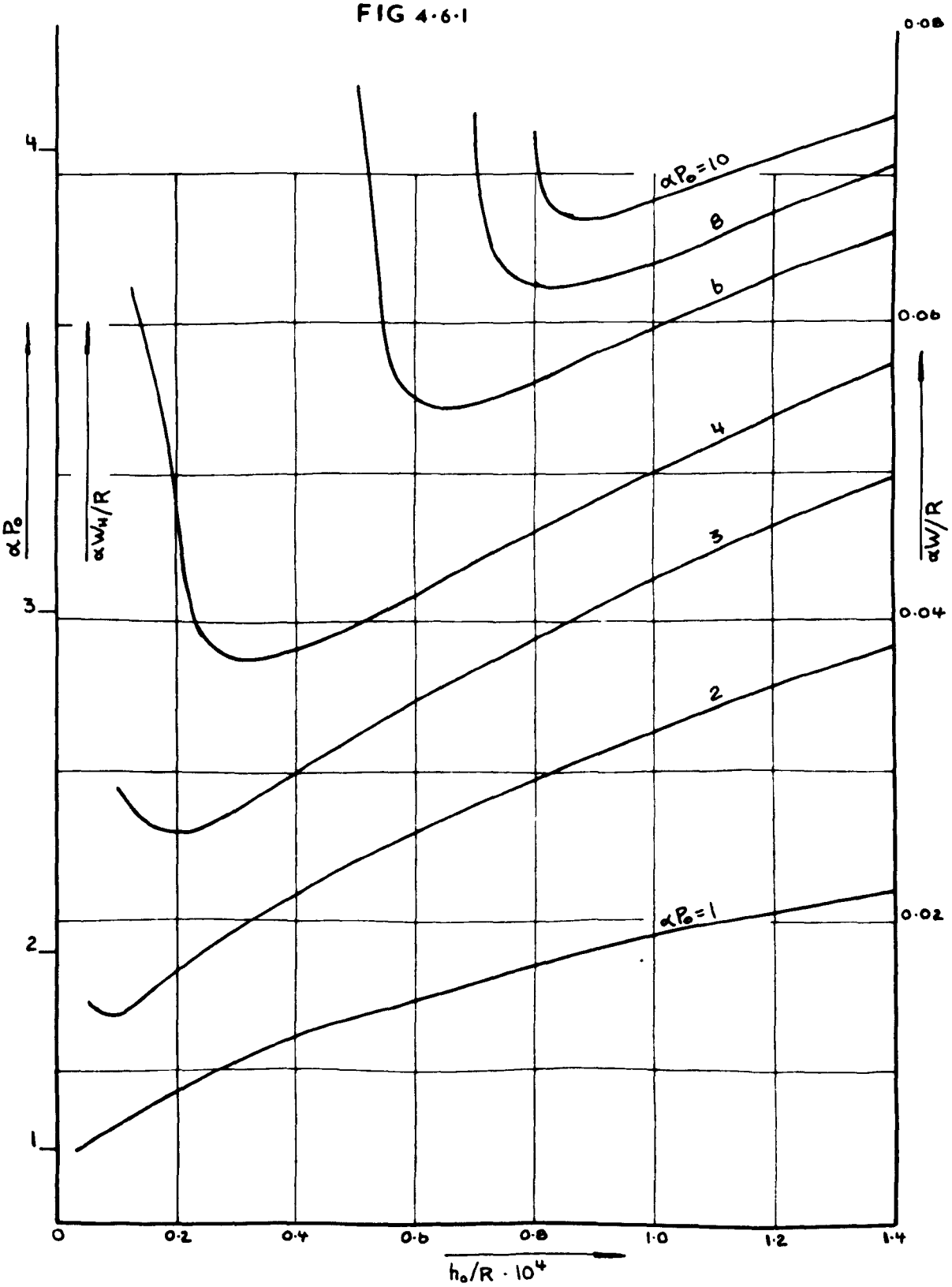

LOAD
$\alpha E = 1000$

FIG 4·6·2

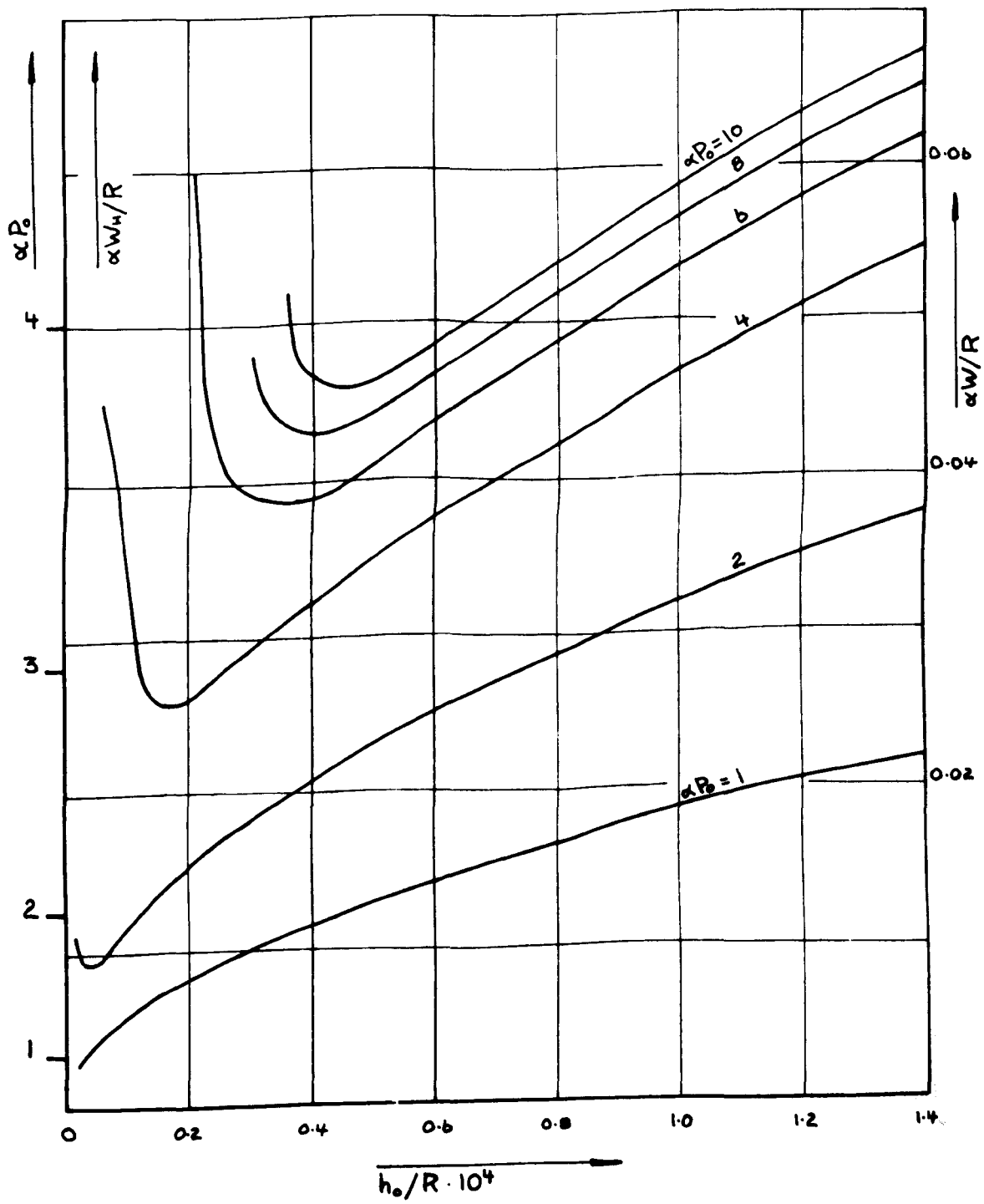

LOAD
$\alpha E = 1400$

FIG 4·6·3

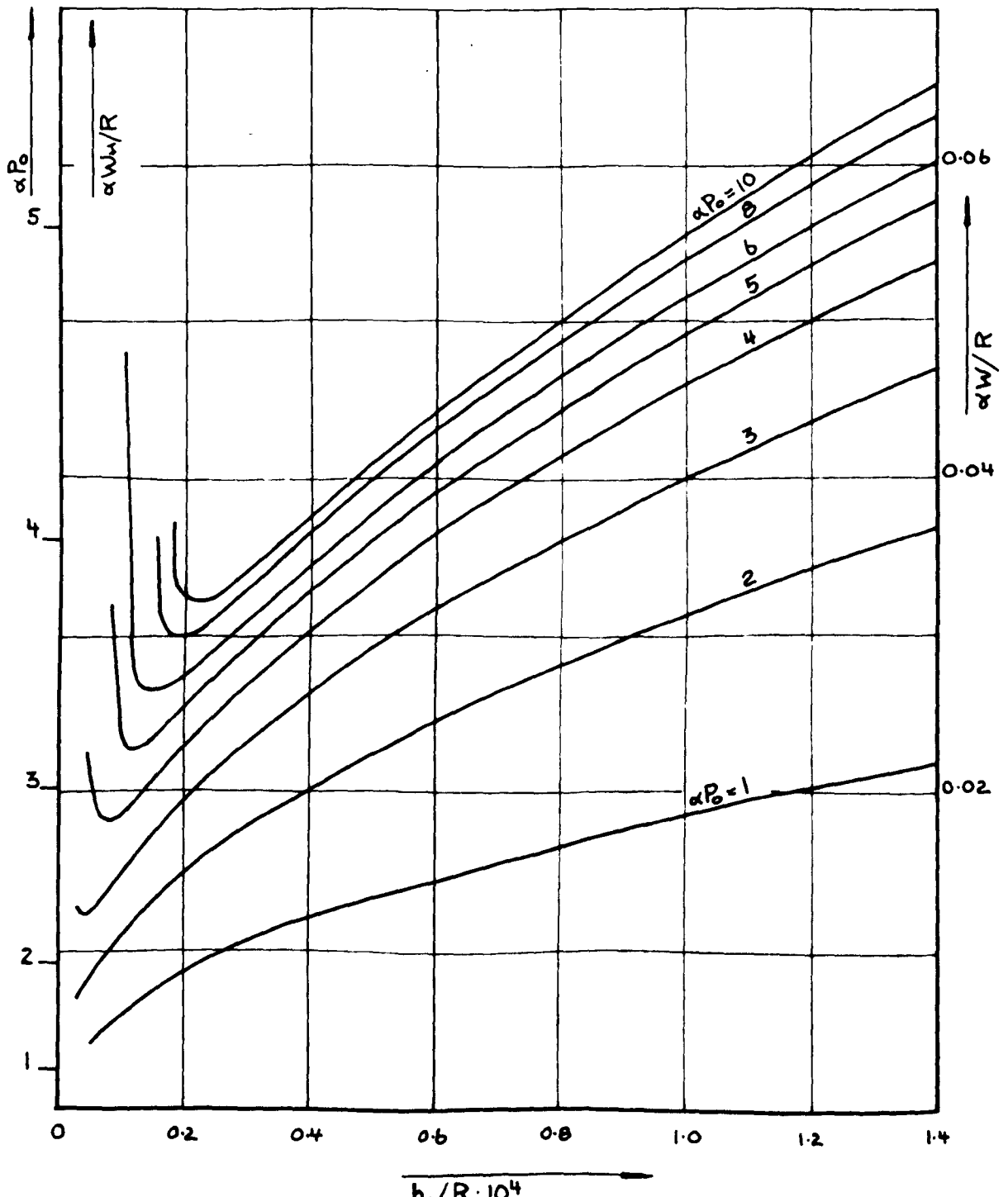

LOAD

CONSTANT VISCOSITY

FIG 4·6·4

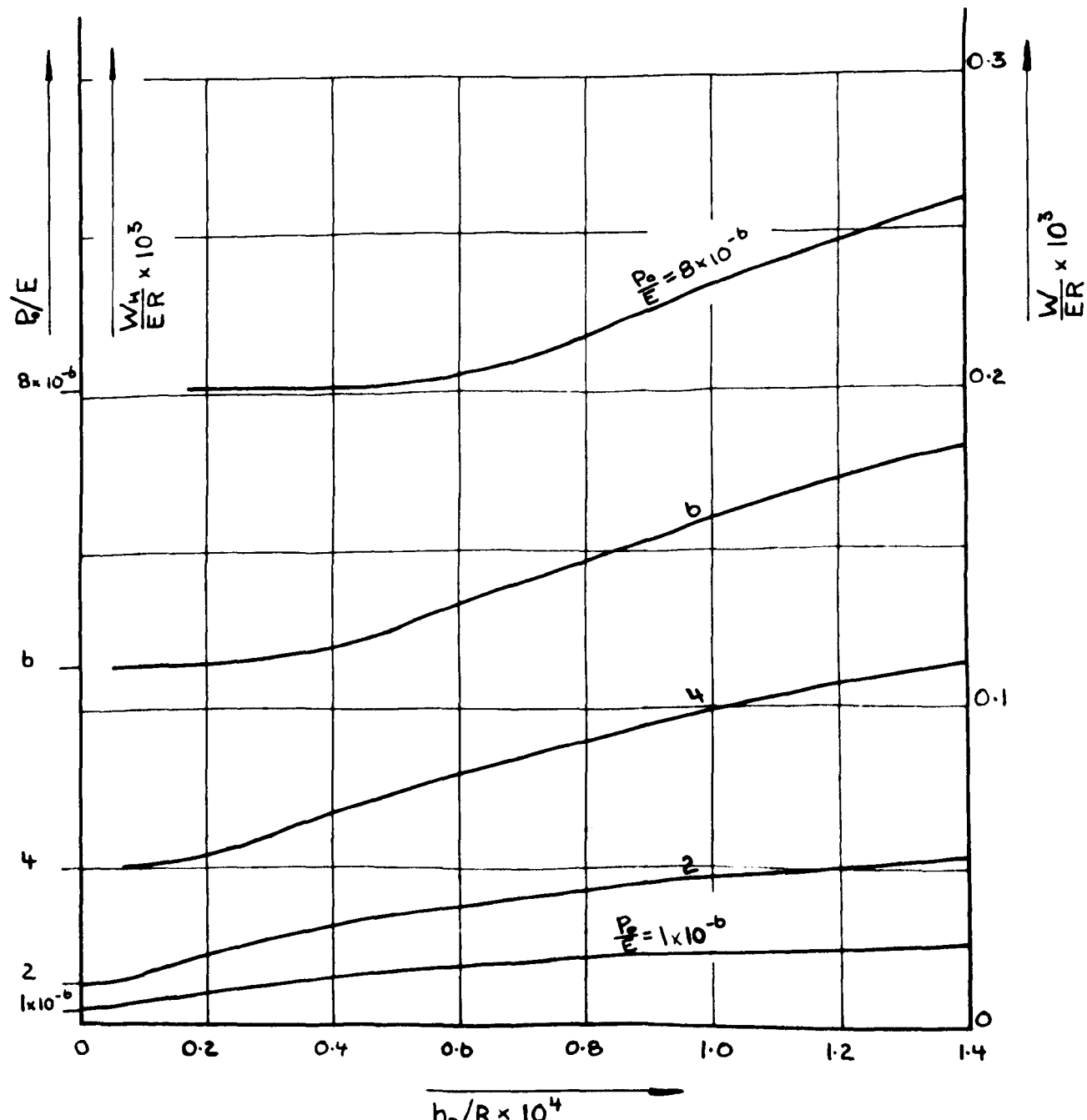

FIG 4·6·5

FILMSHAPES
αE 1000
αP_0 4

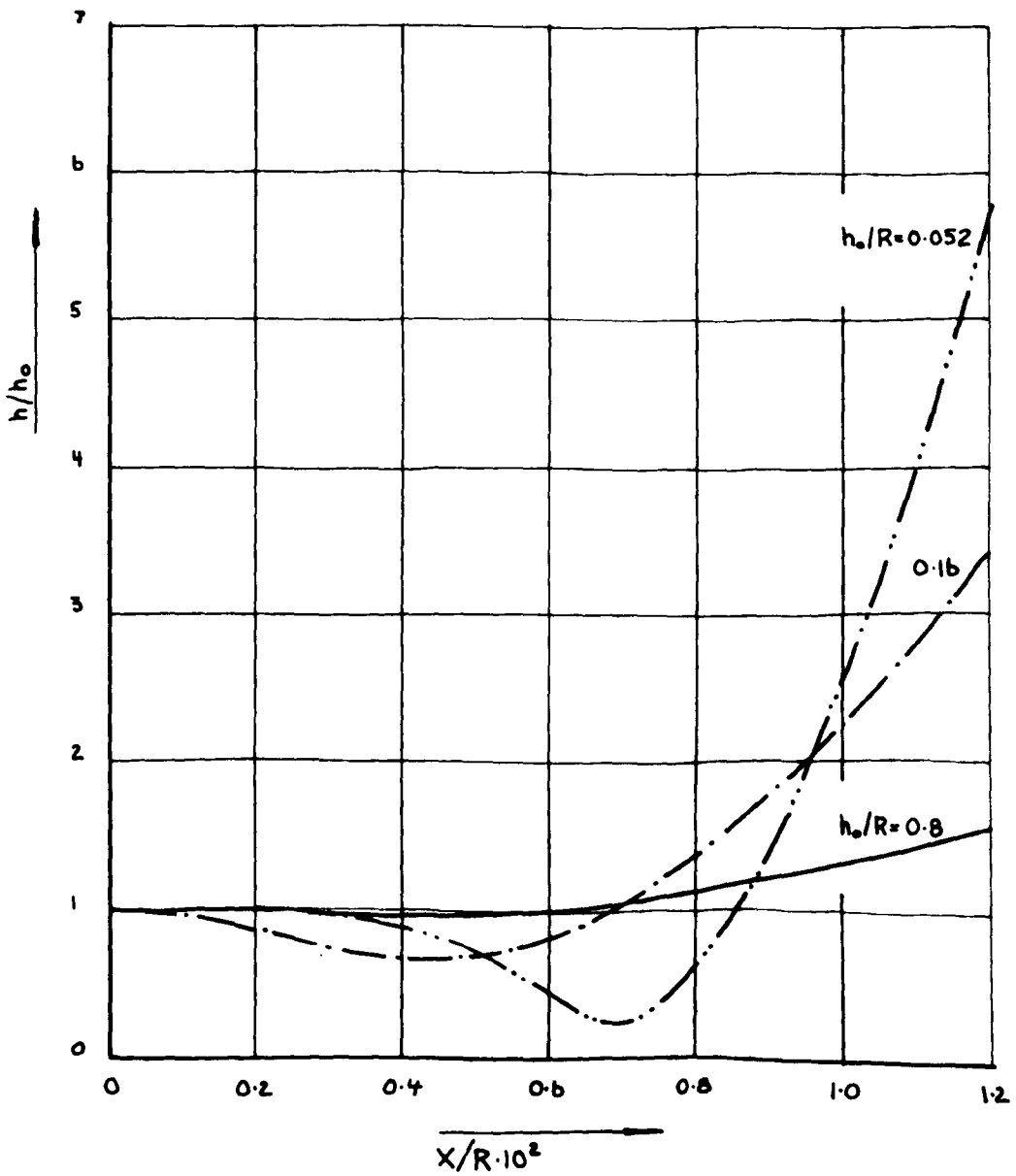

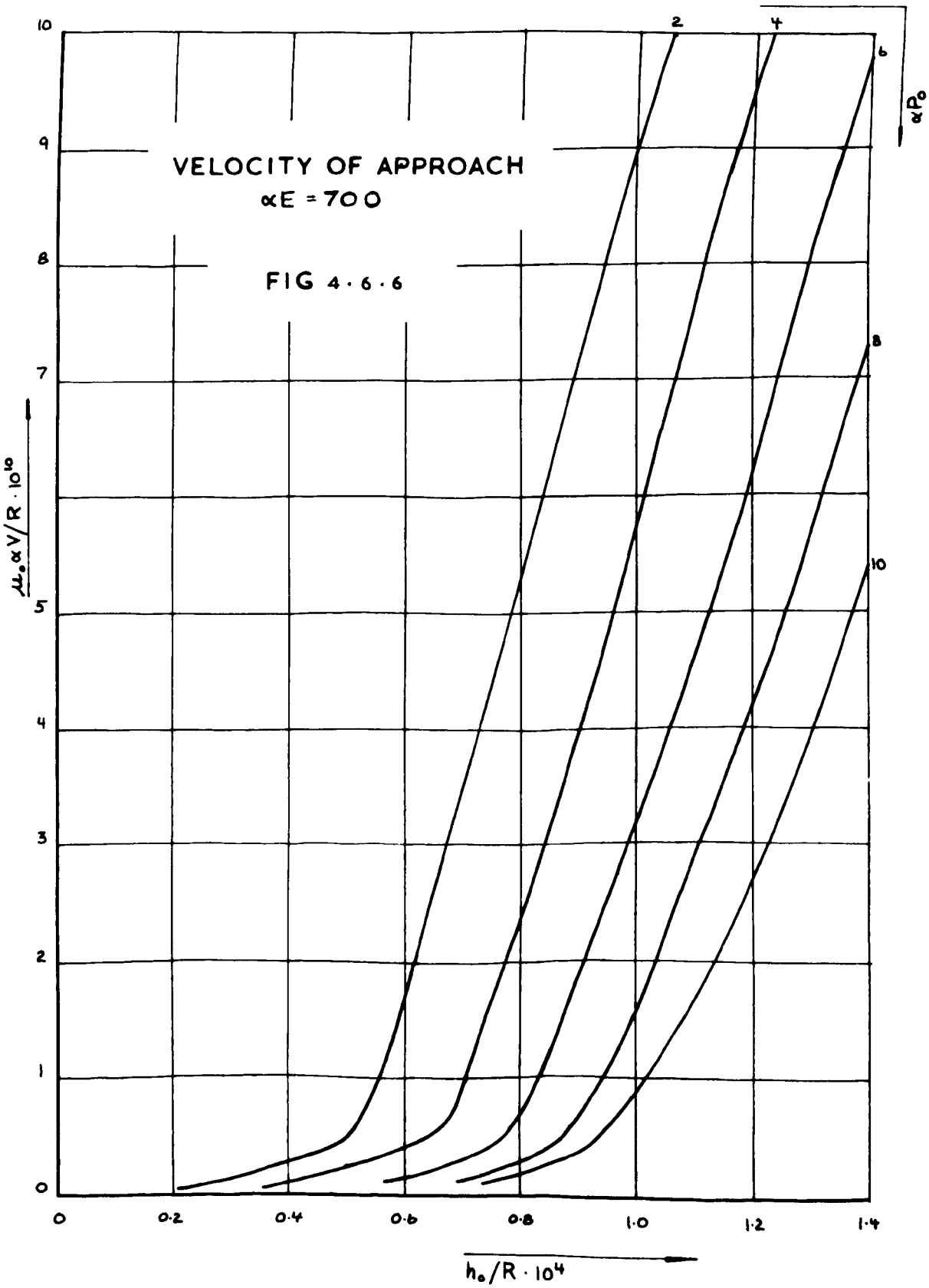
VELOCITY OF APPROACH
∝E = 700
FIG 4·6·6
2
4
6
8
10
∝P₀
μ₀∝V/R·10¹⁰
h₀/R·10⁴
0
0·2
0·4
0·6
0·8
1·0
1·2
1·4
1
2
3
4
5
7
8
9
10

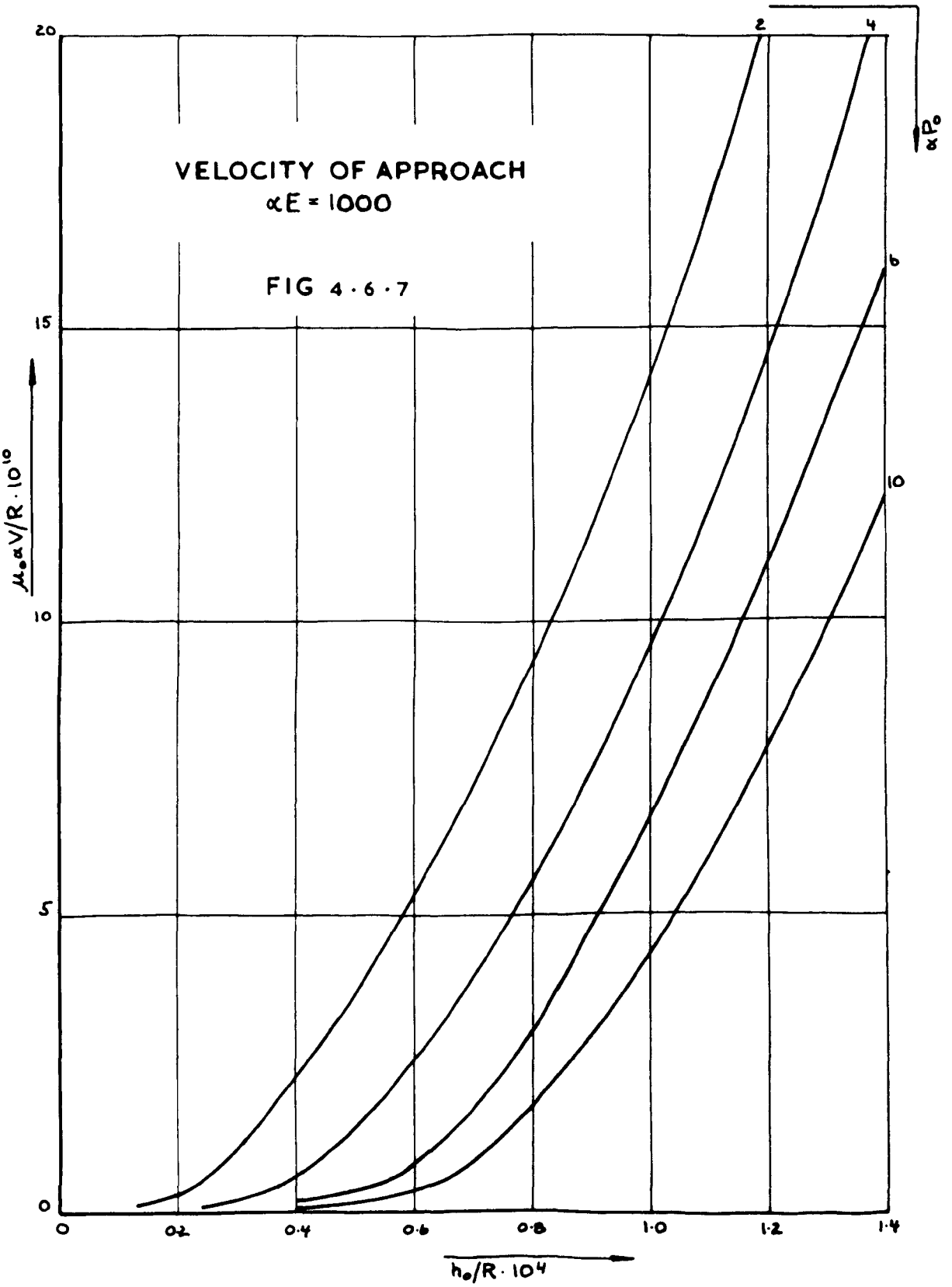
VELOCITY OF APPROACH
αE = 1000
FIG 4·6·7
2
4
6
10
∝P₀
20
15
10
5
0
0
0·2
0·4
0·6
0·8
1·0
1·2
1·4
μ₀αV/R·10¹⁰
h₀/R·10⁴

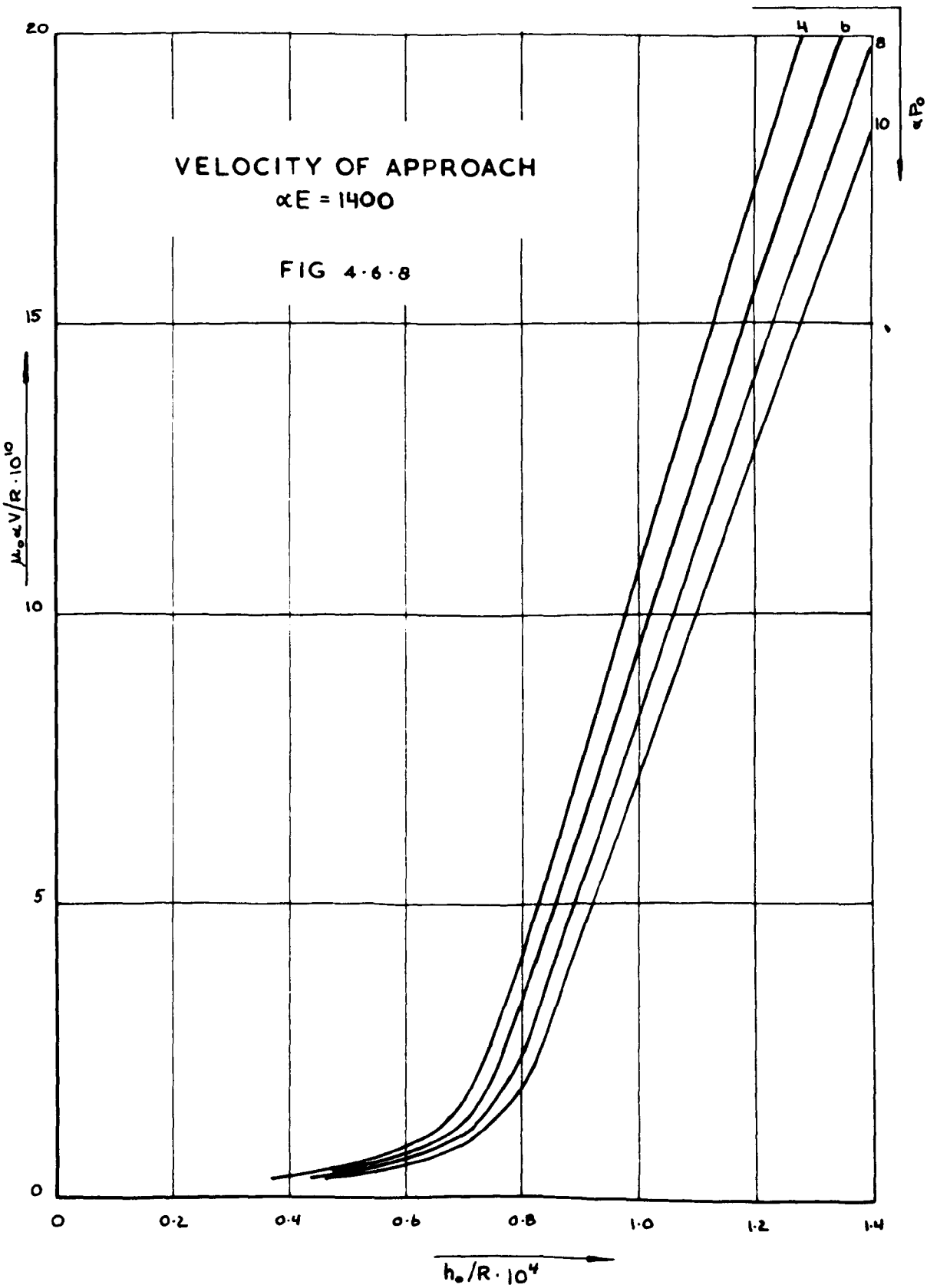
VELOCITY OF APPROACH
∝E = 1400
FIG 4·6·8
20
15
10
5
0
0
0·2
0·4
0·6
0·8
1·0
1·2
1·4
4
6
8
10
∝P₀
μ₀∝V/R·10¹⁰
h₀/R·10⁴

Chapter 5

Discussion

5.1 Discussion of validity of assumptions

In chapter II where the mathematical equations governing the problem were described, it was found necessary to introduce a number of physical assumptions and approximations.

These assumptions can be viewed as being on two levels, i.e., those implicit in the general equation, and secondly the additional assumptions and approximations that had to be introduced in order to reduce these general equations sufficiently to solve them.

One of the first level assumptions not often discussed in the literature is the assumption of constant viscosity introduced into the Navier-Stokes equations, in order to reduce them from their general form 2.2.16 to the form 2.2.17 usually given.

This approximation is checked numerically for the present case, and it is found that only for the highest pressures used would the variable viscosity influence the results appreciable and cause a reduction in the pressure gradient near the centre line.

The analysis is given in appendix A.

Of the more important approximations introduced on the second level, was the assumption that the inertia terms in the momentum equation could be dropped. The argument was supported by an order of magnitude analysis.

This assumption implies a finite discontinuity in the velocities at zero time and hence cannot hold in the initial

stages of the motion. If, however, the initial film thickness is taken large enough, the prescence of inertia reaction will not influence the later stages of the motion, and for this stage the assumption is acceptable.

In the case of the energy equation, it was found necessary to introduce the assumption that the temperature would be constant across the film. It was argued that since the film thickness considered was so small, it was unlikely that any great temperature gradients would exist across it. An argument similar to the one that was used to show that if metals were used for the boundary materials, isothermal conditions would approximately be realized in the oil film, could also be used in order to justify this assumption. Since, in that case, adiabatic conditions were postulated, it would be necessary to put the coefficient of heat conduction of the boundary material equal to zero, and assume some form for the space distribution of the heat sources. This analysis is given in appendix B.

Finally, the results obtained are all derived for a two dimensional space, which implies they would only be valid if the length of the bodies was very much larger than the width of the pressure zone. If this condition is not fullfilled, discrepancies might be expected due to side leakage of the lubricant.

5.2 Discussion of Results

The results presented in the previous chapter fall into two categaries, characterized by the assumptions made about the temperature condition. The adiabatic assumption is the more general in that it includes the isothermal assumption as a particular case. However, as was pointed out earlier, difficulties are met with in its solution. In addition to this, it was also felt that the adiabatic case was too ambitious, in the sense that the solution contains a comparatively large number of parameters. In order to determine the influence of these parameters, a large number of cases in which these parameters would have to be varied in an orderly fashion, would have to be worked out. This would be very time consuming, especially as the program was inherently slow. Therefore, when it also turned out that the isothermal condition seemed to be the more realistic one, the main attention was focused on this case.

This does not mean to say that the work spent on the adiabatic case was considered to be wasted. Apart from the interest of the results themselves, considerable experience of programming for an electronic computer was gained during this phase. Also, a better understanding of the physical and

mathematical problems involved were obtained.

Turning to the results obtained in the adiabatic case, it is seen from fig. 5.2.1 that the introduction of variable viscosity considerably alters the pressure distribution. The maximum pressure obtained for a given film thickness is higher for variable than for constant viscosity. In addition, very high pressure gradients occur in the region of the peak pressure, and this provides the pressure distribution with a very pointed appearance.

On the other hand, the pressure of elastic boundaries does not seem to affect the pressure appreciably for the film thickness considered, even though the surfaces are considerably deformed. The reason for this will be clearer when the isothermal results are considered.

Turning to the temperature distribution, the increase in film temperature is slow when the film thickness is large, but it increases repidly as the film thickness approaches zero. Since the temperature is a cumulative quantity, the actual increase obtained at any film thickness is dependant on the initial film thickness. However, if this is chosen sufficiently large, no great difference will occur between different initial states as the rate of increase at the beginning of the motion is slow.

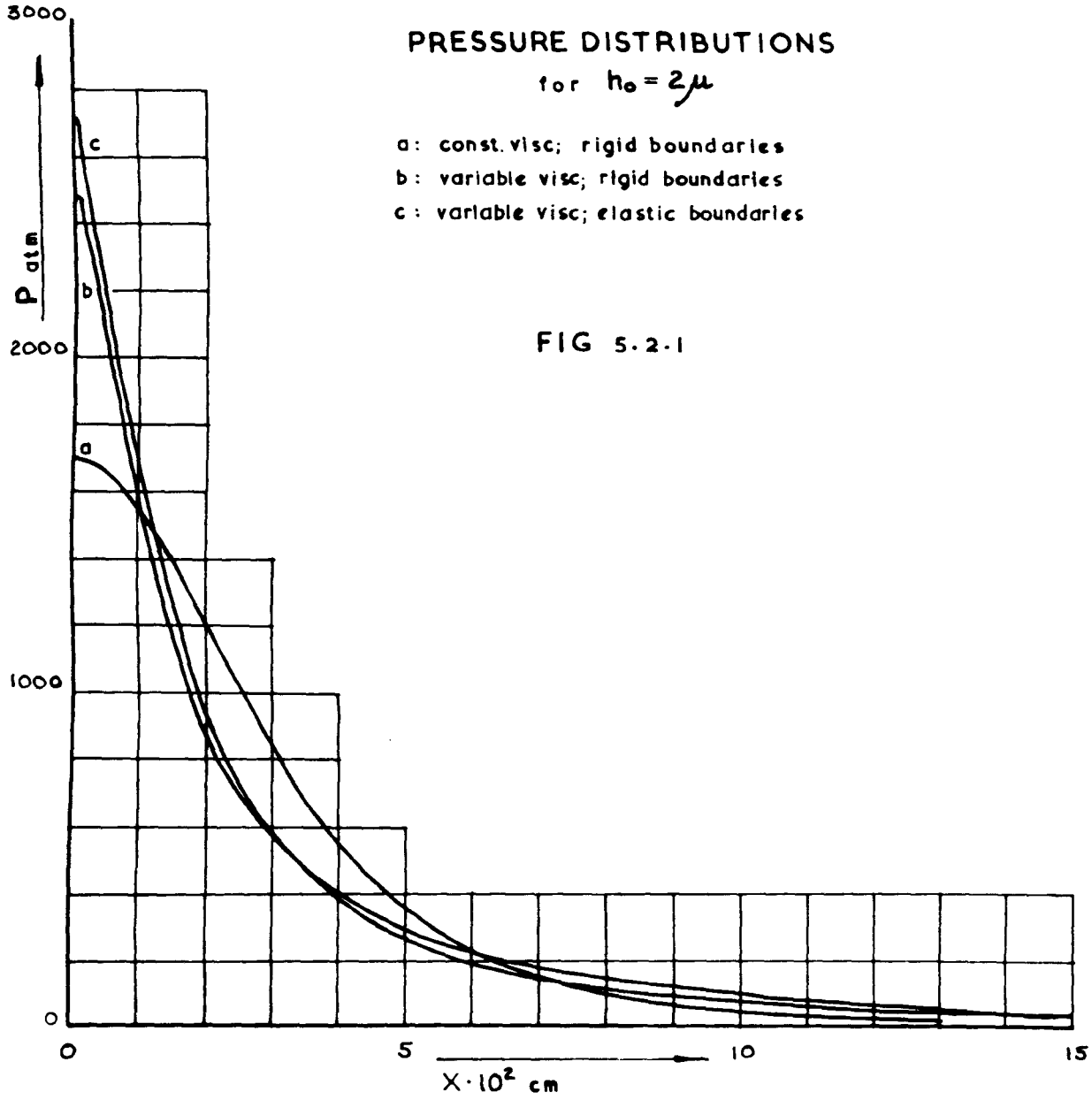
PRESSURE DISTRIBUTIONS
for $h_0 = 2\mu$
a: const. visc; rigid boundaries
b: variable visc; rigid boundaries
c: variable visc; elastic boundaries
FIG 5.2.1
3000
2000
1000
0
P_{atm}
c
b
a
0
5
10
15
$X \cdot 10^2$ cm

5.2

Computing the total heat content as a function of central film thickness, this comes out as a linear function of h_o. This must obviously be so, since the heat generated is due to the work done by the load i.e. $\int_{h_1}^{h_2} W dh_o$

Introduction of variable viscosity have again a marked effect. As was found for the pressures, the temperature gradient in the region of the maximum temperature becomes very steep and the maximum temperature is increased. At the same time the position of the maximum has moved closer to the centre of the cylinder. This is clearly due to the influence of pressure and temperature upon the viscosity.

This effect is illustrated in fig. 4.3.2, which showes the viscosity distribution for various values of h_o. The presence of a high central pressure together with a low temperature in this region produces a very high value for the viscosity. At a little distance from the centre the pressure is considerably reduced, while on the other hand the temperature is a maximum. This will cause a rapid reduction in viscosity, depending upon the sensitiveness of viscosity on pressure and temperature. At larger distance from the centre, viscosity will asymptotically approach its normal value. Consequently, over a large portion of the range, viscosity may be appreciably lower than the value under normal conditions and this, one might expect, would have

TOTAL HEATCONTENT & MAX. TEMPERATURE

case a: const. visc; rigid boundaries
case b: variable visc; rigid boundaries

FIG 5·2·2

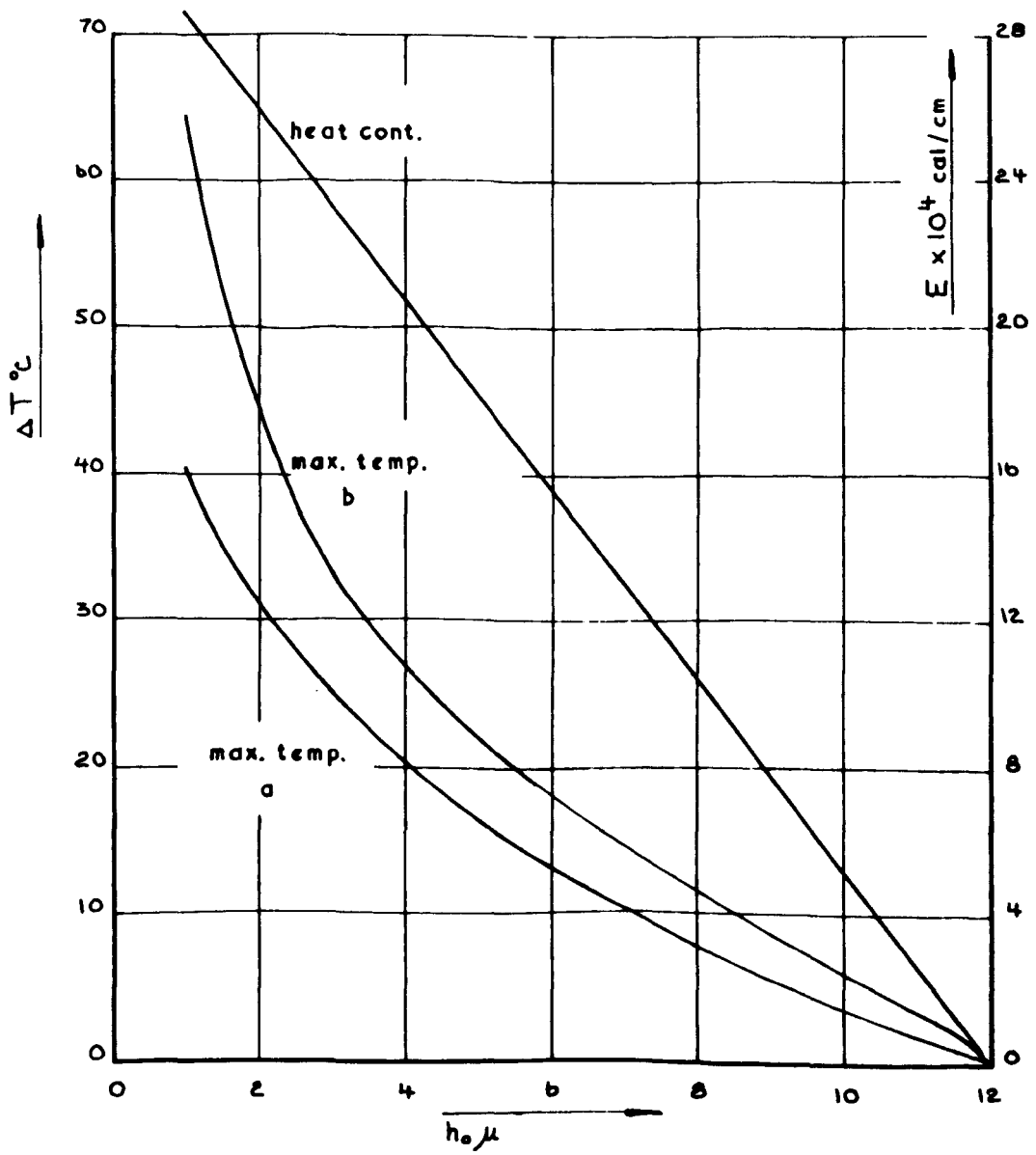

a considerable influence upon the motion. A single parameter that will perhaps best measure this influence for constant load is the velocity of approach. From previous the velocity of approach is expressed by

$$V = \frac{W}{24S}$$

where

W = constant load

$$S = \int_0^{\infty}\int_x^{\infty} \frac{\mu x\, dx}{h^3}$$

i.e., the velocity of approach is only dependant upon viscosity and its distribution in the case of rigid boundary materials.

Fig. 4.5.1, showes the velocity of approach as a function of central film thickness h_o for the various cases, and showes the influence of viscosity very clearly.

At some value of film thickness $h_o < H$, the velocity of approach of the variable viscosity case is larger than for the corresponding constant viscosity case. In fig. 4.5.1, the estimated value of velocity of approach for the isothermal case has also been plotted. As expected this always is lower than the constant viscosity velocity.

These curves also show the small influence of the elastic deformation for the range of film thicknesses considered. Apart

from an approximate constant difference, corresponding curves for rigid and elastic cases are nearly identical. The constant difference arises from the fat that what is computed is the relative velocity of the two surfaces. Since in the elastic case, deformation produces a surface velocity opposite in sense to the general motion of the cylinders, this will have the effect of reducing the velocity of approach as defined here.

Isothermal case:

The simplifications brought about by the assumption of isothermal conditions are considerable in two ways. First the mathematical relations themselves can be expressed in a simpler form that is more amenable to numerical treatment. Secondly, the number of parameters involved is reduced, and this makes the results easier to interpret.

Dimensional analysis of the isothermal problem reveals the following possible set of non-dimensional main parameters:

$$\Pi_1 = \alpha P_o$$
$$\Pi_2 = \alpha E$$

where

α is the pressure coefficient of viscosity

P_o is maximum pressure

E is an expression involving the elastic constants of the boundary materials

5.2

The non-dimensional form of the main independant variables is

$$\pi_3 = h_c/R$$

$$\pi_4 = x^2/2Rh_c$$

The form of the equation 2.13.7, show that the condition of constant load is not a matural one from a mathematical point of view, and it is better to solve for constant maximum pressure rather than constant load. That such a procedure is rarely realized in nature does not matter if one assumes that the equations have a unique solution, which seem to be a reasonable assumption from physical considerations.

In contradistinction to the adiabatic case where numerical solution of several particular cases such as rigid boundaries, constant viscosity etc., had interest, the isothermal case only have two particular cases, ie., elastic boundaries, with constant or variable viscosity. This is so since in the isotherm problem the rigid solution can be obtained by analytic methods. Since viscosity is expressed by a law of the form $\mu = \mu_0 e^{\alpha P}$ the case constant viscosity can strictly speaking be obtained as the limit of the general case with $\alpha \to 0$
As, however, the limit can never be obtained by numerical means, this property has not been employed. No fundamental numerical differences occur between the two cases, and since the case of

variable viscosity yields the more interesting results, emphasis have been given to this case.

The main results are given in fig. 4.6.1 - 4.6.3. Here the load is plotted as a function of central film thickness for a range of values of maximum pressure. The three figures correspond to the three different values of the parameter αE

Fig. 4.6.3	αE	= 1,400
4.6.2	αE	= 1,000
4.6.1	αE	= 700

By comparing these curves with the corresponding rigid solutions fig. 2.13.2, some conclusions can immediately be drawn. It is apparent that the elastic loads for a given h_o and P_o are always greater than the rigid load, and furthermore as the film thickness increases, this difference becomes smaller so that the two loads will approach each other asymtotically as h_o increases. Furthermore, by comparing corresponding curves for the three values of the parameter αE, it is seen that for a given h_o, the largest difference occurs for the case with the lower value of αE, i.e., $\alpha E = 700$ and the least difference for the case $\alpha E = 1,400$. The reason for this is readily apparent when we consider that for constant value of α in the three cases, the case with the lower value of αE represent a "soft" material.

For such a material the deformation for any load will be greater and hence the influence of this deformation will be more strongly felt.

Similarly, for a given value of αE, the difernece for any value of h_o is greater for higher values of αP_o. For the smaller values of αP_o, i.e., for small loads, the elastic loads nearly coincide with the rigid ones, except for very small values of film thickness.

The most conspicuous feature of the load curves is that they all exhibit a minimum at some specific value of film thickness. This feature is completely absent from the rigid loads, which all converges uniformly to zero as film thickness approaches zero. The film thickness at which the minimum occurs, depends upon the value of maximum pressure αP_o and on the parameter αE, growing larger with increasing αP_o and αE. Furthermore, it will be observed that the minimum load necessary to produce a given maximum pressure is less, the higher the value of αE, i.e., the more rigid the boundary material is. Also in order to increase the maximum pressure from αP_o to $\alpha P_o + \delta(\alpha P_o)$ a load increment $\delta(\frac{\alpha W}{R})$ must be applied and this increment is getting smaller the higher the value of αP_o and the lower the value of αE. The result is shown in fig. 5.2.3.

It is observed that for a sufficiently high value of αP_o,

FIG 5·2·3

MINIMUM LOAD

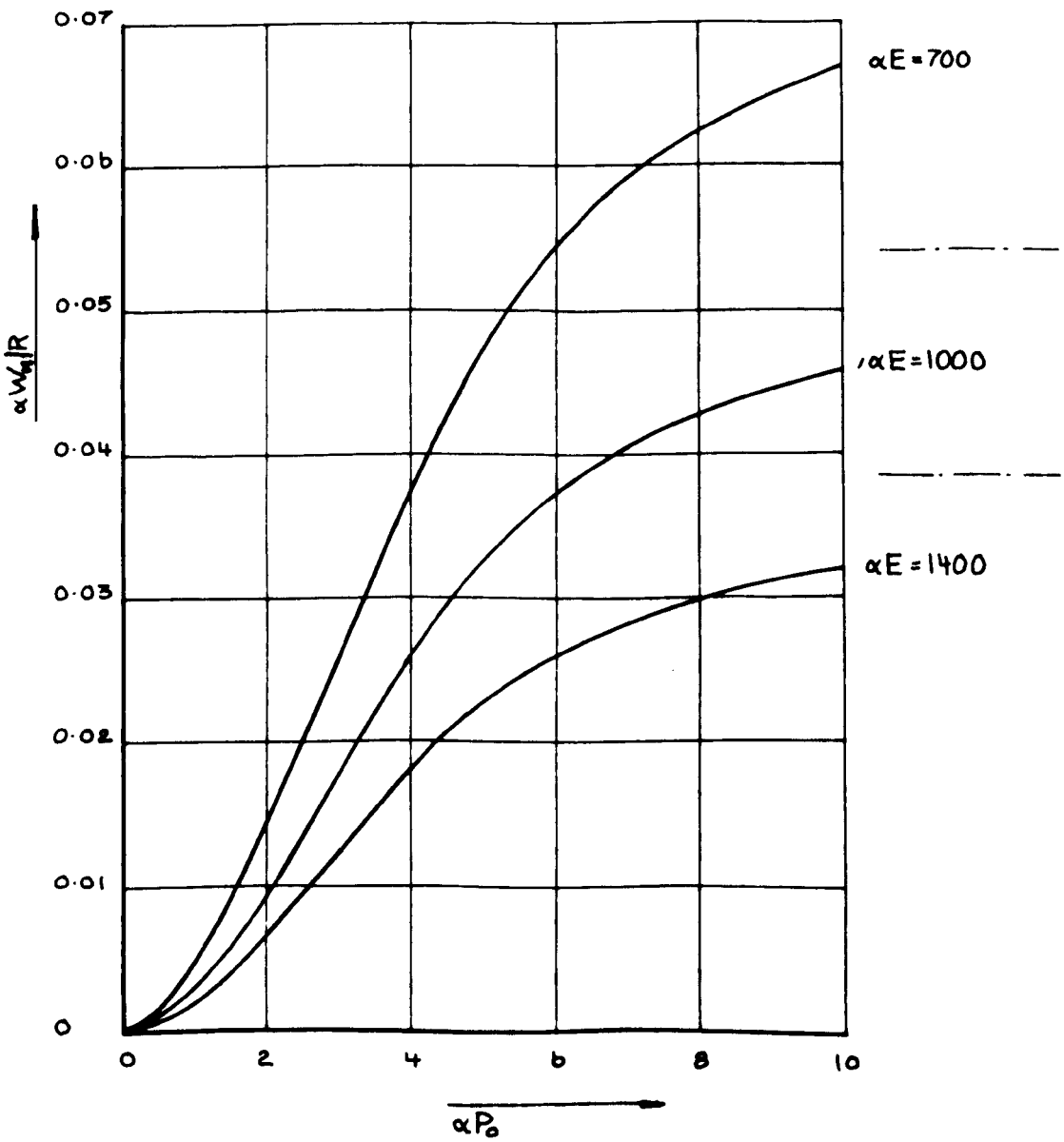

the curve with $\alpha E = 1{,}400$ is drawn with a small gradient, i.e., a small increase in load will result in a large increase in maximum pressure. For the curve $\alpha E = 700$, the gradient is larger, i.e., a larger load increment must be applied in order to effect the same change in pressure, or looked upon in a different way, the value of αP_o must be higher in order to have the same gradient.

The reason for this behaviour is suggested by the appearance of the rigid load curves fig. 2.13.2. At a sufficiently high value of αP_o, a very small increase in load is sufficient to bring about a large increase in central pressure. Indeed, an infinite value of pressure can be obtained at any film thickness by the application of a finite load This is because of the exponential viscosity. When elastic materials are considered, the behaviour is modified by the deformation of the surfaces. The load is still bounded, but due to the deformation, the load that must be applied in order to raise the central pressure to infinity is now a function of the elastic properties of the material, and increases with decreasing values of αE. The result is in any case of theoretical interest only, and would not be realized in practice.

Returning to the load curves figs. 4.6.1 - 4.6.3, another important characteristic of the motion is suggested. If the Hertzian load given by the equation

5.2

$$\frac{\alpha W_h}{R} = \pi \frac{(\alpha P_o)^2}{\alpha E}$$

and which represent the dry contact load between elastic cylindrical bodies as function of the maximum pressure developed and the elastic properties of the bodies, is computed and set out along the load axis, then a "reasonable" extrapolation of the load curves drawn to zero film thickness would terminate the load curves at their corresponding Hertzian loads. This feature is perhaps brought out clearest in Fig. 4.6.2 for values of maximum load of $\alpha P_o = 2, 3$ and 4.

If this conjecture is correct, a corresponding convergence of the pressure distribution towards that of the Hertzian ellipse should be noticable as film thickness is decreased. That this seems to be so is shown in fig. 5.2.4 where pressure distributions are drawn for the values of $\alpha P_o = 4$ and $\alpha E = 1{,}000$. These curves taken in conjuction with the load curves, also show that the pressure distribution is very sharp at the point of minimum load. This must clearly be so and is indeed the reason for the minimum obtained in the loads.

Considering now the change of film shape as film thickness is reduced, this was shown in fig. 4.6.5. The effect of

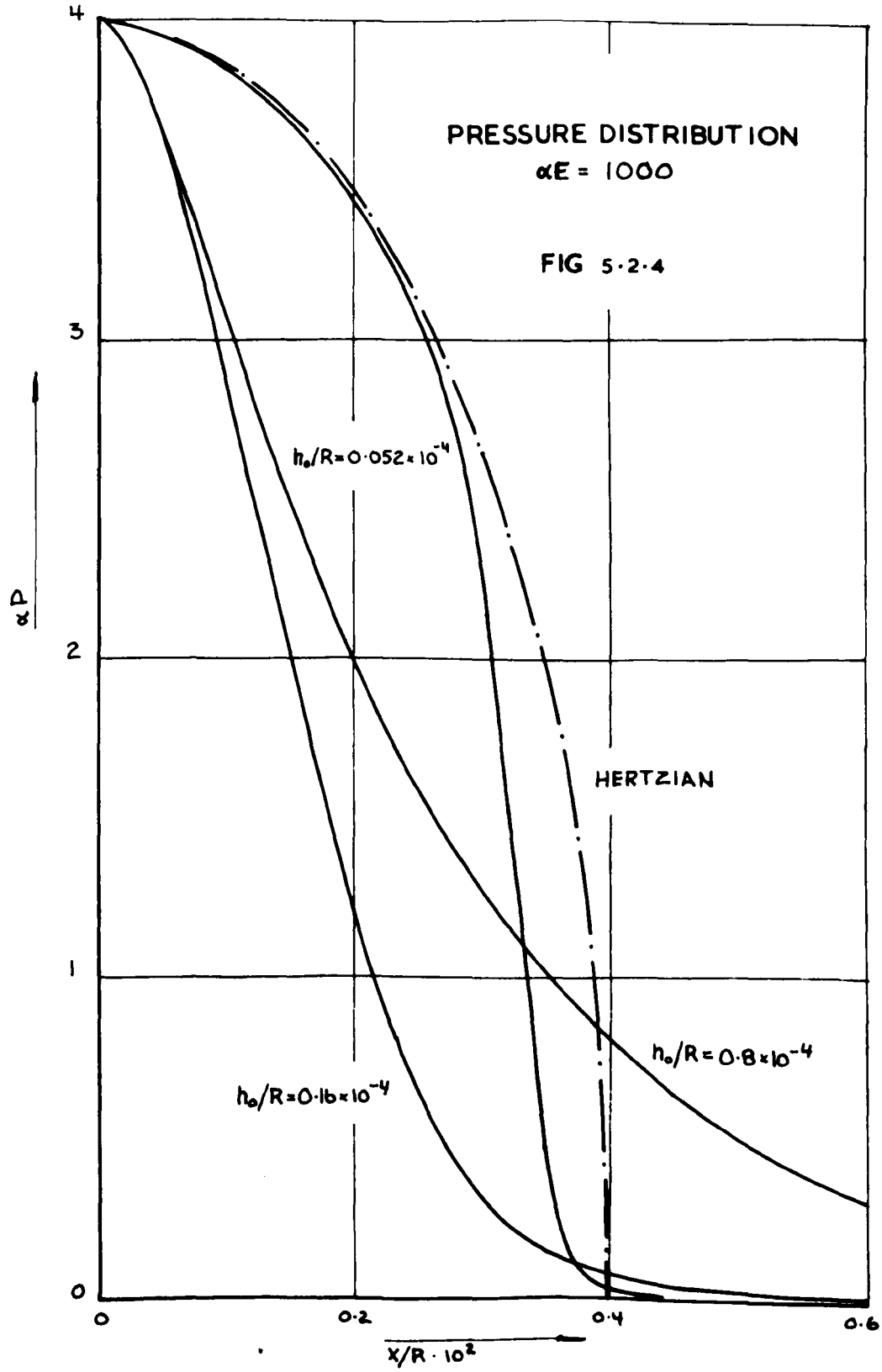
PRESSURE DISTRIBUTION
αE = 1000
FIG 5·2·4
4
3
2
1
0
αP
$h_o/R = 0.052 \times 10^{-4}$
HERTZIAN
$h_o/R = 0.8 \times 10^{-4}$
$h_o/R = 0.16 \times 10^{-4}$
0
0·2
0·4
0·6
$X/R \cdot 10^2$

deformation is seen to reduce the cylinder curvature, and as film thickness is further reduced, to reverse it in a region near the centre line. Thus a bump is produced at some distance away from the centre. This feature of the solution is common to the rolling or sliding solutions which also show a characteristic bump at the outlet end of the loaded zone. As the film thickness approach the minimum load value, the relative amplitude of the bump increases, and at the same time it is moving outwards away from the centre. The region between the bump and the centreline is gradually flattened out and approaches the Hertzian flat.

Returning once more to the load curves, if for any given value of αP_o we form the ratio of the Hertzian load to that of the minimum load corresponding to the chosen value of αP_o then, within the accuracy of the calculation, this ratio appears to be independant of αE.

Forming this ratio for the various values of αP_o, the result is given in the table below.

5.2

αP_o	Wh/Wm				
	αE= 1400	αE= 1000	αE= 700	Mean Value	Max. % Dev.Mean
1				1·12	
2	1·38	1·32	1·28	1·33	3·7
3	1·59	1·61	1·59	1·59	1·25
7	1·99	1·93	1·95	1·96	1·50
5	2·47	2·30	2·38	2·38	3·70
6	3·11	2·92	2·96	2·99	4·0
8	4·80	4·67	4·60	4·69	2·3
10	7·00	6·90	6·75	6·88	1·9

Here the ratio Wh/Wm is formed for the three different values of αE, the arithmetic mean is calculated and the maximum percentage deviation from the mean found. This deviation is within the accuracy with which the load curves were calculated.

If this ratio is now plotted as a function of αP_o, the points indicated by crosses in fig. 5.2.5 is obtained, and attempting to fit a least square parabola to these points, the full line drawn in fig. 5.2.5 appears. This suggests that a simple mathematical relation holds for the ratio

$$\frac{\alpha W_n}{R} \Big/ \frac{\alpha W_m}{R} = 0.0582\ (\alpha P_o)^2 + 1 \qquad 5.2.1$$

FIG 5·2·5

$$\frac{\alpha W_H}{R} \Big/ \frac{\alpha W_M}{R} = 0.0582(\alpha P_o)^2 + 1$$

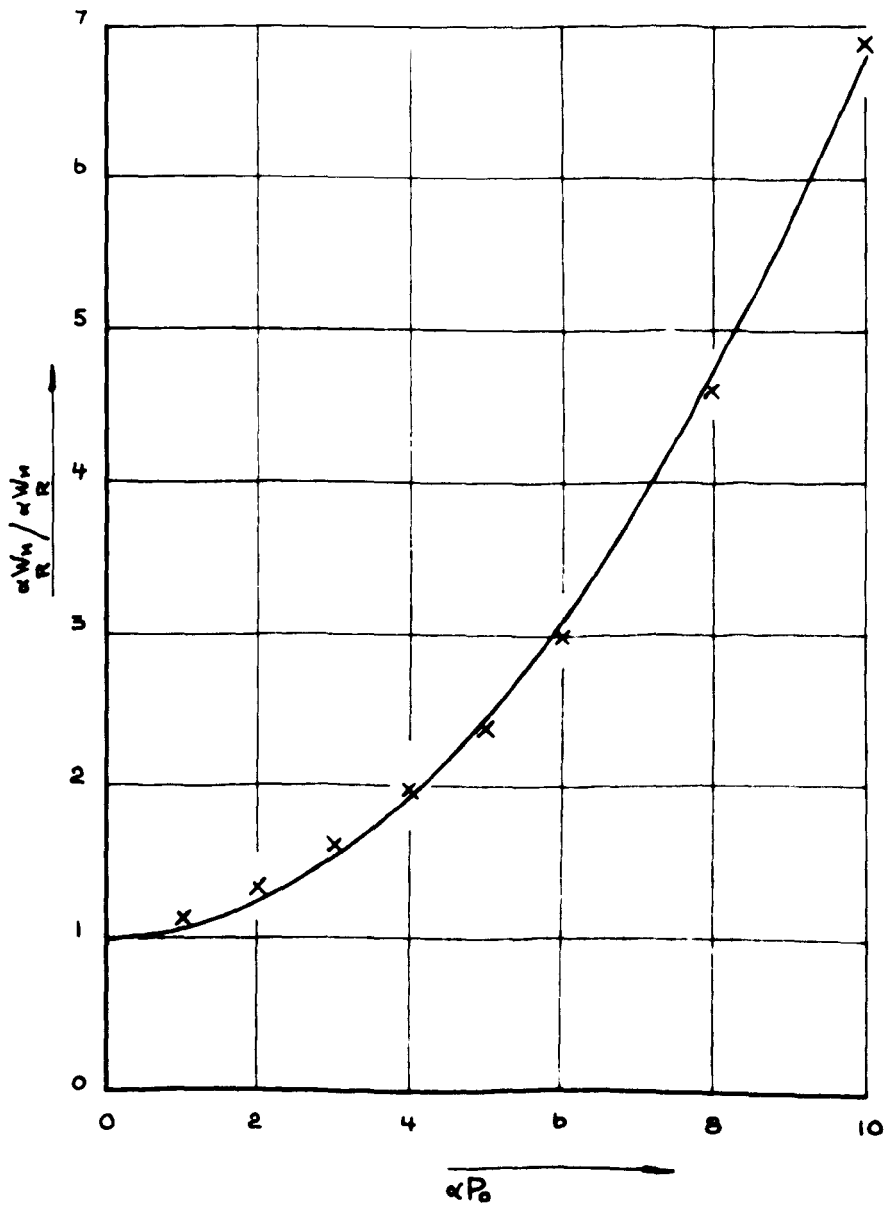

5.2

The deeper significance of this, if any, is not yet clear.

Since the expression for the Hertzian load is known to be

$$\frac{\alpha W_h}{R} = \pi \frac{(\alpha P_o)^2}{\alpha E} \qquad 5.2.2$$

then the equation for the minimum load becomes

$$\frac{\alpha W_m}{R} = \frac{\pi (\alpha P_o)^2}{\alpha E \left[1 + K(\alpha P_o)^2 \right]} \qquad 5.2.3$$

where $K = 0{\cdot}0582$

This must then be the equation for the curves drawn in fig. 5.2.3. Assuming that it also holds for values of $\alpha P_o > 10$ and for different values of αE than the ones used, this expression can be used to extrapolate the curves fig. 5.2.3 to higher value of αP_o and for different αE.

In particular the expression should hold for the case of constant viscosity, i.e., by taking $\alpha = 0$. In this case 5.2.1 gives

$$W_m = W_h$$

i.e., the minimum load should coiside with the Hertzian.

In order to check this prediction, and also for its own intrinsic interest, the constant viscosity case was computed. The load curves for this case was shown in fig. 4.6.4 for $E = 10^{12}$ dyn/cm^2.

The predicted behaviour that the minimum load should coincide with the Hertzian appears to be verified. In addition it is also noticed that the load that must be applied in order to get a specified maximum pressure is very much increased as expected.

In order to describe the various features of the solution in more natural terms, suppose a hypothetical experiment is performed.

Let an elastic cylinder with negligable mass of radius $R = 5$ cm and of unit length, made of a material with the elastic constants $E = 1275 \times 10^9$ dyn/cm^2, $\nu = 0{\cdot}3$ approach an elastic flat plate of the same material under a constant load $W = 150 \times 10^6$ dyn/cm. Furthermore let the lubricant separating the bodies have a pressure coefficient of viscosity of $\alpha = 1 \times 10^{-9}(\text{dyn/cm}^2)^{-1}$

We thus have $\alpha E = 700$. $\frac{\alpha W}{R} = 0{\cdot}03$

The motion will be described by a horizontal straight line in fig. 4.6.1 passing through the value of load $\alpha W/R = 0{\cdot}03$.

5.2

The maximum pressure in the oil film at succeeding stages of the motion is given by the intersections of the straight path with the load curves. The values of maximum pressure is plotted in fig. 5.2.6. If now the experiment is repeated with a harder material i.e., $E = 1820 \times 10^9$ dyn/cm^2, $\nu = 0{\cdot}3$, $\alpha E = 1{,}000$ the motion is described by a similar line in fig. 4.6.2.

The value of maximum pressure in the oil film at any stage of the motion for the three cases

$\alpha E = 700$, $\alpha P_{max} = 3{\cdot}45$

$\alpha E = 1{,}000$, $\alpha P_{max} = 4{\cdot}50$

$\alpha E = 1{,}400$, $\alpha P_{max} = 8{\cdot}00$

is shown in fig. 5.2.6.

From these curves it is apparant that a very high pressure occurs in the oil film at a finite film thickness. The value of the maximum pressure is proportional to αE, and the film thickness at which it occurs is inversly proportional to αE.

If now these experiments are repeated, but this time applying a load 6·6% higher than in the previous series, a new set of curves is obtained. The maximum pressure reached fig. 5.2.7 is now higher, and relative to the first series, increase of maximum pressure is 4·35%, 6·7%, and 25% respectively.

FIG 5·2·6

MAXIMUM PRESSURE

LOAD $\alpha W/R = 0.03$

$\alpha = 10^{-9}[\text{dynes}/\text{cm}^2]^{-1}$

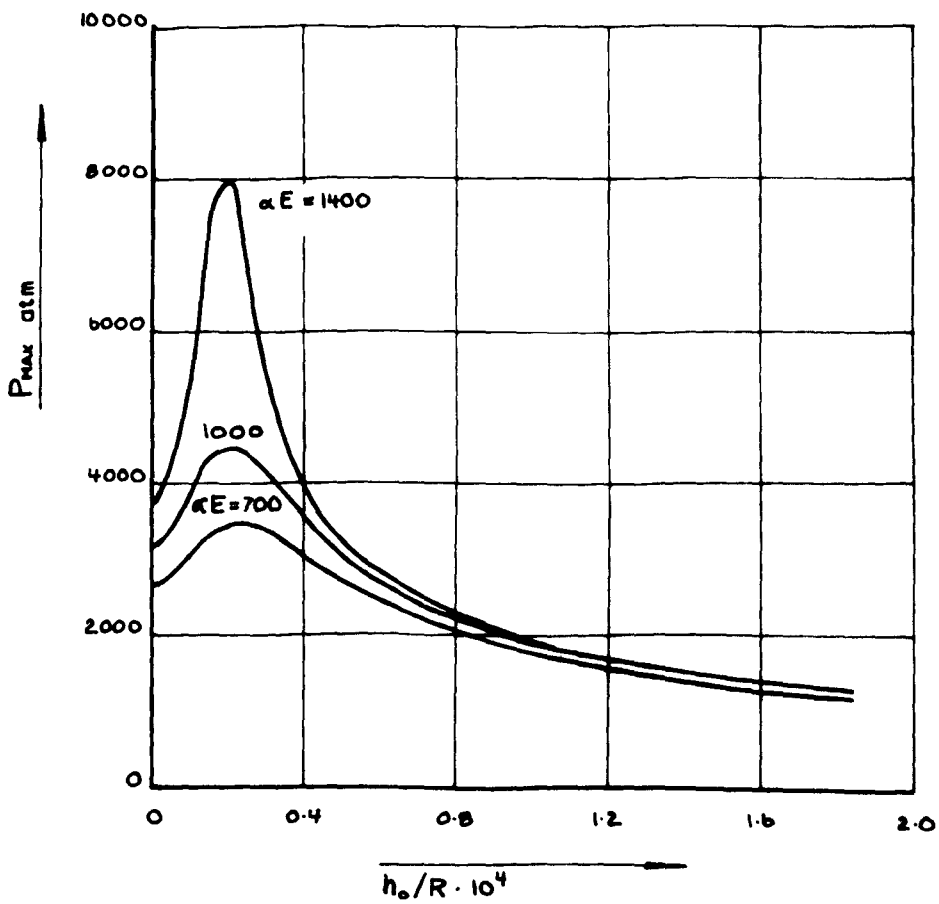

FIG 5·2·7

MAXIMUM PRESSURE
LOAD $\alpha w/R = 0{\cdot}032$
$\alpha = 10^{-9}\,[\text{dynes}/\text{cm}^2]^{-1}$

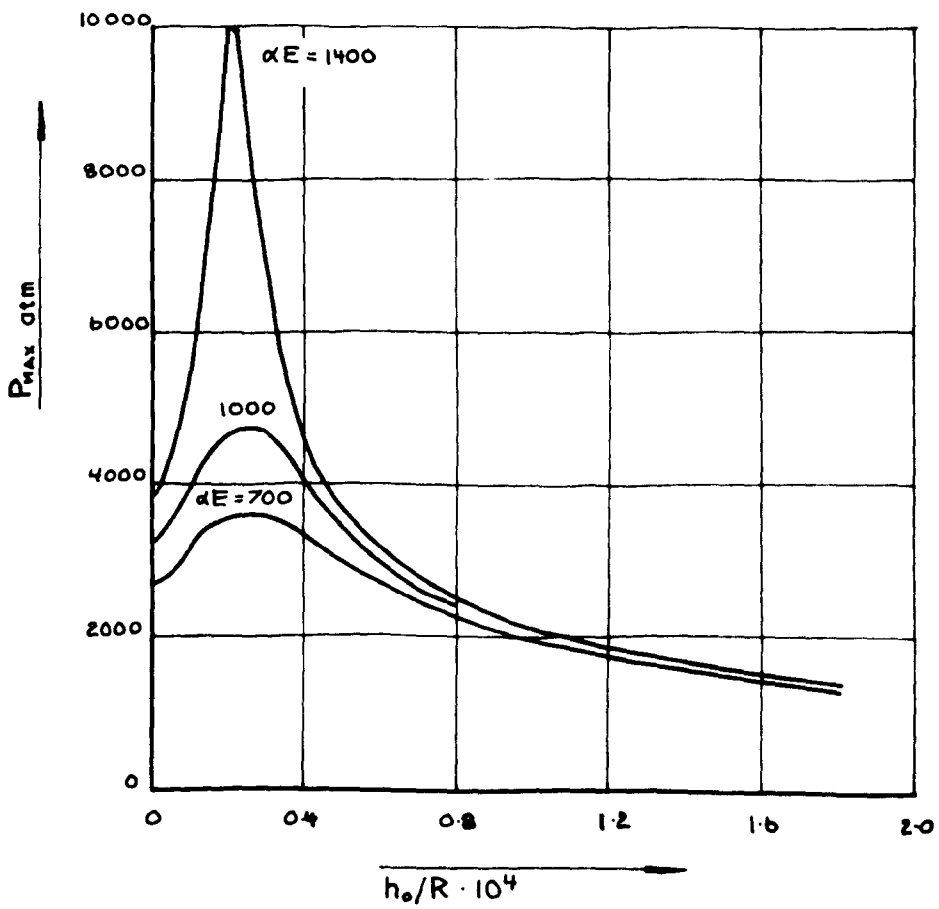

Hence for $\alpha E = 1,400$ for an increase of load of only 6·6%, the maximum pressure has increased by 25%. If the pressure distribution is examined for the film thickness where the maximum pressure peak occurs, this is found to be very sharp and the high pressure will only be applied over a very small area and for a short time. Such a pressure distribution might, however, produce large shear stresses close to the surface of the cylinders, and the material might yield. Furthermore, if the pressures were applied in rapid succession, a large number of times, one might be led to think that this could lead to fatigue failure of the surface.

If the cylinders in our experiment were designed according to the Hertzian criterian, i.e., assuming that the maximum pressure would be obtained at Hertzian dry contact, and then calculating the design load from a suitable maximum value for this pressure, the present results show that the actual pressure obtained would be higher than those predicted by the Hertzian theory. Indeed, fig. 5.2.5 may be looked upon as giving the safety factor by which the Hertzian load must be reduced in order that the maximum pressure shall not exceed a specified value.

In our example for $\alpha P_o = 10$ (say), this factor has the considerable value of 6·8. Hence only about 15% of the Hertzian

load may be applied in order that the maximum pressure shall not exceed 10. This figure might be reduced if compressibility and thermal effects had been considered. Only in the case of constant viscosity would the Hertzian theory have predicted the right maximum pressures. The results here show that the maximum pressure would coincide with the Hertzian.

Generally, these results show that it would be advantageous to use materials with a low value of Youngs modulus, and lubricants with small values of the pressure coefficient. For some lubricants, the value of α decreases with increasing temperatures, hence these considerations point to the use of "soft" materials and lubricants kept at a high temperature. Other considerations might lead to another conclusion. Nothing definite can be decided about these questions at the present time. More work, both theoretical and experimental is needed before the results presented here can be fitted into a general theory of surface failure and used as a basis for design criteria.

CHAPTER 6

EXPERIMENTAL

6.1 Introduction

The experimental work described in this chapter was devised in order to check some of the general predictions made by the theory, and at the same time intended to be as simple as possible.

The experiment consisted of dropping a suitably loaded steel ball from a height under gravity on to the polished surface of a metal specimen. The surface was covered by a film of lubricating oil, and the resulting plastic deformation of the specimen surface, if any, was measured with a Talysurf surface recorder. By varying the load on the ball, and by using varying metals in the specimen, different values of the elasto-hydrodynamic load W and of the parameter αE could be obtained. Only qualitative confirmation of the theoretical results could be hoped for from an experiment of this kind, because of the following two main reasons.

a. The theory was worked out for the normal approach of two cylindrical bodies or, as a special case, on an elastic cylinder moving normal to an elastic flat plate. For reasons of simplicity an elastic ball rather than a cylinder was used in the experiment. The governing equations for the special case can be shown to have much the same form as for the cylindrical case. Hence, we might expect that the

solutions would be of similar form although the numerical values might be widely different.

b. It was shown in section 2 that under certain conditions the inert of the fluid could be neglected, and these conditions are probably satisfied in the present system. The inertia of the gravitating ball system cannot be ignored, however, and hence the governing equation is

$$M\ddot{Z} + Mg = W(h_o, V) \qquad 6.1.1$$

where

M is total mass of falling ball system.

W is the elasto-hydrodynamic force developed.

V is the velocity of approach as defined in Section 2.

Z the coordinate of the centre of ball.

with initial conditions

$$\left.\begin{aligned} Z(o) &= H + R \\ \dot{Z} &= o \end{aligned}\right\} \quad t = o$$

We then have

$$Z = R + h_o - \delta \qquad 6.1.2$$

where δ is the deformation of the elastic surfaces.

Differentiating w.r.t time:

$$\dot{Z} = \dot{h}_o - \dot{\delta}$$

6.1

$$V_A = V + V_\delta$$

where

V_A is the absolute velocity of the ball system relative to the fixed coordinate system.

V is the relative velocity between the elastic surfaces as defined in section 2.

V_δ is the deformation velocity.

Also

$$\ddot{z} = \ddot{h}_c - \ddot{\delta}$$

If we neglect $\dot{\delta}$ and $\ddot{\delta}$ as small we get

$$MV\frac{dV}{dh_c} = W(h_c, V) - Mg \qquad 6.1.3$$

$$V_A = V$$

or

$$W(h_c, V) = M\left(g + V\frac{dV}{dh_c}\right) \qquad 6.1.4$$

The equation 6.1.3 can be solved for the given physical system provided the appropriate function $W(h_o, V)$ is available. This is not so in the present case and hence eqn. 6.1.3 cannot be solved .

For this reason, although no quantitative agreement between theory and experiment is possible, there are nevertheless some general predictions made by the theory that

the experiments are capable of testing.

In fig. 5.2.3 it is observed that for two materials having the same dynamic yield characteristics, but having different values of αE, then the minimum load necessary to cause yielding will be smaller for the material having the larger value of αE, other conditions being equal. To detect the onset of yield would be difficult. We might expect, however, this could also be interpreted so that for the same load, the size (depth) of the plastic deformation would be larger in the material having the larger value of αE. If therefore the experiment is performed on say aluminium bronze ($E = 1.3 \times 10^{12}$ dyn/cm^2) and steel ($E = 2{\cdot}1 \times 10^{12}$ dyn/cm^2) using in each case the same lubricant and dropping the ball from the same initial height, one might expect that the depth of the resulting plastic deformation would be larger in the steel than in the aluminium bronze, provided the dynamic yield characteristics of the two materials could be assumed to be comparable.

It might also be of some interest to see how depth of deformation varies with yield stress for a constant value of Youngs modulus. Refering to fig. 5.2.3 it is observed that for higher values of αP_o, the gradient of the curve is small, this is particularly noticeable for the higher values of the

parameter αE. This suggests that the load necessary to cause yielding would be fairly insensitive to the yield stress of the material. Or again, because of the difficulty of detecting the onset of yield, the depth of the impressions for any load would be fairly independant of yield stress.

There is one snag to this extrapolation to finite plastic deformation. The depth of the depression depends not only on the magnitude of the pressure applied, but one would also expect that it would depend on the length of time this pressure was being applied. From fig. 5.2.7 it appears that the time of application of a sufficiently high pressure, decreases with increasing value of yield stress. Thus, the variation of depth with yield stress would be larger than one would be led to expect from a consideration of fig. 5.2.3 alone.

There is also the complication that with finite deformations the material might considerably work-harden.

For this last reason it was thought that when finite deformations were considered, tensile fracture strength rather than some proof stress would provide a fairer basis for comparison, and this has been adopted in the following.

6.2 Description of apparatus and experimental procedure.

The main details of the apparatus is shown in fig. 6.2.1, 6.2.2 and 6.2.3.

① is a ⅞" thick plate supporting the 4 steel columns. In a horizontal groove milled out, it also supports and guides the metal specimens ②. The specimens themselves were closely machined to size 5" x ¼" x ⅛", the top surface being carefully ground and polished. The columns support the top plate to which an electro-magnet ③ is fixed. The height of the magnet can be slightly adjusted by the micrometer ⑤, which allow adjustment to an accuracy of a few microns. A larger and coarser adjustment is provided by the nuts ④. Round the lower end of the magnet is fixed a brass ring ⑥ which serves as a guide for the magnet armature.

Fig. 6.2.2 shows details of the way the test ball is clamped, and the loading arrangements. ⑦ is the test ball, a ¼"ϕ hardened steel ball-bearing ball, held by the nut ⑧ which screws onto the brass fixing ⑨. The plate ⑨ also serves as supports for the loose steel disc weights ⑩. At the top of the spindle is fastened the magnet armature ⑪. The photograph fig. 6.2.3 shows the apparatus assembled and ready for an experiment.

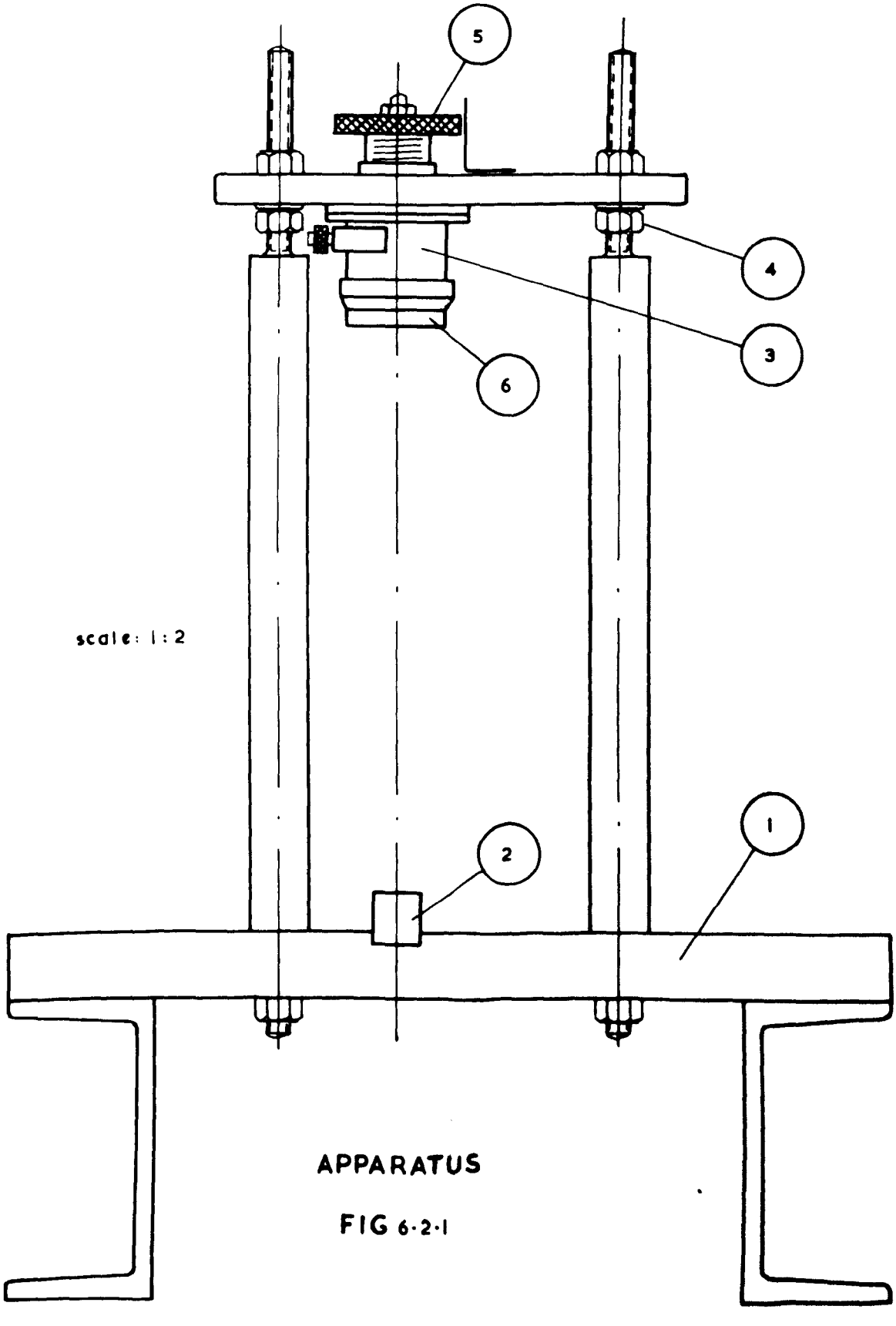

APPARATUS

FIG 6·2·1

FIG 6·2·2

BALL ASSEMBLY

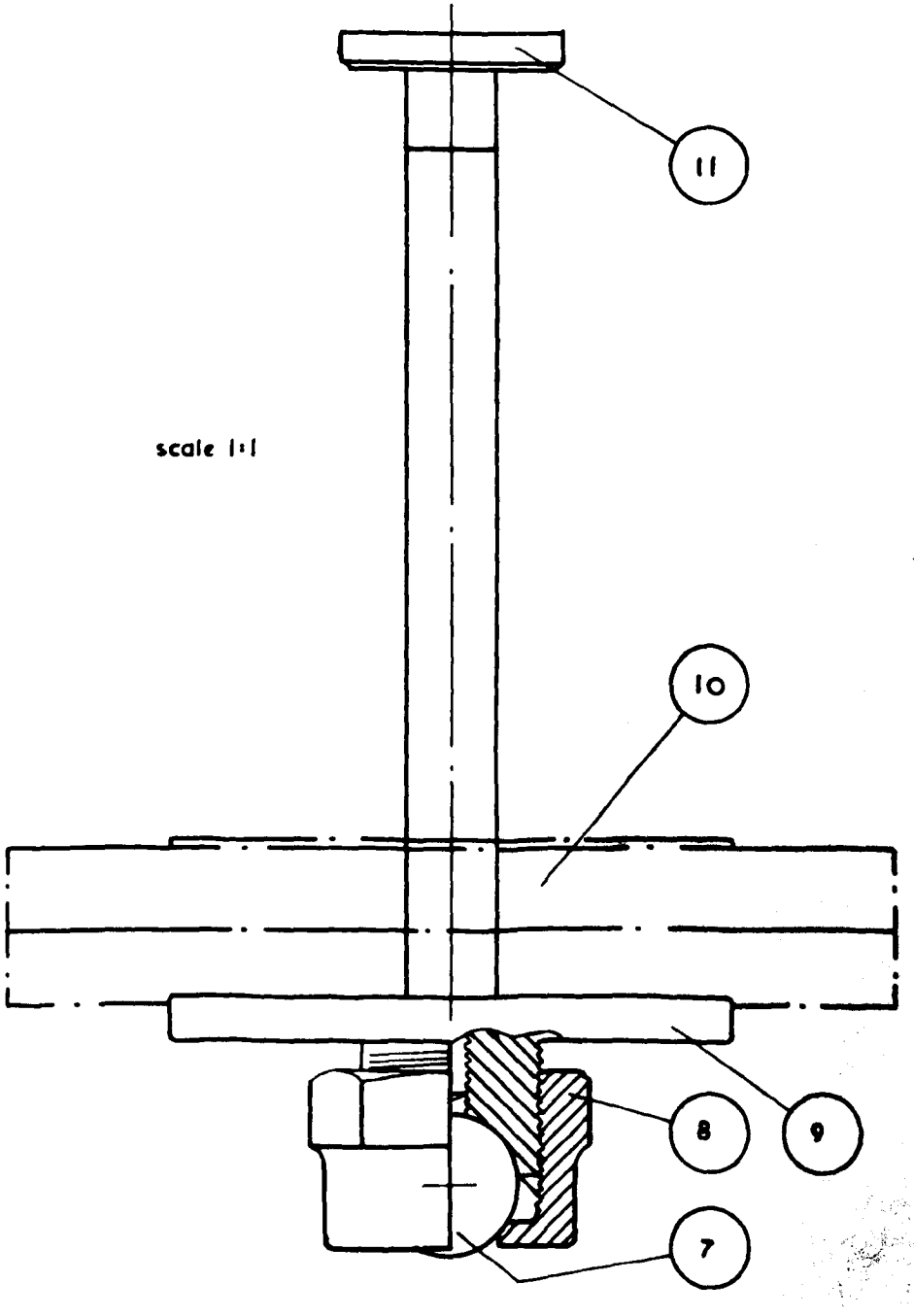

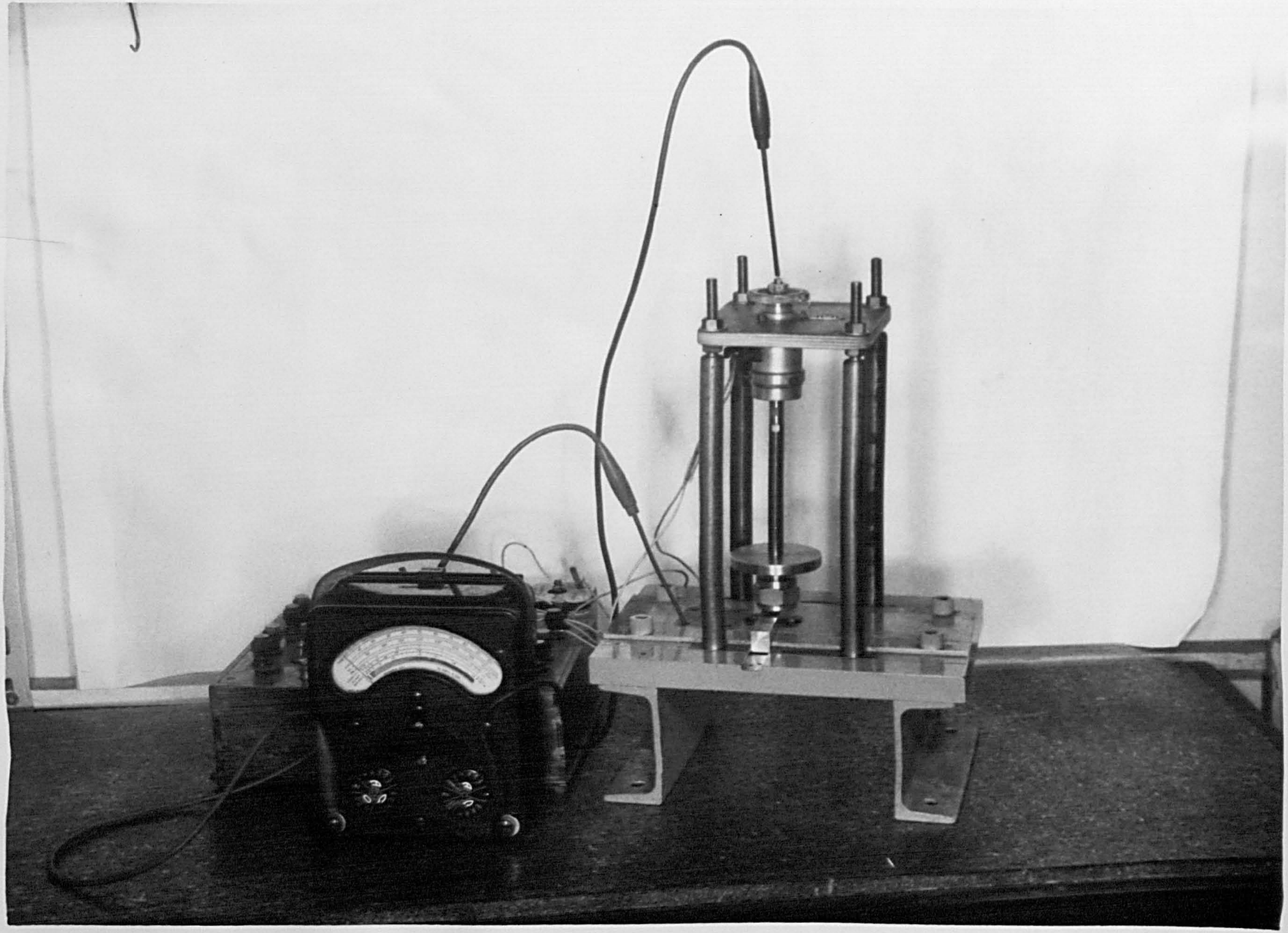

FIG 6.2.3

6.2

To prepare the apparatus for an experiment, the vertical level of the magnet was adjusted by the coarse adjustment, until the distance between the ball and the specimen was of the order of a few hundred microns and the axis of the spindle vertical. Fine adjustment of the level was made with the micrometer.

To prepare the specimen, the surface of this and of the ball was thoroughly cleaned by washing with alcohol. After drying, the lubricant was put onto the surface, care being taken to see that no dirt or air bubbles was present near the area where contact was to be made. In order to stop the lubricant from flowing away from the surface, a thin strip of cellotape was put round the edges of the specimen, thus forming a shallow trough. The oil film could thus be kept at a thickness of a few hundred microns.

Switching on the current activating the magnet, the ball assembly could then be fitted into place and would be held up by the magnet, and the ball assembly loaded up with the required number of weights.

In order to set the initial height of the drop accurately, the ball was lowered by means of the micrometer until it just touched the specimen surface. This could be detected by measuring the electrical resistance across the oil film. The resistance dropping instantly when metallic contact was

established. For measuring the resistance, an ordinary Avo meter was connected across the specimen and the ball assembly. Having by this means fixed the zero level, the ball was raised the required amount by means of the micrometer.

Checking the accuracy of this procedure with the help of slip gauges, it was found that the initial height of the drop could be set with an accuracy of a few microns.

Switching off the current to the magnet, the armature would be released and the ball drop on to the specimen surface. For suitably chosen values of load and initial height, the specimen surface would plastically deform under the pressure developed in the lubricant.

The deformation was measured up by means of a Talysurf surface roughness recorder. On account of the small dimensions involved, care was taken to ensure that profile sections across a diameter was obtained.

In most cases the diameters of the depression could also be measured by means of a travelling microscope. This method, however, using very oblique lighting, proved unsatisfactory, since the edges of the impressions frequently were ill defined and this caused considerable scatter in the microscope measurements. Also, no information of the depth of the deformation could be obtained from the microscope measurements. However, when the size of the deformations were so small that they were of the same oder as the general surface roughness,

it became very difficult to distinguish these on the Talysurf records. For these cases, microscope measurements of the diameters were used.

6.3 Results.

The experimental results are divided into three groups. Group I contains the results designed to bring out any correlations between depth of depression and the value of the parameter αE.

The results in group II were designed to show the connection between depth of impression and strength, while the results in group III were intended to show the variation of impression with initial height of the drop for a constant load. The lubricant used was T.N. 1074, described earlier. In group I and II the initial height was kept at 50 , the loads running from 710 grams. to 6120 grams. in steps of ~900 grams. In group III the load was kept constant at 6120 grams., and the initial height of the drop varied.

Group I:

Three different specimens were used here, i.e., aluminium-alloy, aluminium-bronze and steel, the elastic constants of which is given in table below. These were measured from tests done on the same bars from which the specimens had been made.

6.3

Group I, Specimens

TABLE 6.3.1.

Code	Material	Tensile strength Kg/mm^2	Youngs mod. Kg/cm^2	Vickers hardn. VPN
1A	Alum.-alloy	38·0	$0·715 \times 10^6$	110
3B	Alum.bronze	78·5	$1·3 \times 10^6$	240
2S	KF46 steel	81·5	2.1×10^6	248

The tensile failure stress is taken as being representative of the strength of the material.

The approximate values of the diameter of the depression and its depth as obtained from the Talysurf records are given in Table 6.3.4. Reproductions of the records themselves are shown in figs. 6.3.1 - 6.3.3 incl.

In order to clearly bring out the influence of the lubricant, the experiments in group I was repeated with no lubricant present. These results are given in Table 6.3.5, and the records reproduced in figs. 6.3.1 and 6.3.2.

Group II:

Three different steel specimens, having approximately the same value of Youngs modulus but different strengths, were used. The measured elastic constants are given in the table below.

6.3

Group II, Specimens

TABLE 6.3.2

Code	Material	Tensile strength Kg/mm^2	Youngs mod. Kg/cm^2	Vickers Hrdn. VPN
1S	Mild steel	63·0	$2{\cdot}1 \times 10^6$	200
4S	KF 1b	90·0	$2{\cdot}2 \times 10^6$	254
5S	KF1b Hardn.	142·0	$2{\cdot}0 \times 10^6$	363

The results are shown in table 6.3.6. Reproductions of the records are given in figs. 6.3.4 and 6.3.5. As for the previous group, the experiments in group II were repeated with no lubricant present. These results are given in Table 6.3.7, and the records reproduced in figs. 6.3.4.

Group III:

Only one steel specimen was used in this group. The constants for the specimen were measured to be

6.3

Group III, Specimen

TABLE 6.3.3.

Code	Material	Tensile strength Kg/mm^2	Youngs mod. Kg/cm^2	Vickers hardn. VPN
3S	Steel	175·0	$1·9 \times 10^6$	464

The results are given in Table 6.3.8, and the records reproduced in Figs. 6.3.6. As usual, the no lubricant test was also performed. In this case, no surface deformation at all could be detected under a microscope.

6.3

TABLE 6.3.4

Group I, with lubricant

Code	1A		3B		2S	
load grams	Diam μ	Depth μ	Diam μ	Depth μ	Diam μ	Depth μ
710						
1608			100	1)	175	1)
2511			175		175	
3411			175	0·50	175	1·00
4313	175	0·75	200	0·80	225	1·35
5216	300	1·40	200	0·85	250	1·60
6120	400	1·50	225	1·10	275	1·75

1) Microscope measurement only.

6.3

TABLE 6.3.5

Group I: No lubricant

Code	1A		3B		2S	
load grams	Diam μ	Depth μ	Diam μ	Depth μ	Diam μ	Depth μ
710						
1608		2)		2)		
2511						
3411			200			
4313			250	1)		
5216	450	0.65	300			2)
6120	550	0.75	325			

1) Microscope measurements only

2) Could be seen under the microscope as a faint marking of the surface, but could not be measured.

6.3

TABLE 6.3.6

GROUP II: with lubricant

Code	1S		4S		5S	
Load grams	Diam μ	Depth μ	Diam μ	Depth μ	Diam μ	Depth μ
710						
1608	162	1)	150	1)	100	1)
2511	200		250	1·00	150	
3411	275	1·15	275	1·25	175	
4313	325	1·50	350	1·35	225	
5216	400	2·00	350	1·50	225	0·65
6120	425	2·10	350	1·60	225	0·75

1) Microscope measurements only.

6.3

TABLE 6.3.7

GROUP II: no lubricant

Code	1S		4S		5S	
Load grams	Diam μ	Depth μ	Diam μ	Depth μ	Diam μ	Depth μ
710						
1608						
2511		2)		3)		3)
3411						
4313						
5216						
6120	350	0·60				

1) Microscope measurements only

2) Could be seen under the microscope as a faint marking of the surface, but could not be measured

3) Could not be seen neither with the naked eye or under the microscope.

6.3

TABLE 6.3.8

GROUP III

Code	3S	
Initial height μ	Diam μ	Depth μ
50	125	1)
100	175	
150	250	0·70
200	300	1·00
250	400	1·12
300	450	1.20

1) Microcsope measurement only.

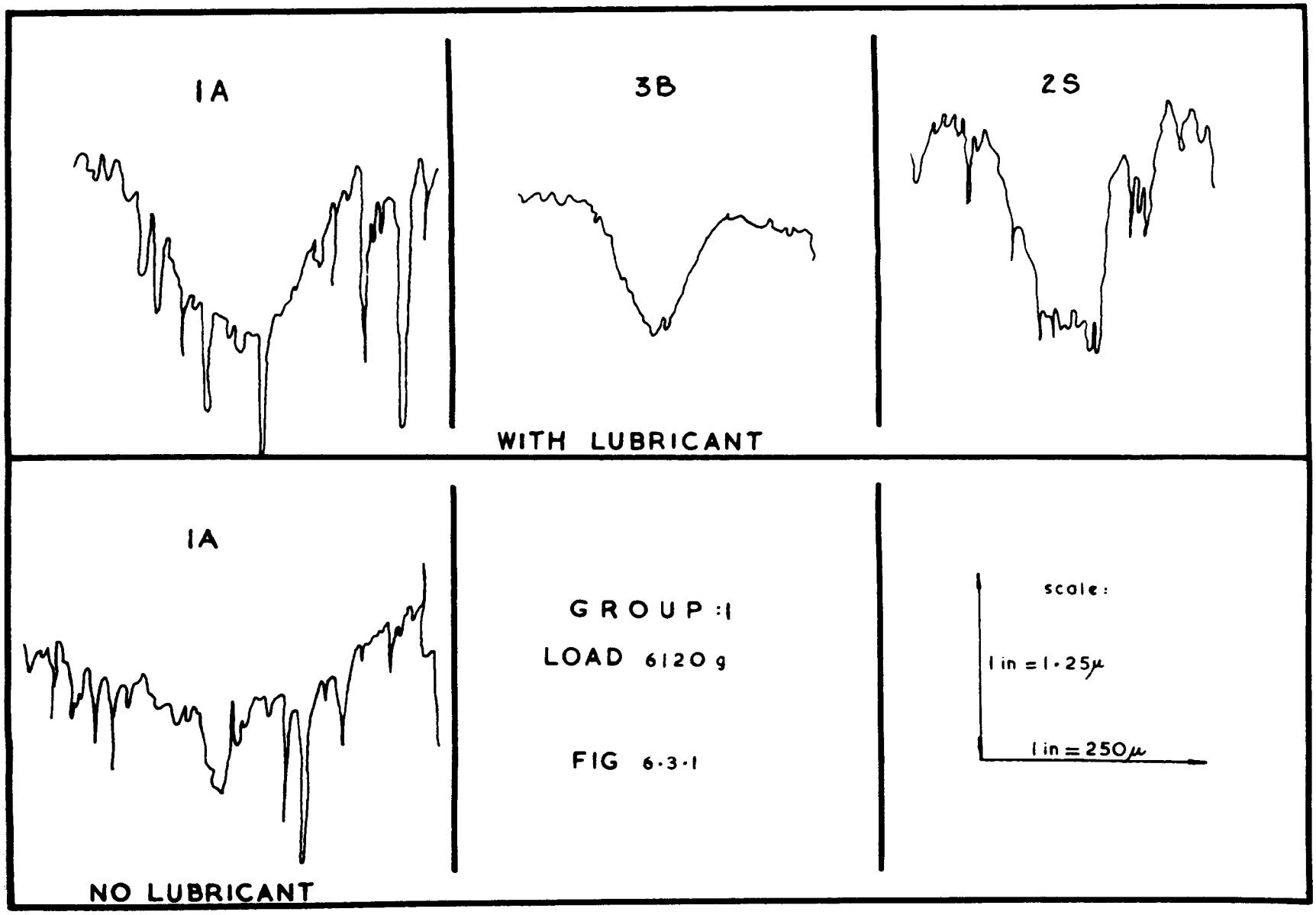
1A
3B
2S
WITH LUBRICANT
1A
NO LUBRICANT
GROUP : 1
LOAD 6120 g
FIG 6·3·1
scale :
1 in = 1·25μ
1 in = 250μ

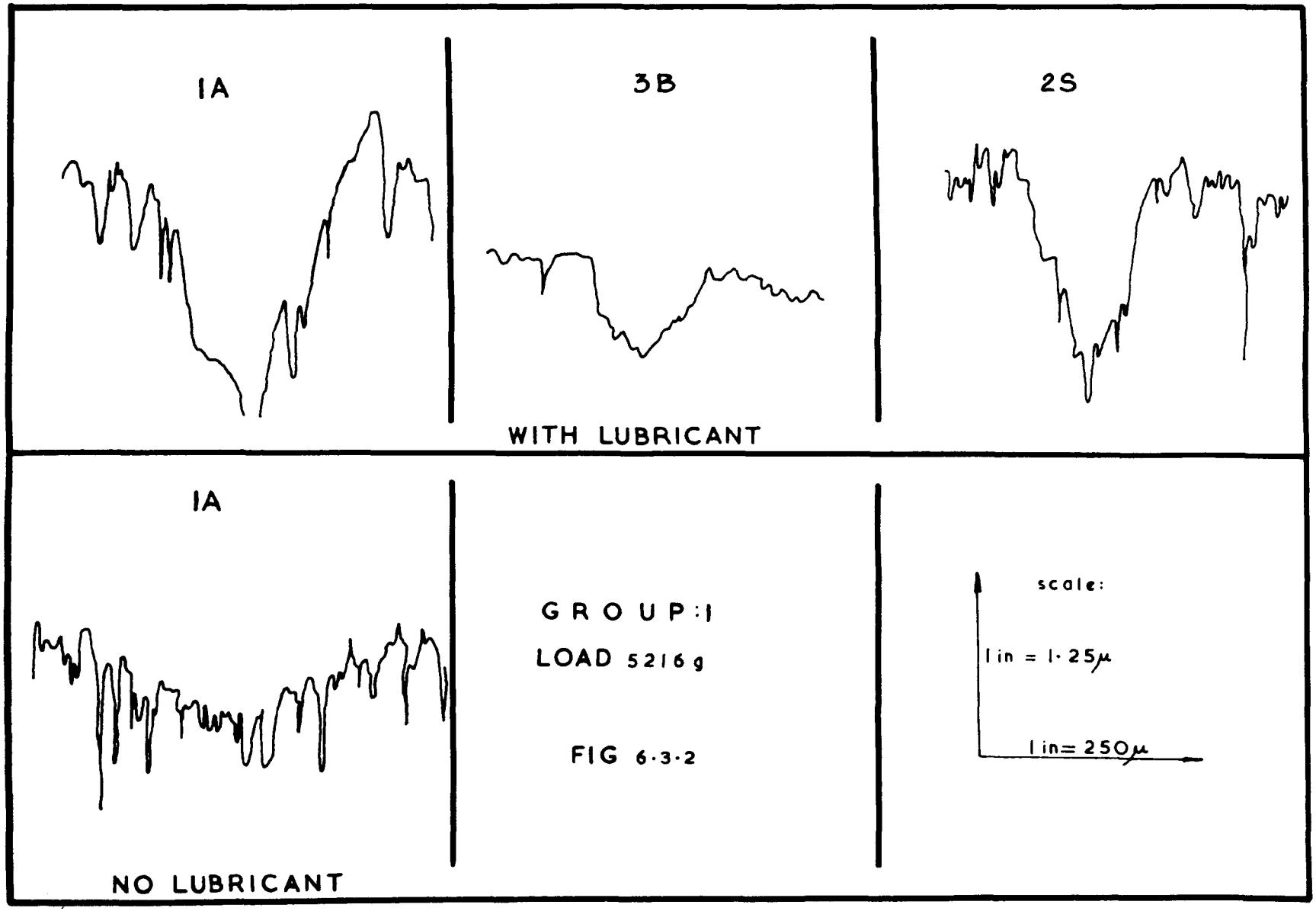
1A
3B
2S
WITH LUBRICANT
1A
NO LUBRICANT
GROUP:1
LOAD 5216 g
FIG 6·3·2
scale:
1 in = 1·25μ
1 in = 250μ

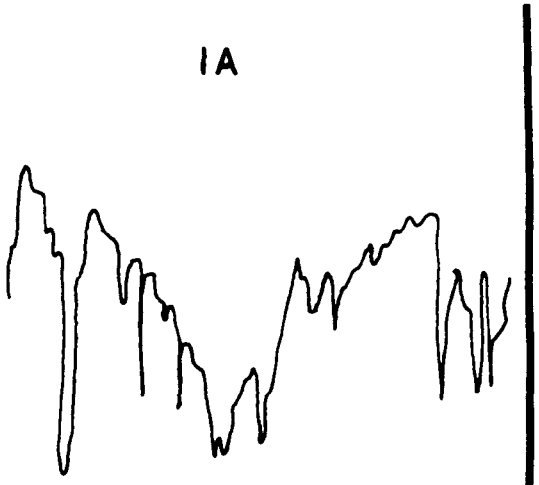

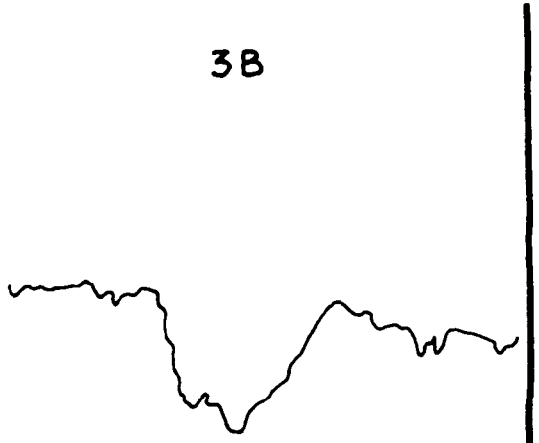

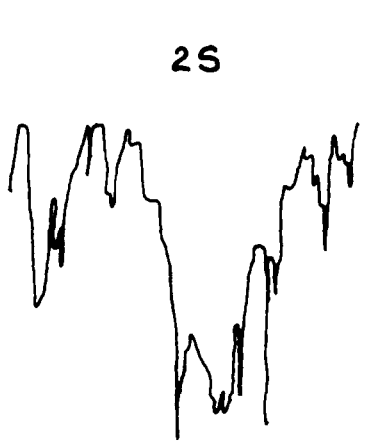

WITH LUBRICANT

GROUP :1

LOAD 4313 g

FIG 6·3·3

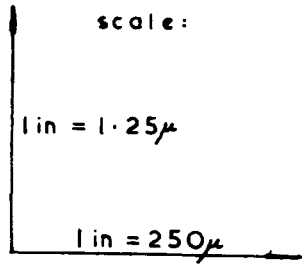

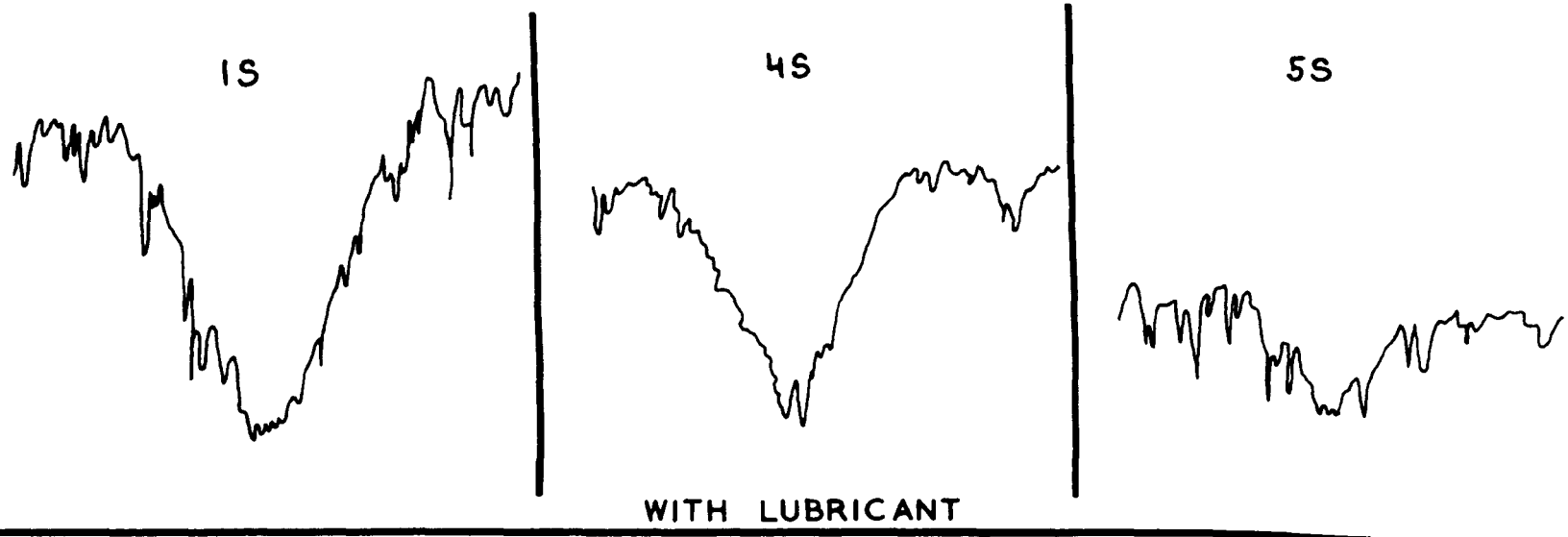
1S
4S
5S
WITH LUBRICANT

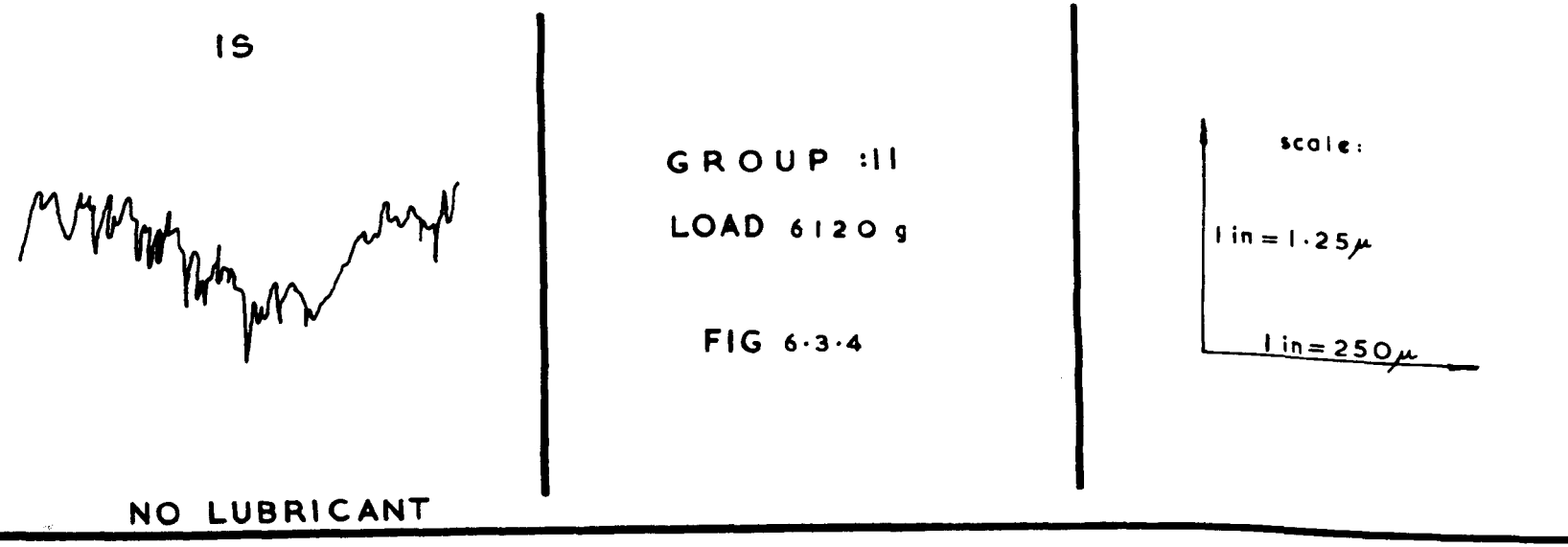
1S
NO LUBRICANT
GROUP :11
LOAD 6120 g
FIG 6·3·4
scale:
1 in = 1·25μ
1 in = 250μ

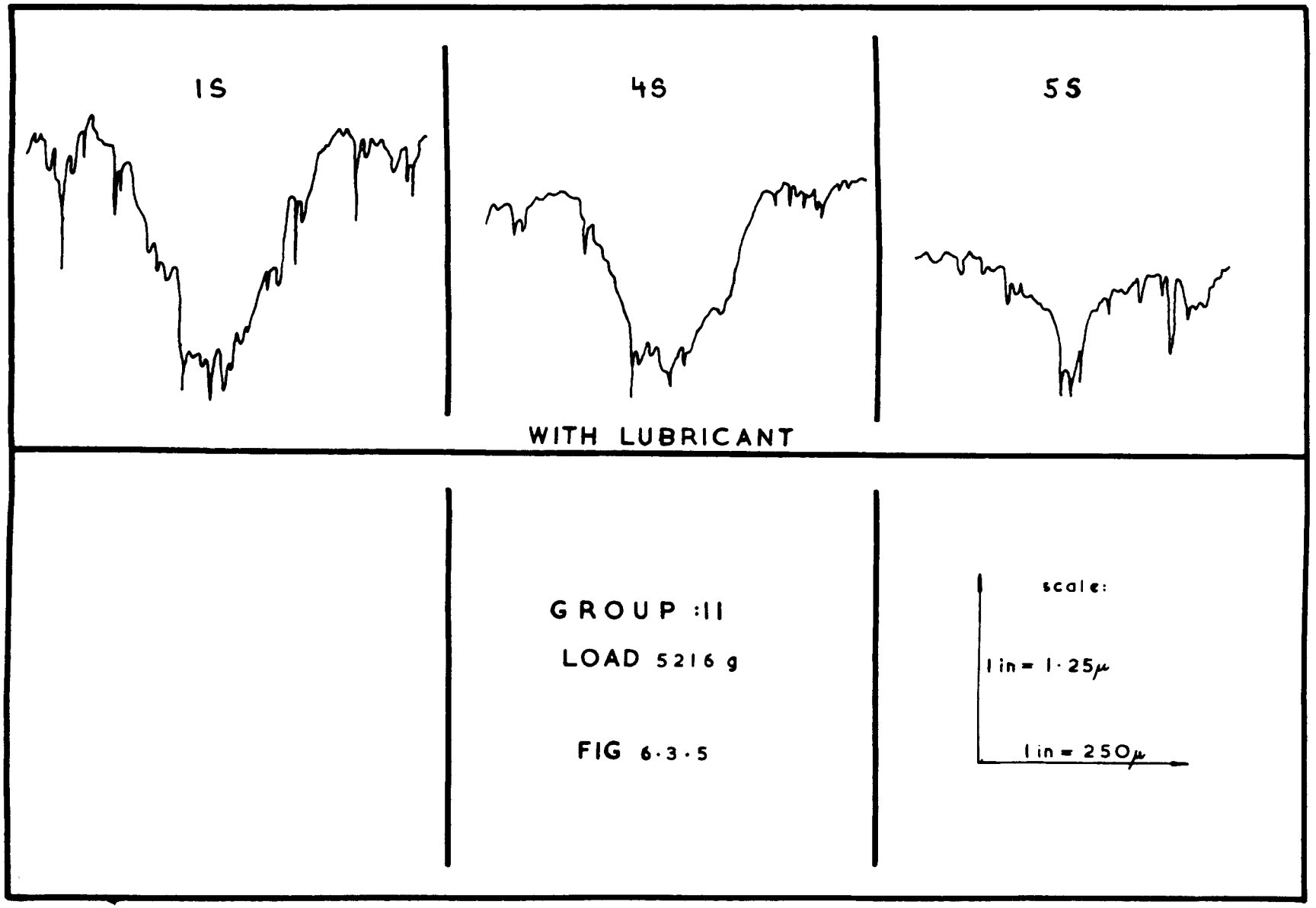
1S
4S
5S
WITH LUBRICANT
GROUP :II
LOAD 5216 g
FIG 6·3·5
scale:
1 in = 1·25μ
1 in = 250μ

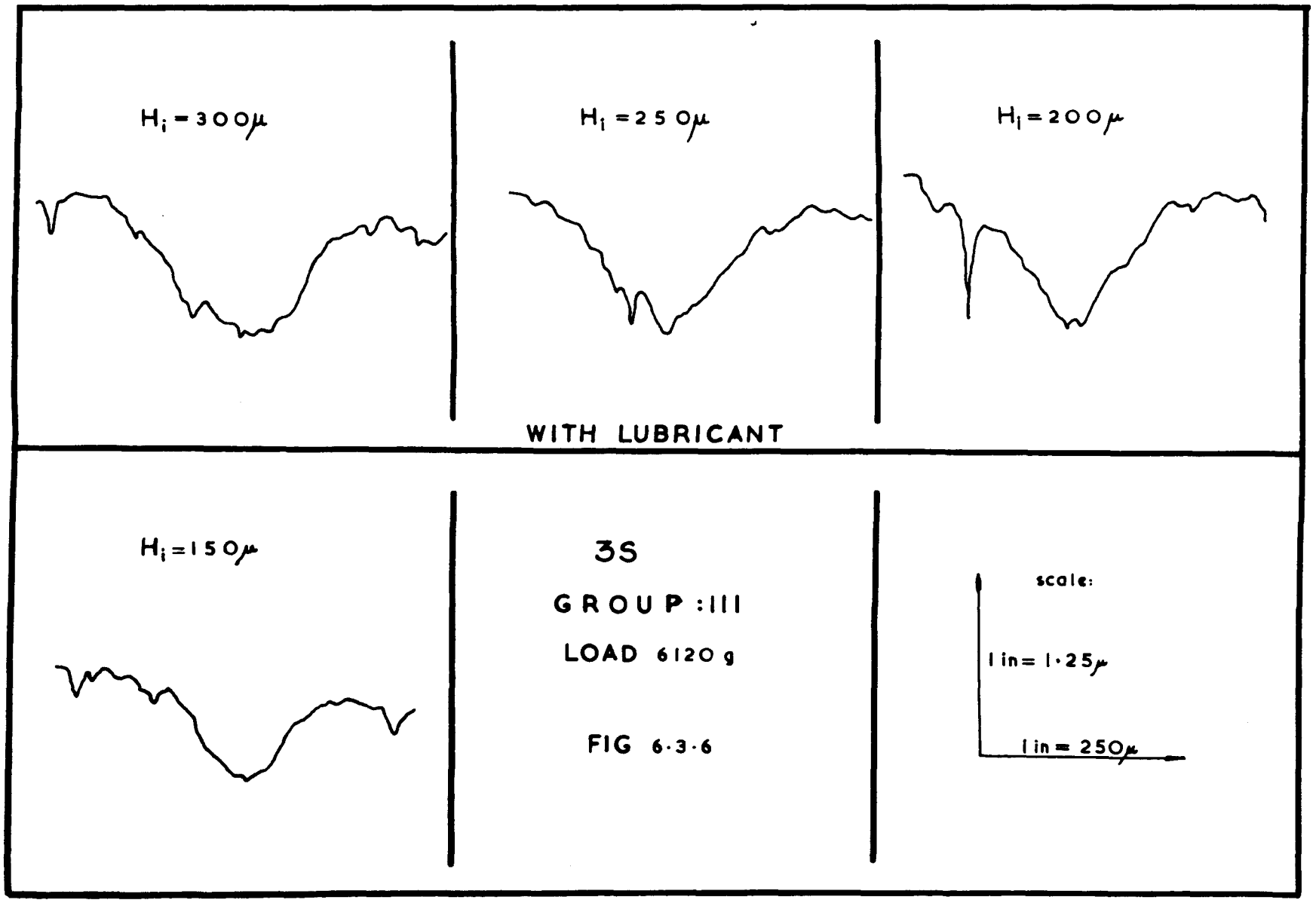
$H_i = 300\mu$
$H_i = 250\mu$
$H_i = 200\mu$
WITH LUBRICANT
$H_i = 150\mu$
3S
GROUP : III
LOAD 6120 g
FIG 6·3·6
scale:
1 in = 1·25μ
1 in = 250μ

6.4 Conclusions

Comparing the deformations obtained with lubricant with the Hertzian, or dry contact deformations, under otherwise equal conditions, it is seen that the influence of the lubricant on the shape of the plastic deformations is considerable. Compared with the dry contact, the deformations in the presence of lubricant are in every case deeper and sometimes also having a smaller diameter, thus causing the depressions to appear more conical. If the average radius of curvature of a depression is defined as

$$\bar{R} = \frac{D^2}{8d}$$

where D is the maximum diameter of the depression
d is the depth.

Then this quantity is smaller for the depressions made in the presence of the lubricant. Sometimes this quantity is even smaller than the original radius of the indenting ball.

In the experiments, where in particular the harder specimens were used, no dry contact deformations at all, or at best very faint markings which could not be measured, were found, even for the highest loads used. The corresponding deformations with lubricant were easily detectable, even for much smaller loads. This again demonstrates the considerable influence of the lubricant.

6.4

Turning now to the results of Group I given in table 6.3.4, these seem to bear out the theoretical prediction of the inverse relationships between the parameter αE and the maximum pressure developed in the oil film. Comparing the reults for the aluminium-bronze (3)B and the steel (2S), it is seen that for all loads the deformation in the steel is deeper than the corresponding one in the aluminium-bronze. Indeed even for the harder steel(4S) table 6.3.6, the deformation is deeper than in the bronze, even though this steel has a strength 15% higher.

Unfortunately, the results for the aluminium-alloy (1A) are not as conclusive. A comparison with the bronze (3B) shows that the deformations are larger for equal loads in spite of the fact that E for aluminium-alloy is some 45% lower than for bronze. However, the strength of the bronze is nearly twice as high, and this may account for the discrepancy, Hardness tests of the surface of the aluminium-alloy seem to indicate that the top surface layers are softer than the bulk of the material. The stress quoted was measured in a tensile test, and thus represents the bulk of the material while, as far as the experiments are concerned, it is the stress of the

surface that is relevant. This softening and lowering of the stress of the surface layer may have been brought about by the grinding and polishing operations done. At any rate, comparing the aluminium with the steel, the discrepancy vanishes. The impressions in the steel are considerably larger, even though the strength of the steel is also very much higher.

Turning to the results in Group II, it is seen that the depth of the deformations decrease with increasing stress, and that the decrease is more pronounced in the regions of lower stress. This may mainly be due to difference in the times of application of the pressures. In fig. 6.4.1 is drawn the depth of the deformation against tensile fracture stress for the highest load.

In the case of the results in Group III, these are much as expected and show an increase for increasing initial height of the drop.

Since in this case a high tensile steel was used in the specimen, no Hertzian or dry contact deformations were obtained at all.

CORRELATION BETWEEN MAX. DEPTH OF DEFORMATION AND SPECIMEN STRENGTH LOAD 6120 grams

FIG 6·4·1

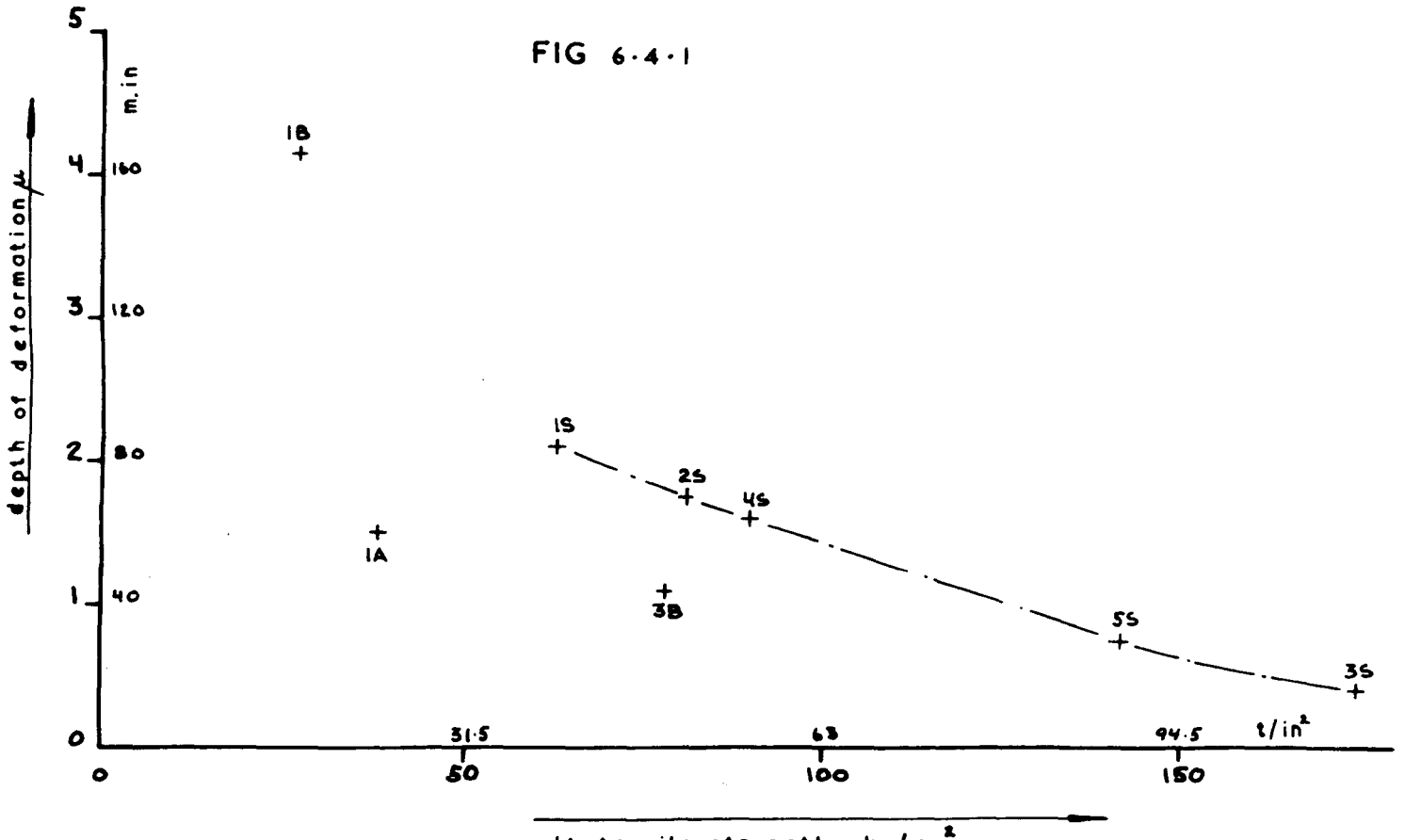

Appendix A.

The effect of Variable Viscosity on the Navier-Stokes Equations.

The x component of the general equation of motion without making the assumption of constant viscosity is as previously shown

$$\rho \frac{Du}{Dt} = \rho X - \frac{\partial P}{\partial x} + \frac{2}{3}\frac{\partial}{\partial x}\mu\left(\frac{\partial u}{\partial x} - \frac{\partial v}{\partial y}\right) + \frac{2\partial}{3\partial x}\mu\left(\frac{\partial u}{\partial x} - \frac{\partial w}{\partial z}\right) +$$

$$+ \frac{\partial}{\partial y}\mu\left(\frac{\partial v}{\partial x} + \frac{\partial u}{\partial y}\right) + \frac{\partial}{\partial z}\mu\left(\frac{\partial u}{\partial z} + \frac{\partial w}{\partial x}\right) \qquad A1$$

Rearranging the viscous terms these becomes

$$\frac{1}{3}\mu\frac{\partial}{\partial x}\Delta + \mu\nabla^2 u - \frac{2}{3}\Delta\frac{\partial \mu}{\partial x} + 2\frac{\partial \mu}{\partial x}\frac{\partial u}{\partial x} + \left(\frac{\partial v}{\partial x} + \frac{\partial u}{\partial y}\right)\frac{\partial \mu}{\partial y} + \left(\frac{\partial u}{\partial z} + \frac{\partial w}{\partial x}\right)\frac{\partial \mu}{\partial z}$$

where $\Delta = \frac{\partial u}{\partial x} + \frac{\partial v}{\partial y} + \frac{\partial w}{\partial z}$

Restricting the treatment to the two dimensional case, assuming constant properties across the film and neglecting terms arising from compressibility, this becomes

$$\mu\nabla^2 u + 2\frac{\partial \mu}{\partial x}\frac{\partial u}{\partial x} \qquad A2$$

With the previous approximations the equation of motion now becomes

$$\frac{\partial P}{\partial x} = \mu\frac{\partial^2 u}{\partial y^2} + 2\frac{\partial \mu}{\partial x}\frac{\partial u}{\partial x} \qquad A3$$

By incompressible continuity

$$\frac{\partial u}{\partial x} = - \frac{\partial v}{\partial y}$$

$$\therefore \frac{\partial P}{\partial x} = \mu \frac{\partial^2 u}{\partial y^2} - 2 \frac{\partial \mu}{\partial x} \frac{\partial v}{\partial y} \qquad A4$$

Integrating:

$$\frac{\partial P}{\partial x} y = \mu \frac{\partial u}{\partial y} - 2 \frac{\partial \mu}{\partial x} v + C_1$$

$$\frac{\partial P}{\partial x} \frac{y^2}{2} = \mu u - 2 \frac{\partial \mu}{\partial x} \int v \, dy + C_1 y + C_2$$

Boundary conditions are:

$u = 0$ for $y = 0$ and $y = h$

$$\therefore C_1 = \frac{\partial P}{\partial x} \frac{h}{2} + \frac{2}{h} \frac{\partial \mu}{\partial x} \int_0^h v \, dy$$

$$u = \frac{1}{2\mu} \frac{\partial P}{\partial x} (y^2 - yh) - \frac{2}{\mu} \frac{\partial \mu}{\partial x} \left(\frac{y}{h} \int_0^h v \, dy - \int_0^y v \, dy \right) \qquad A5$$

Defining the average value of v:

$$\bar{v} = \frac{1}{h} \int_0^h v \, dy$$

Then for terms in the last bracket, we have

$$\left(y\bar{v} - \int_0^y v \, dy \right) < Vh$$

If we define,

A.

$$\epsilon = \epsilon(x,y,t) = \frac{1}{Vh}\left(y\bar{v} - \int_o^y v\, dy \right)$$

it follows that $0 \leqslant \epsilon < 1$

Substituting into 5 we get

$$u = \frac{1}{2\mu}\frac{\partial P}{\partial x}\left(y^2 - yh \right) - \frac{2}{\mu}\frac{\partial \mu}{\partial x}\epsilon Vh \qquad A6$$

As previously

$$V = \frac{\partial}{\partial x}\int_o^h u\, dy$$

$$\therefore V = \frac{\partial}{\partial x}\left\{ -\frac{h^3}{12\mu}\frac{\partial P}{\partial x} \right\} - \frac{\partial}{\partial x}\left\{ \frac{2}{\mu}\frac{\partial \mu}{\partial x} Vh\bar{\epsilon} \right\}$$

where $\bar{\epsilon} = \frac{1}{h}\int_o^h \epsilon\, dy \qquad \bar{\epsilon} = \bar{\epsilon}(x,t) < \epsilon_{max}$

$$\therefore V = -\frac{\partial}{\partial x}\left\{ \frac{h^3}{12\mu}\frac{\partial P}{\partial x}\left(1 + \frac{24V\bar{\epsilon}}{h}\frac{\partial \mu}{\partial x} \right) \right\} \qquad A7$$

assuming that viscosity is a function of pressure only. The last term is due to the variable viscosity. If this term is small and is neglected, eqn. 7 reduces to

$$V = \frac{\partial}{\partial x}\left(\frac{h^3}{12\mu}\frac{\partial P}{\partial x} \right)$$

as was previously obtained.

The influence of the variable viscosity on the pressure can be seen by solving for $\partial P/\partial x$

$$\frac{\partial P}{\partial x} = - \frac{12\mu V x}{h^3 \left[1 + \frac{24 V \bar{\epsilon}}{h} \frac{\partial \mu}{\partial P} \right]} \qquad A8$$

In this case, since the term $\frac{24V}{h}\bar{\epsilon}\frac{\partial \mu}{\partial P}$ is non-negative, its influence is to reduce the pressure gradient. In terms of a fix ed central pressure P_o, this means that the load necessary to produce this P_o at a given h_o is larger than if this term is neglected.

Assuming that the viscosity is given by

$\mu = \mu_o \exp(\alpha P)$

the variable viscosity correction may conveniently be expressed in the form

$$K_\mu = \frac{\alpha \mu_o V}{R} \frac{24 \bar{\epsilon} \exp(\alpha P)}{h/R} \qquad A9$$

If this quantity is < 1, the influence of the variable viscosity on the Navier-Stokes equation is small and may be neglected.

In order to establish bounds for the function $\bar{\epsilon}$, assume that v is expressible in the form

$$v = \sum_{n=0} a_n \left(\frac{y}{h} \right)^n \qquad A10$$

where the coefficients are functions of x and t i.e.

$a_n = a_n(x,t)$

The boundary conditions on v demands

$V = \Sigma a_n$ and $a_o = 0$

$$\bar{v} = \sum_n \frac{a_n}{(n+1)}$$

A.

Substituting this, the expression for ϵ becomes

$$\epsilon = \frac{1}{\bar{v}h}\left\{ \frac{y}{h}\int_0^h \sum_n a_n \left(\frac{y}{h}\right)^n dy - \int_0^y \sum_n a_n \left(\frac{y}{h}\right)^n dy \right\} \qquad A11$$

$$= \frac{1}{\bar{v}h}\left\{ \sum_n \frac{a_n y}{n+1} - \sum_n \frac{a_n y}{n+1}\left(\frac{y}{h}\right)^n \right\}$$

and the average value of ϵ becomes

$$\bar{\epsilon} = \frac{1}{2V}\sum_n \frac{n}{(n+1)(n+2)} a_n$$

and substituting the series for V we get

$$\bar{\epsilon} = \frac{1}{2}\,\frac{\sum_n \frac{n a_n}{(n+1)(n+2)}}{\sum_n a_n} \qquad A12$$

In order to proceed further, some knowledge of the analytical form of the function v must be obtained or assumed.

From previous, ignoring variable viscosity, we have

$$-v = \int \frac{\partial u}{\partial x}\,dy = \frac{\partial}{\partial x}\left\{ \frac{1}{12\mu}\frac{\partial P}{\partial x}\left(2y^3 - 3y^2 h \right) \right\}$$

This form suggests taking for the a_n:

$$\left.\begin{aligned} a_3 &= -h^3 \frac{\partial}{\partial x}\left\{ \frac{2}{12\mu}\frac{\partial P}{\partial x} \right\} \\ a_2 &= \quad h^2 \frac{\partial}{\partial x}\left\{ \frac{3h}{12\mu}\frac{\partial P}{\partial x} \right\} \end{aligned}\right\} \quad n = 2,3 \qquad A13$$

A.

These values give for the parameter $\bar{\epsilon}$:

$$\bar{\epsilon} = \frac{1}{12}\left(1.2 - 0.6 \frac{x}{h} \frac{\partial h}{\partial x} \right) \qquad \text{A14}$$

after substitution of the a_n's.

This show that the variation of $\bar{\epsilon}$ is

$$0 \leqslant \bar{\epsilon} \leqslant 0.1$$

The max imum value is obtained for x = 0, which gives

$$\bar{\epsilon} = 0.10; \; x = 0$$

This value of $\bar{\epsilon}$ is used in expression 9. The result is given in fig. A1, computed for various values of αP_o, for three different values of αE.

INFLUENCE OF VARIABLE VISCOSITY ON NAVIER STOKES EQUATIONS

FIG A·1

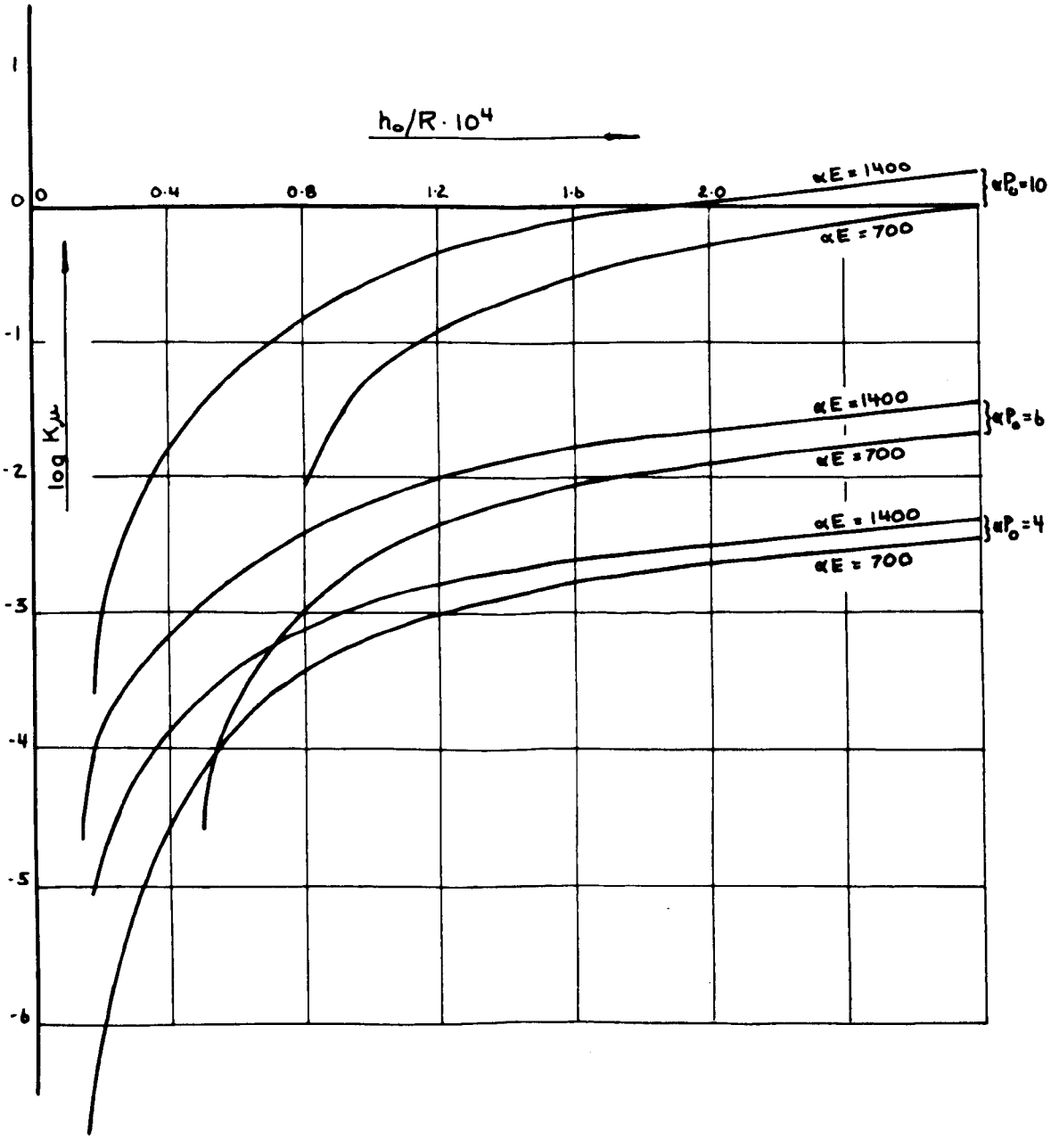

Appendix B.

Solution of the Linear Heatconduction Equation for a Composite Solid.

Consider a composite solid consisting of a finite medium $-1 \leqslant x \leqslant 0$, of temperature T_1 and properties K_1, c_1, ρ_1 etc. in contact with a semi-infinite medium $x \geqslant 0$, of temperature T_2 and properties K_2, c_2, ρ_2 etc.

Consider further that heat is generated in the finite medium at a rate $\Phi(x)\, t^{m/2-1}$ where m may take integral values.

The governing equations are,

$$\left.\begin{aligned} \frac{\partial^2 T_1}{\partial x^2} - \frac{1}{\alpha_1}\frac{\partial T_1}{\partial t} &= -\frac{\Phi t^{m/2-1}}{K_1} && -1 \leqslant x \leqslant 0 \quad \text{B1} \\ \frac{\partial^2 T_2}{\partial x^2} - \frac{1}{\alpha_2}\frac{\partial T_2}{\partial t} &= 0 && x \geqslant 0 \quad \text{B2} \end{aligned}\right\}$$

where $\alpha_1 = \dfrac{K_1}{\rho_1 c_1}$ and $\alpha_2 = \dfrac{K_2}{\rho_2 c_2}$

The initial and boundary conditions will be taken as

$$\left.\begin{aligned} K_1 \frac{\partial T_1}{\partial x} &= K_2 \frac{\partial T_2}{\partial x} \\ T_1 &= T_2 \end{aligned}\right\} \quad x = 0;\ t > 0 \qquad \text{B3, B4}$$

$$K_1 \frac{\partial T_1}{\partial x} = 0 \qquad x = -1;\ t > 0 \qquad \text{B5}$$

$$\lim_{x \to \infty} T_2 = 0 \qquad t > 0 \qquad \text{B6}$$

$$T_1(x,0) = T_2(x,0) \qquad t = 0 \qquad \text{B7}$$

Taking the Laplace transform defined by

$$\mathcal{L}[f(t)] = \int_c^\infty f(t) e^{-st} dt$$

B.

the subsidiary equations become

$$\frac{d^2v_1}{dx^2} - q_1^2 v_1 = -\frac{\Phi\Gamma(\frac{m}{2})}{K_1 s^{m/2}} \qquad \text{B8}$$

$$\frac{d^2v_2}{dx^2} - q_2^2 v_2 = 0 \qquad \text{B9}$$

where $v = \mathcal{L}[T]$

$$q_1 = \sqrt{s/\alpha_1} \qquad q_2 = \sqrt{s/\alpha_2}$$

The boundary conditions transforms into

$$K_1 \frac{dv_1}{dx} = K_2 \frac{dv_2}{dx} \qquad \text{B10}$$

$$v_1 = v_2 \qquad x = 0 \qquad \text{B11}$$

$$K_1 \frac{dv_1}{dx} = 0 \qquad x = -1 \qquad \text{B12}$$

$$\lim_{x\to\infty} v_2 = 0 \qquad \text{B13}$$

A formal solution to eqn. 8 is

$$v_1 = Be^{q_1 x} + Ce^{-q_1 x} + \frac{\Gamma(\frac{m}{2})}{K_1 q_1^2 s^{m/2}} \sum_{\lambda=0}^{\infty} \left(\frac{D}{q_1}\right)^{2\lambda} \Phi \qquad \text{B14}$$

where D is the ordinary differential operator d/dx.

Boundary condition 12 gives

$$0 = Bq_1 e^{-q_1 \ell} - Cq_1 e^{q_1 \ell} + \frac{\Gamma(\frac{m}{2})}{K_1 q_1^2 s^{m/2}} \sum_{\lambda} \frac{D^{2\lambda+1}}{q_1^{2\lambda}} \Phi(-\ell)$$

The restriction will now be placed on the function Φ that it is symmetric about the point $x = -1$. This implies that $D^{2\lambda+1}\,\Phi(-1) = 0; \quad \lambda = 0,1,2,3\cdots$

$\therefore\quad C = Be^{-2q_1\ell}$

B.

The solution of 9 with boundary condition 13 is

$$v_2 = E\, e^{-q_2 x} \qquad \text{B15}$$

The remaining constants can now be found from boundary condition 10 and 11

$$\therefore B = -\frac{\Gamma(\frac{m}{2})[\sigma\sum(\frac{D}{q_1})^{2\lambda} + \sum(\frac{D}{q_1})^{2\lambda+1}\ ]\ \Phi(0)}{(\sigma+1)[\ 1 + \beta e^{\ 2q_1 \ell}\ ]\ K_1 q_1^2 s^{m/2}} \qquad \text{B16}$$

$$E = \frac{\Gamma(\frac{m}{2})\sum(\frac{D}{q_1})^{2\lambda}}{K_1 q_1^2 s^{m/2}} \left\{ 1 - \frac{1 + e^{-2q_1\ell}}{1 + \beta e^{-2q_1\ell}} \frac{(\sigma + \frac{D}{q_1})}{(\sigma+1)} \right\} \Phi(0) \qquad \text{B17}$$

where, following Carslaw and Jaeger (9) we define :

$$K = q_2/q_1 \ ; \quad \sigma = (K_2/K_1)K \ ; \quad \beta = (\sigma - 1)/(\sigma + 1)$$

Expanding the denominator in a binomial series, substituting into eqn. 14 and rearranging,

$$v_1 = \frac{\alpha_1 \Gamma(\frac{m}{2})}{K_1} \left\{ \sum_{\lambda} \frac{\alpha_1^{\lambda} D^{2\lambda}}{s^{1+\lambda+m/2}} \Phi \ - \right.$$

$$- \left[\frac{\sigma}{\sigma+1} \sum_{\lambda} \frac{\alpha_1^{\lambda} D^{2\lambda} \Phi(0)}{s^{1+\lambda+m/2}} + \frac{\sigma}{\sigma+1} \sum_{\lambda} \frac{\alpha_1^{\lambda+1/2} D^{2\lambda+1}\ \Phi(0)}{s^{1+\lambda+(m+1)/2}} \right]$$

$$\left. \sum_{n=0}^{\infty} (-1)^n \beta^n [\ e^{-q_1(2n\ell - x)} + \ e^{-q_1[\ell(n+1) + x]}\ ] \right\} \qquad \text{B18}$$

Treating 17 in a similar way and substituting into eqn. 15 gives

B.

$$v_2 = \frac{\alpha_1 \Gamma(\frac{m}{2})(1 + \frac{D}{q_1}) \sum_{\delta} (\frac{D}{q_1})^{2\lambda} \Phi(0)}{K_1 \ (\sigma + 1) \ s^{1+m/2}}$$

$$\sum_{n=0}^{\infty} (-1)^n \beta^n \ [\ e^{-q_1 [2n\ell + kx]} \ + \ e^{-q_1 [2\ell(n+1) + kx]} \ ] \qquad \text{B19}$$

Taking the inverse transform, 18 transform into

$$T_1 = \frac{\alpha_1 \Gamma(\frac{m}{2})}{K_1} \left\{ \sum_{\lambda=0}^{\infty} \alpha_1^{\lambda} D^{2\lambda} \ \frac{t^{\lambda + m/2}}{\Gamma(1+\lambda+m/2)} \Phi \ - \right.$$

$$- \frac{\sigma + 2\sqrt{\alpha_1 t} \ iD}{\sigma + 1} \sum_{\lambda=0}^{\infty} \sum_{n=0}^{\infty} \alpha_1^{\lambda} D^{2\lambda} \Phi(0) (4t)^{\lambda + m/2} (-1)^n \beta^n i^{2\lambda+m}$$

$$\left. \left[\ \text{erfc} \ \frac{2n\ell - x}{2\sqrt{\alpha_1 t}} + \text{erfc} \ \frac{2\ell(n+1) + x}{2\sqrt{\alpha_1 t}} \ \right] \right\} \qquad \text{B20}$$

Similarly 19 transform into

$$T_2 = \frac{\alpha_1 \Gamma(\frac{m}{2})}{K_1} \ \frac{1 + 2\sqrt{\alpha_1 t} \ iD}{\sigma + 1} \sum_{\lambda=0}^{\infty} \sum_{n=0}^{\infty} \alpha_1^{\lambda} D^{2\lambda} \Phi(0) (4t)^{\lambda + m/2} i^{2\lambda+m} (-1)^n \beta^n$$

$$\left[\ \text{erfc} \ \frac{2n\ell + Kx}{2\sqrt{\alpha_1 t}} + \text{erfc} \ \frac{2\ell(n+1) + Kx}{2\sqrt{\alpha_1 t}} \ \right] \qquad \text{B21}$$

where the D operates on $\Phi(x)$ at $x = 0$, and the i operator is operating on the errorfunctions.

Adiabatic conditions are characterized by $K_2 = \alpha_2 = 0$ i.e. putting $\beta = -1$; $\sigma = 0$; $K = \infty$ in the above equations.

B.

The average adiabatic temperature $\bar{T}_1$ cannot be influenced by the presence of the heatconduction terms, since these only serve to shift the temperatures about.

Defining the average adiabatic temperature

$$\bar{T}_1 = \int_{\xi}^{1} T_1 d\xi$$

we get

$$\bar{T}_1 = \frac{\alpha_1 \Gamma(\frac{m}{2})\, t^{m/2}}{K_1 \Gamma(1 + m/2)} \int_{0}^{1} \Phi d\xi \qquad \text{B24}$$

where we have defined the non-dimensional variables

$\xi = x/l$; $\chi^2 = \alpha_1 t/l^2$

and redefined Φ to be a function of x/l

For the special case Φ = constant; m = 1 we get

$$\bar{T}_1 = \frac{2\alpha_1 \sqrt{t}}{K_1} \Phi \qquad \text{B25}$$

$$T_1/\bar{T}_1 = 1 - \frac{\sigma}{\sigma+1} \sum_{n=0}^{\infty} (-1)^n \beta^n \left[\text{ierfc} \frac{2n-\xi}{2\chi} + \text{ierfc} \frac{2(n+1) + \xi}{2\chi} \right] \qquad \text{B26}$$

Equation 20 may also be used to investigate the varia tion of temperature across the film under adiabatic conditions. Putting $\beta = -1$; $\sigma = 0$; $K = \infty$ and also applying the coordinate transform $y = 1 + x$, redefining ξ to mean y/l we get

B.

$$T_1 = \frac{\alpha_1 \Gamma(\frac{m}{2}) t^{m/2}}{K_1} \left\{ \sum_{\lambda=0}^{\infty} \frac{\chi^{2\lambda}}{\Gamma(1+\lambda+m/2)} D^{2\lambda}\Phi - \right.$$

$$- \sum_{\lambda=0}^{\infty} \sum_{n=0}^{\infty} 2^{m+1} \chi^{2\lambda+1} D^{2\lambda+1}\Phi(0)(4t)^{\lambda} i^{2\lambda+m+1}$$

$$\left. \left[\operatorname{erfc} \frac{(2n+1) - \xi}{2\chi} + \operatorname{erfc} \frac{(2n+1) + \xi}{2\chi} \right] \right\} \qquad \text{B27}$$

Now, taking Φ to be a quadratic in ξ restricted by the boundary condition $\Phi(0) = 0$, i.e. $\Phi = A\xi^2$, and taking $m = 1$ we obtain

$$T_1 = \frac{2\alpha_1 \sqrt{t}\, A}{3K_1} \left\{ 3\xi^2 + 4\chi^2 - 12\sqrt{\pi}\chi \right.$$

$$\left. \sum_{n=0}^{\infty} \left[i^2 \operatorname{erfc} \frac{(2n+1) - \xi}{2\chi} + i^2 \operatorname{erfc} \frac{(2n+1) + \xi}{2\chi} \right] \right\} \qquad \text{B28}$$

$$\bar{T}_1 = \frac{2\alpha_1 \sqrt{t}\, A}{3K_1}$$

$$\frac{T_1 - \bar{T}_1}{\bar{T}_1} = 3\xi^2 + 4\chi^2 - 12\sqrt{\pi}\chi \sum_{n=0}^{\infty} i^2 \operatorname{erfc} \frac{(2n+1)-\xi}{2\chi} + i^2 \operatorname{erfc} \frac{(2n+1)+\xi}{2\chi} - 1$$

B29

The variation of 29 with χ is shown in fig. B1.

Equation 29 was solved on the computer for three values of l_0 corresponding to the x-stations 6, 10 and 14×10^{-2}cm from the cylinder axis. In all cases the parameter ξ was taken as $\xi = 1$. The relation required between l and t was taken from the velocity of approach curve for the case a: constant viscosity, rigid material.

B.

The solution is showm in fig. B2.

It is not so much the function $(T - \bar{T})/\bar{T}$ that is of interest but rather $(T - \bar{T})$, since if this is small, temperature variation across the film will have little effect on the physical properties such as viscosity and density. Taking the values of $\bar{T}$ from the computer solution for the case a : constant viscosity, rigid material, the obtained values of $(T - \bar{T})$ are shown in fig. B2. The value of the thermal diffusivity used in the calculation was taken as $\alpha_1 = 0.81 \times 10^{-3}$ cm^2/sec.

It is believed that the results obtained are more severe than the true solution allowing for the motion of the boundaries, and hence provide an upper limit for the temperature variation.

SOLUTION OF

$$(T-\bar{T})/\bar{T} = 3\xi^2 + 4\chi^2 - 12\sqrt{\pi}\,\chi \sum_{N=0}^{\infty} i^2\mathrm{erfc}\,\frac{2N+1+\xi}{2\chi} + i^2\mathrm{erfc}\,\frac{2N+1-\xi}{2\chi}$$

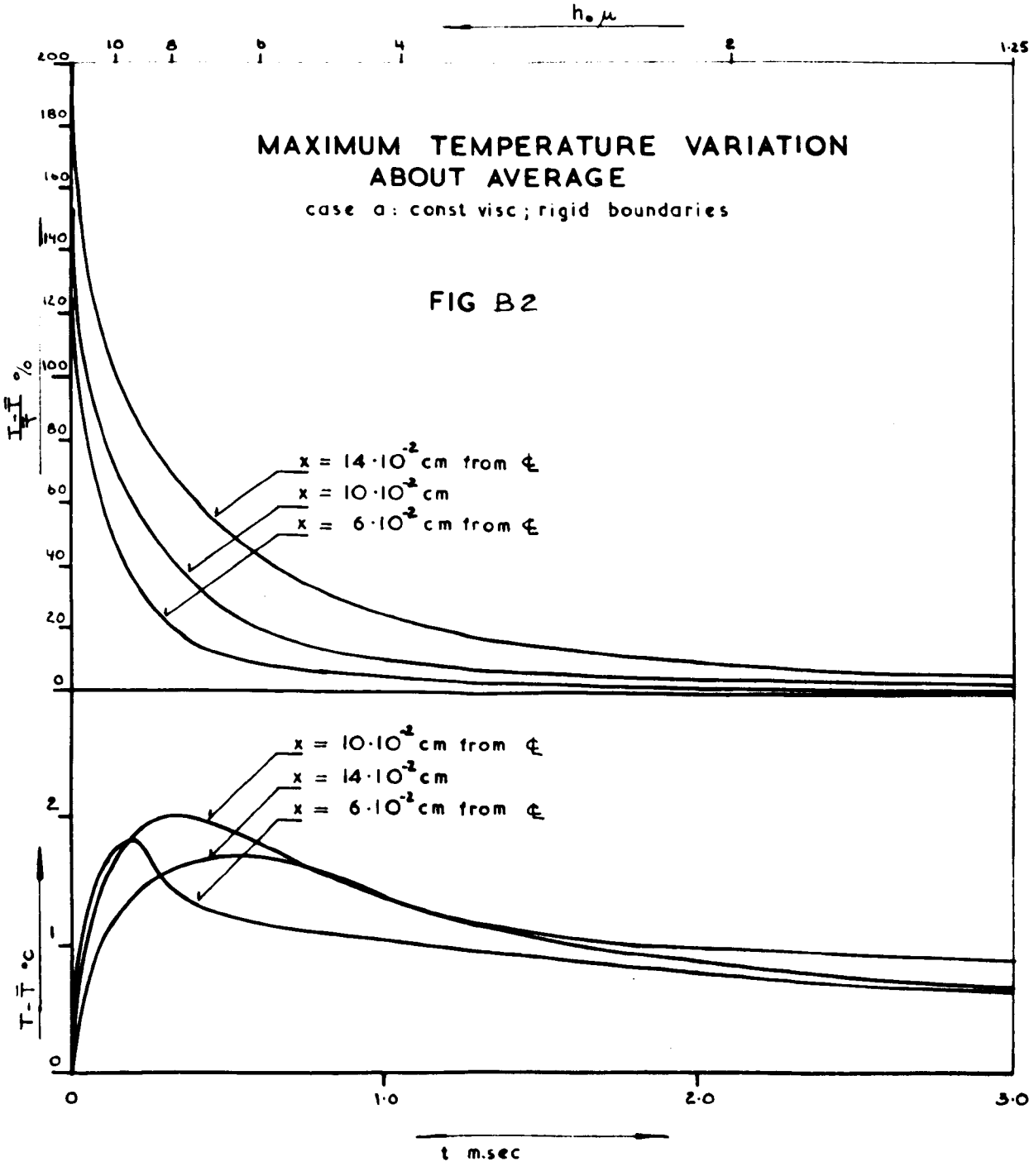
h. μ
200
10
8
6
4
2
1·25
180
160
140
120
100
80
60
40
20
0
MAXIMUM TEMPERATURE VARIATION
ABOUT AVERAGE
case a: const visc; rigid boundaries
FIG B2
$\frac{I-\bar{I}}{\bar{I}}$ %
x = 14·10⁻² cm from ℄
x = 10·10⁻² cm
x = 6·10⁻² cm from ℄
x = 10·10⁻² cm from ℄
x = 14·10⁻² cm
x = 6·10⁻² cm from ℄
2
1
0
T-T̄ °c
0
1·0
2·0
3·0
t m.sec

References

1) Martin, H.M 1916 Engineering, vol. 102, p.119 "The Lubrication of Gear Teeth".

2) Grubin, A.N. 1949 Central Scientific Research Institute for Technology and Mechanical Engineering. Moscow, Book No. 30, English Translation D.S.I.R.

3) Petrusevich, A.I. 1951 Izv. uzbekist. Fil. Akad. Nauk. SSSR., "Fundamental Conclusions from the Contact-hydrodynamic Theory of Lubrication".

4) Poritsky, H. 1952 Amer. Soc. Lubric. Engrs., National Symposium, p.98, "Lubrication of Gear Teeth, Including the Effect of Elastic Displacement".

5) Weber, C. and Saalfeld, K. 1954 Z. angew. Math. Mech., vol.34 p.54, "Schmierfilm bei Walzen mit Verformung".

6) Dowson, D. and Higginson, G.R. 1960 J. Mech. Eng. Science vol. 1, p.6. "A Numerical Solution to the Elasto-hydrodynamic Problem".

7) Halton, J.H. 1956 "The Lubrication of Plain Bearings: An Examination of Reynolds' Hydrodynamic Theory" (Engineering).

8) Galvin, G.D. 1957 Thornton Research Centre; Technical Note. "The effect of pressure on the viscosities of a paraffinic H.V.I. 650 oil, and an equiviscous blend of naphthenic L.V.I. oils supplied to the Department of Mechanical Engineering, Leeds University".

9) Carslow, H.S. and Jaeger, J.E. 1947 "Conduction of Heat in Solids" (Clarendon, Oxford).

I would like to thank Professor D. C. Johnson for his understanding and helpful supervision.

My thanks are also due to Dr. G. R. Higginson for interest and advice.

To Dr. A. S. Douglas, director of the University's electronic computing laboratory, for permission to use the computing facilities there, and to Dr. G. B. Cook and Mr. A. J. Mitchell of the Computing laboratory staff for helpful discussions and assistance.

In particular I would like to offer my gratitude to Dr. D. Dowson for his invaluable help and guidance throughout the period of my research.

For the construction of the experimental apparatus and the specimens I wish to thank W. H. Bickerton of the Research Workshop Staff.

Finally, I would like to take this opportunity to express my gratitude to my wife Randi Christensen for her patience and understanding.